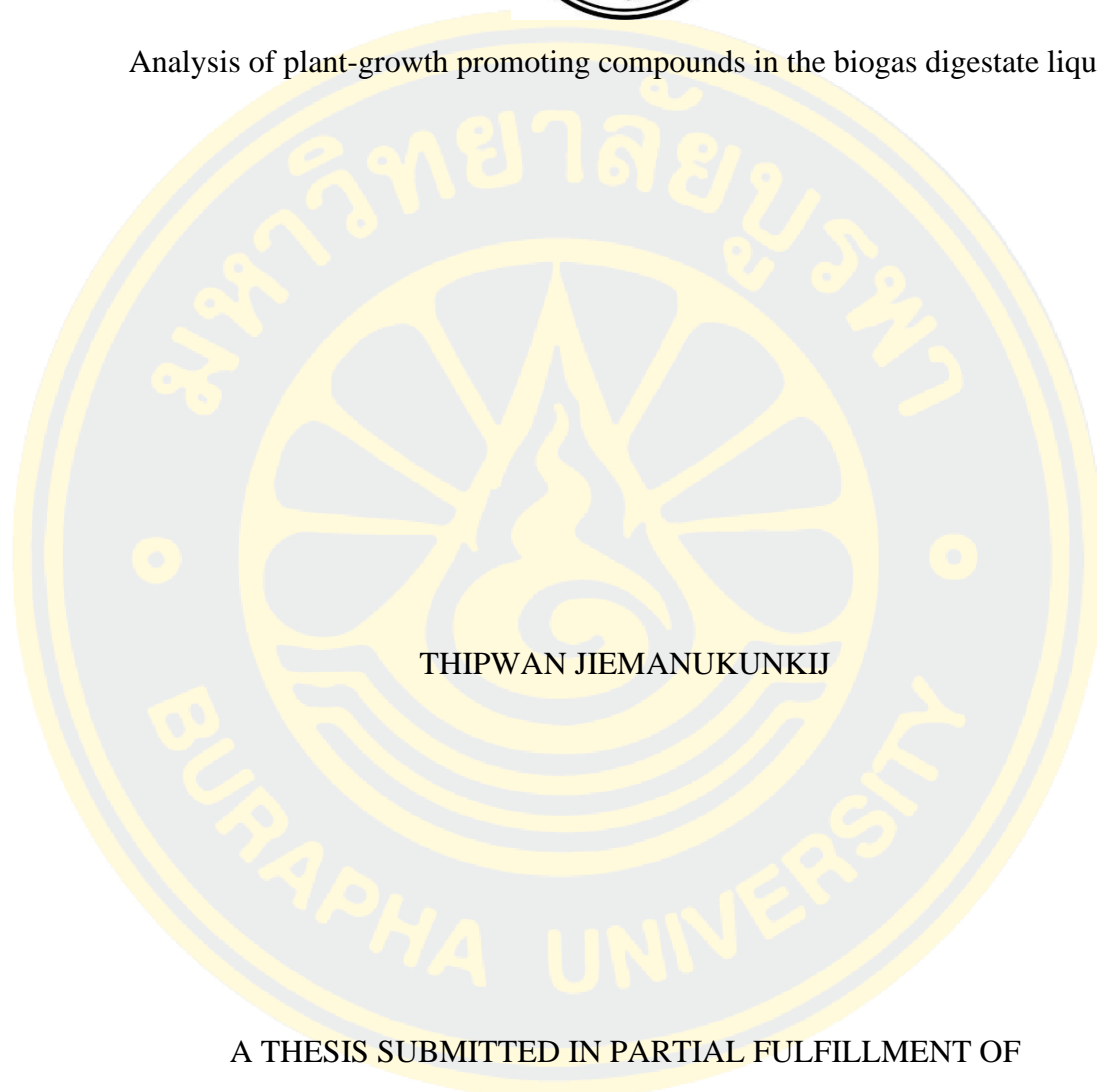




Analysis of plant-growth promoting compounds in the biogas digestate liquid



THIPWAN JIEMANUKUNKIJ

A THESIS SUBMITTED IN PARTIAL FULFILLMENT OF  
THE REQUIREMENTS FOR THE MASTER DEGREE OF SCIENCE  
IN BIOCHEMISTRY  
FACULTY OF SCIENCE  
BURAPHA UNIVERSITY

2022

COPYRIGHT OF BURAPHA UNIVERSITY

การวิเคราะห์สารในของเหลวจากระบบหมักก๊าซชีวภาพที่ส่งเสริมการเจริญของพืช



ทิพย์วรรณ เจียมอนุกุลกิจ

วิทยานิพนธ์นี้เป็นส่วนหนึ่งของการศึกษาตามหลักสูตรวิทยาศาสตรมหาบัณฑิต

สาขาวิชาชีวเคมี

คณะวิทยาศาสตร์ มหาวิทยาลัยบูรพา

2565

ลิขสิทธิ์เป็นของมหาวิทยาลัยบูรพา

Analysis of plant-growth promoting compounds in the biogas digestate liquid



THIPWAN JIEMANUKUNKIJ

A THESIS SUBMITTED IN PARTIAL FULFILLMENT OF  
THE REQUIREMENTS FOR THE MASTER DEGREE OF SCIENCE  
IN BIOCHEMISTRY  
FACULTY OF SCIENCE  
BURAPHA UNIVERSITY

2022

COPYRIGHT OF BURAPHA UNIVERSITY

The Thesis of Thipwan Jiemanukunkij has been approved by the examining committee to be partial fulfillment of the requirements for the Master Degree of Science in Biochemistry of Burapha University

Advisory Committee

Examining Committee

Principal advisor

.....  
(Assistant Professor Somchart Maenpuen)

.....  
(Wannasiri Wannarat)

Principal examiner

.....  
Member  
(Assistant Professor Somchart Maenpuen)

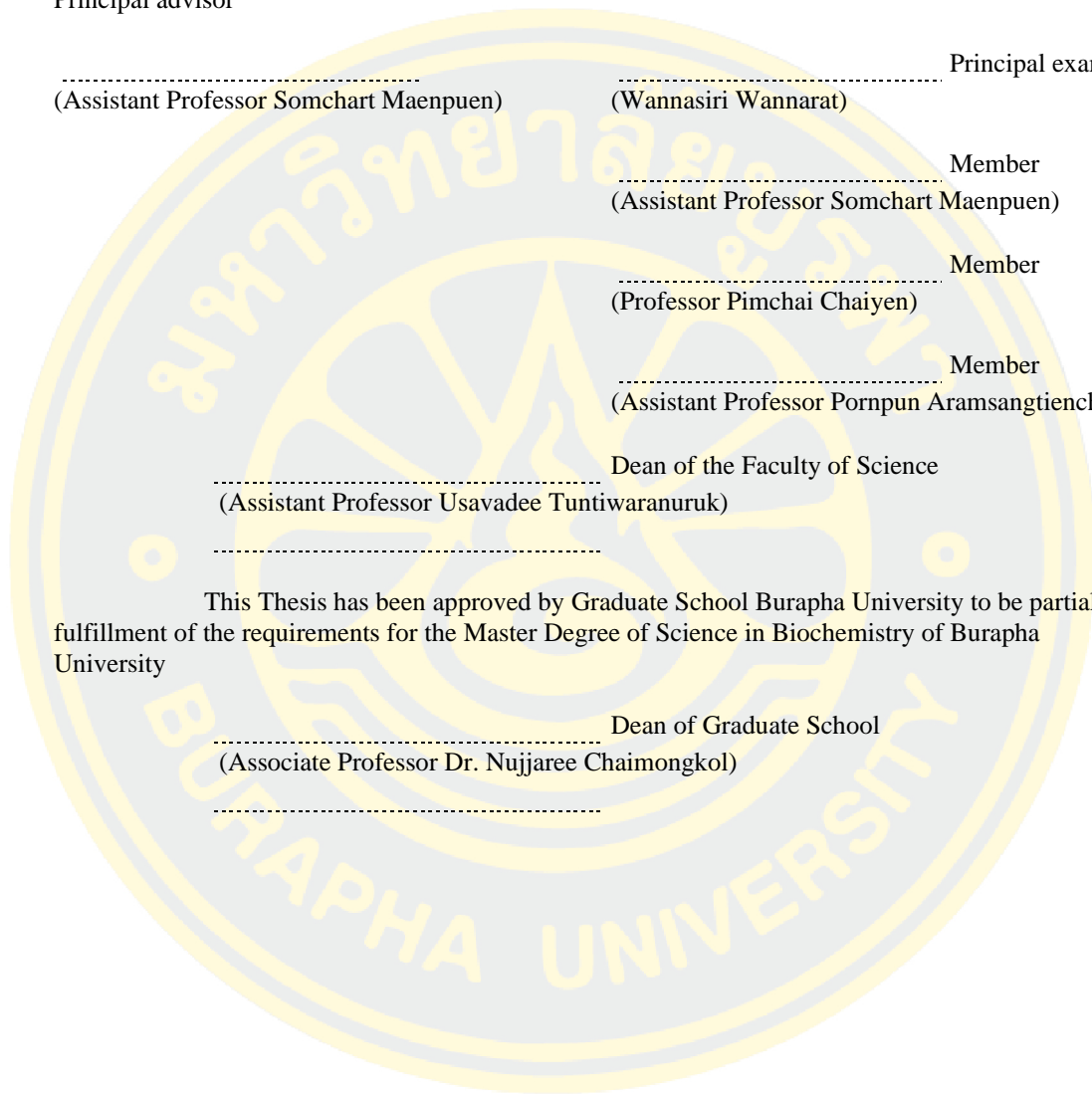
.....  
Member  
(Professor Pimchai Chaiyen)

.....  
Member  
(Assistant Professor Pornpun Aramsangtienchai)

.....  
Dean of the Faculty of Science  
(Assistant Professor Usavadee Tuntiwaranuruk)

.....  
This Thesis has been approved by Graduate School Burapha University to be partial fulfillment of the requirements for the Master Degree of Science in Biochemistry of Burapha University

.....  
Dean of Graduate School  
(Associate Professor Dr. Nujjaree Chaimongkol)



62910154: MAJOR: BIOCHEMISTRY; M.Sc. (BIOCHEMISTRY)

KEYWORDS: Biogas digestate liquid, Plant nutrient, Plant hormone

THIPWAN JIEMANUKUNKIJ : ANALYSIS OF PLANT-GROWTH PROMOTING COMPOUNDS IN THE BIOGAS DIGESTATE LIQUID.

ADVISORY COMMITTEE: SOMCHART MAENPUEN, Ph.D. 2022.

Biogas digestate liquid (BDL) is a byproduct derived from the anaerobic (co)-digestion of organic wastes, which can be applied as an organic fertilizer since it usually contains plant nutrients. In this work, we aim to analyze plant nutrients and plant hormones/plant-growth promoting compounds in unheated and heated BDL sample sets (fresh, 1-month-, 2-month-, and 3-month-storage sets), obtained from the anaerobic co-digestion of animal manure inoculum and food waste, by analytical techniques, CNS analyzer, AAS, and LC-MS/MS. The results obtained from the CNS and AAS analysis showed that all of the BDL sample sets contained high concentrations of essential plant macronutrients (N, P, K, Ca, and Mg) and micronutrients (Fe, Cu, Zn, Mn, and Mo), and very low concentrations of toxic elements (As, Pb, Cd, and Cr). The LC-MS/MS analysis using ampicillin as an internal standard demonstrated that only five plant hormones including, indole 3-acetic acid (IAA), abscisic acid (ABA), salicylic acid (SA), kinetin, and zeatin were detected in unheated BDL samples of the fresh set with an approximate concentration of 1.5  $\mu\text{M}$ , 1.7 nM, 0.18  $\mu\text{M}$ , 1 nM, and 0.2 nM, respectively. However, it was found that these plant hormones, except zeatin, were trivially decreased after storage for 1 month and could not be detected after storage for more two months. It was interesting to note that all of the plant hormones detected, except zeatin, were likely stable over heat treatment, which was agreed well with the finding that these plant hormones were stable at 40 and 100 °C. To evaluate all of BDL sample sets with different treatments could promote plant growth, we hence employed a hydroponic assay using green oak lettuce as a model. The bioassay results showed that only the 1H0+ formula (heated BDL sample of 1-month-storage set mixed with 170X-diluted hydroponic fertilizer) can promote the growth of green oak lettuce. The results

suggested that heated BDL sample of the 1-month-storage set was suitable for plant growth in the presence of hydroponic fertilizer. Taken together, the data indicated that BDL obtained from the anaerobic co-digestion of animal manure inoculum and food waste can serve as an environmentally friendly organic supplement for plant growth.



## ACKNOWLEDGEMENTS

I would like to thank my advisor, Asst. Prof. Dr. Somchart Maenpuen, for his kind academic support, suggestions, and comments throughout this study. I would like to thank Prof. Dr. Pimchai Chaiyen for valuable Guidelines for setting up a research problem. I would like to thank Dr. Thanyaporn Wongnate from (VISTEC) for valuable suggestions on this project. I would like to thank Dr. Wannasiri Wannarat from Kasetsart University for her valuable advice on bioassay. I would like to express my appreciation to the technical staff of Science Innovation Facility (SIF) IN54300018, Burapha University, for training me to use AAS. I would like to thank the School of Biomolecular Science and Engineering, VISTEC and Faculty of Science, BUU for the access and use the instruments for compound analysis. I also would like to thank the Biosynthai Biotechnology Co., Ltd. for kindly providing the BDL samples for this study. I would like to thank Dr. Aisaraphon Phintha (P' Tarn) and P' Nook for their kind helps and supports the use of LC-MS/MS. And I also would like to thank the Biogas team, P' Jum, P' Game, P' Non, and P' Pleng for the suggestions and support. Finally, I would like to thank the PC & TW lab members for their support and training me on having more skill sets. Finally, I would like to express all of my gratitude to my family for their support with love and understanding. Thank you for their patience.

Thipwan Jiemanukunkij

## TABLE OF CONTENTS

	<b>Page</b>
ABSTRACT.....	D
ACKNOWLEDGEMENTS.....	F
TABLE OF CONTENTS.....	G
TABLES .....	J
FIGURES.....	K
CHAPTER 1 .....	1
INTRODUCTION .....	1
1.1 Objective .....	3
1.2 Hypothesis.....	3
1.3 Advantage.....	3
1.4 Scope of research.....	3
CHAPTER 2 .....	4
LITERATURE REVIEWS .....	4
2.1 Food waste.....	4
2.2 Anaerobic digestion.....	6
2.3 Plant nutrients.....	10
2.4 Plant hormones .....	13
2.4.1 Indole-3-acetic acid (IAA) .....	15
2.4.2 Abscisic acid ( .....	19
2.4.3 Gibberellic acid (GA).....	22
2.4.4 Cytokinin (CK).....	26
2.4.5 Ethylene (ET) .....	32
2.4.6 Jasmonic acid (JA) .....	34
2.4.7 Salicylic acid (SA).....	39
2.4.8 Brassinosteroids (BRs) .....	43



2.4.9 Strigolactones (SLs) .....	47
2.5 Other compounds involving in plant growth/development.....	54
2.5.1 Pipecolic acid (Pip) .....	54
2.5.2 5-Aminolevulinic acid (ALA) .....	57
2.5.3 L-Ornithine .....	58
2.5.4 2,3-Butanediol (2,3-BD).....	59
2.6 Bioactive compounds detected in the biogas digestate liquid derived from the anaerobic digestion system.....	60
2.7 Hydroponic assay .....	63
CHAPTER 3 .....	68
RESEARCH METHODOLOGY.....	68
3.1 Chemicals and instruments.....	68
3.2 Acquirement of biogas digestate liquid (BDL) .....	69
3.3 BDL sample handlings .....	69
3.4 Metal analysis of heated and unheated BDL samples .....	71
3.5 CNS analysis of heated and unheated BDL samples .....	71
3.6 The condition optimization for LC-MS/MS analysis of authentic plant hormones and plant-growth promoting compounds.....	72
3.7 Determination of the optimal internal standard for LC-MS/MS analysis ...	74
3.8 Determination of limit of detection (LOD) and limit of quantitation (LOQ) from the calibration curve plot of each authentic plant hormone and plant- growth promoting compound .....	74
3.9 Optimization of the extraction method for future separating plant hormones and plant-growth promoting compounds from the BDL samples .....	75
3.10 Quantitation of plant hormones and plant-growth promoting compounds in heated and unheated BDL samples .....	78
3.11 Temperature effect on plant hormone stability .....	80
3.12 Hydroponic assay .....	80
CHAPTER 4 .....	83
RESULTS .....	83
4.1 The basic physicochemical properties of BDL samples .....	83

4.2	Plant nutrients and toxic elements.....	85
4.2.1	Macronutrients.....	85
4.2.2	Micronutrients .....	90
4.2.3	Toxic elements .....	94
4.3	The optimal condition for HPLC-MS/MS analysis of authentic plant hormones and plant growth promoting compounds.....	98
4.4	The optimal condition of internal standard (IS) for HPLC-MS/MS analysis .....	104
4.5	Temperature effect on stability of plant hormones and plant-growth promoting compounds as well as internal standard.....	107
4.6	The calibration curves of plant hormones and plant-growth promoting compounds and their limit of detection (LOD) and limit of quantitation (LOQ) values .....	109
4.7	The recovery yield of authentic plant hormones and plant-growth promoting compounds under solid phase extraction (SPE) method .....	115
4.7.1	The recovery yield of authentic compounds under an initial workflow.....	115
4.7.2	The optimal desalting step for yield recovery of authentic compounds.....	119
4.7.3	The optimal elution step for yield recovery of authentic compounds .....	125
4.8	Quantitation of plant hormones and plant-growth promoting compounds in unheated and heated BDL samples .....	127
4.9	Hydroponic bioassay .....	132
CHAPTER 5	.....	139
DISCUSSION AND CONCLUSION	.....	139
APPENDIX	.....	143
REFERENCES	.....	146
BIOGRAPHY	.....	154

## TABLES

	<b>Page</b>
Table 1 The limits of heavy metal in soil issued by several countries .....	12
Table 2 The established parameters for quantitative analysis of plant hormones by LC-MS/MS. ....	53
Table 3 Bioactive substances in anaerobic digestates.....	61
Table 4 The optimized distribution of Solvents A and B for compound separation in C <sub>18</sub> column chromatography and MS/MS analysis with negative and positive modes. ....	73
Table 5 The optimized conditions of source parameters for QqQ analyzer. ....	73
Table 6 The pH and electrical conductivity of unheated and heated BDL sample sets. ....	84
Table 7 Summary of the quantitation of macronutrients, micronutrients, and toxic elements in unheated and heated BDL sample sets. ....	97
Table 8 The optimized multiple reaction mode (MRM) parameters for electrospray ionization measurement of plant hormones and plant-growth promoting compounds. ....	103
Table 9 The summary of concentration ranges, coefficient of determination (R <sup>2</sup> ) values for linear regression, and LOD and LOQ values from the calibration curve of each plant hormone and plant-growth promoting compound. ....	114

## FIGURES

	Page
Figure 1 The anaerobic digestion (AD) process. ....	9
Figure 2 Location of each plant hormone binding with their receptors.....	14
Figure 3 Structure and biosynthetic pathways of indole-3-acetic acid (IAA). (A) The chemical structure of IAA. The biosynthetic pathway of IAA via (B) indole-3-acetamide (IAM) and (C) indole-3-pyruvic acid (IPA). ....	16
Figure 4 The transcription of auxin-responsive genes regulated by protein/transcription factors upon the cellular levels of auxin.....	18
Figure 5 Structure and biosynthetic pathways of abscisic acid (ABA). (A) The chemical structure of ABA. (B) The biosynthesis of ABA via multi-step enzymatic conversion of zeaxanthin. ....	20
Figure 6 Role of ABA in abiotic stress response via cascade phosphorylation process. ....	21
Figure 7 Structure of gibberellic acid derivatives.....	23
Figure 8 Decomposition of GA <sub>3</sub> into different forms under aqueous solution at different pHs, temperatures or reaction times.....	23
Figure 9 The transcription of gibberellin-responsive genes regulated by protein/transcription factors upon the cellular levels of gibberellin. ....	25
Figure 10 The chemical structures of cytokinin derivatives.....	27
Figure 11 The reaction of adenosine phosphate-isopentenyltransferase (IPT) that catalyzes the isopentane transfer to nucleotide, yielding the nucleotide-isopentene linkage, which is a CK precursor. ....	28
Figure 12 The proposed model for biosynthesis of CK derivatives from DMAPP derived from MVA and MEP pathways in higher plants via multi-step enzymatic processes. Some key enzymes involved in biosynthesis such as adenosine phosphate-isopentenyltransferase (IPT) catalyzing the linkage of isopentene and nucleotide, cytochrome P450 mono monooxygenase (CYP735A) catalyzing the hydroxylation of isopentane moiety, and cytokinin riboside 5'-monophosphate phosphoribohydrolase (LOG) catalyzing the removal of the nucleotide moiety via hydrolysis process.....	29
Figure 13 The CK molecular action by signaling transduction <i>via</i> the phosphotransfer process.....	31

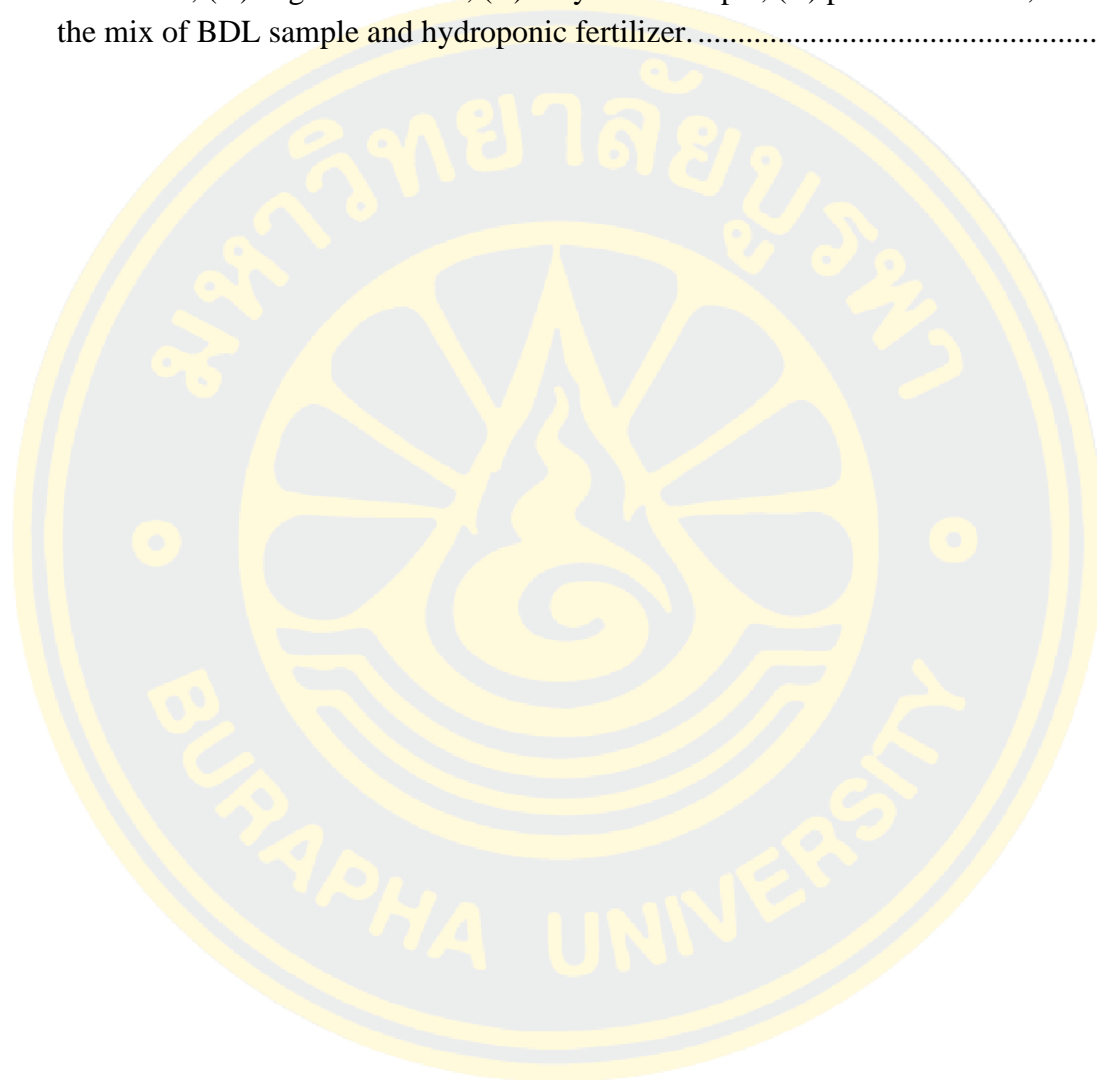
Figure 14 The mode of action of ET towards transcription of ET-responsive genes through the regulated protein turnovers and ET concentrations.....	33
Figure 15 The biosynthetic pathway of JA derivatives. ....	35
Figure 16 The chemical structures of JA derivatives.....	36
Figure 17 The transcription of JA-responsive genes regulated by protein/transcription factors upon the cellular levels of JA. (reproduced from (Santner & Estelle, 2009))	38
Figure 18 Structure of salicylic acid (SA). ....	40
Figure 19 Biosynthetic pathway of SA from chorismite-derived phenylalanine. ....	40
Figure 20 Different levels of SA in binding with the NPR transcription co-activators in response to pathogen infection. ....	42
Figure 21 The chemical structures of three BRs isolated in plants.....	44
Figure 22 The BR signaling pathway controlled by phosphorylation/dephosphorylation and acetylation/deacetylation of the key negative regulator BR-INSENSITIVE 2 (BIN2). ....	46
Figure 23 The possible pathway to synthesize SL via oxidative cleavage of $\beta$ -carotene catalyzed by carotenoid-cleavage dioxygenases, CCD7 and CCD8.....	48
Figure 24 Structure of SL derivatives.....	48
Figure 25 The SL signaling pathway to regulate the expression of the SL-responsive genes to response plant stress and development.....	50
Figure 26 Fragmentation patterns of authentic compounds, ABA (A), GA <sub>3</sub> (B), JA (C), and SA (D), analyzed in a negative mode of LC-MS/MS.....	52
Figure 27 Fragmentation patterns of authentic compounds, IAA (A), t-ZR (B), and t-Z (C), analyzed in a positive mode of LC-MS/MS.....	52
Figure 28 The chemical structure of Pip.....	54
Figure 29 The biosynthesis of Pip in response to pathogen infection. ....	56
Figure 30 The chemical structure of ALA.....	57
Figure 31 The chemical structure of Orn.....	58
Figure 32 The chemical structure of 2,3-BD with difference specific stereoisomer. .	59
Figure 33 The wick system of hydroponic assay.....	65
Figure 34 The ebb-flow system of hydroponic assay.....	65
Figure 35 The drip system of hydroponic assay.....	66
Figure 36 The deep-water culture of hydroponic assay.....	66

Figure 37 The nutrient film technique system of hydroponic assay .....	67
Figure 38 The overview summary of a schematic representation for production of BDL and BDL sample handlings.....	70
Figure 39 The overview of SPE workflow for optimization of compound extraction and separation. ....	77
Figure 40 The scheme represents the workflow of extraction of plant hormones and plant-growth promoting compounds from the BDL samples. ....	79
Figure 41 The planting of green oak lettuce in the deep-water culture system of the hydroponic assay. (A) The greenhouse applied for the hydroponic assay. (B) Seed germination of green oak lettuce inside the tap-water wet sponge. (C) The planting pots were placed on foam boxes filled with tested solution. ....	82
Figure 42 Quantitation of macronutrients (N, P, K, Mg, and Ca) in each of unheated and heated BDL sample set (fresh, 1-month-, 2-month-, and 3-month-storage set). The N contents were analyzed by CNS analyzer (A), while the P (B), K (C), Mg (D), and Ca (E) contents were analyzed by AAS technique. Error bars represent standard deviations (S.D.) from three replications of the data. All concentrations of macronutrients determined were summarized in Table 7. ....	87
Figure 43 Quantitation of micronutrients (Fe, Cu, Zn, Mn, and Mo) in each of unheated and heated BDL sample set (fresh, 1-month-, 2-month-, and 3-month-storage set). All of the micronutrients, Fe (A), Cu (B), Zn (C), Mn (D), and Mo (E), were analyzed by AAS technique. Error bars represent standard deviations (S.D.) from three replications of the data. All concentrations of micronutrients determined were summarized in Table 7. ....	91
Figure 44 Quantitation of toxic elements (As, Pb, Cd, and Cr) in each of unheated and heated BDL sample set (fresh, 1-month-, 2-month-, and 3-month-storage set). All of the toxic elements, As (A), Pb (B), Cd (C), and Cr (D), were analyzed by AAS technique. Error bars represent standard deviations (S.D.) from three replications of the data. All concentrations of toxic elements determined were summarized in Table 7.....	95
Figure 45 The chromatograms of plant hormones and plant-growth promoting compounds together with their structures of (A) IAA, (B) GA <sub>3</sub> , (C) ABA, (D) zeatin, (E) JA, and (F) SA detected by LC-MS/MS in a negative mode. ....	100
Figure 46 The chromatograms of plant hormones and plant-growth promoting compounds together with their structures of (A) kinetin, (B) Pip, and (C) ALA detected by LC-MS/MS in a positive mode.....	102

- Figure 47 The peak chromatogram of ampicillin (A and C) and IPTG (B and D) in the negative and positive modes. .... 105
- Figure 48 Effect of temperatures at 40 and 100 °C on the stability of plant hormones and plant-growth promoting compounds including IAA, GA<sub>3</sub>, ABA, SA, zeatin, kinetin, ALA, and Pip as well as ampicillin (an internal standard). Error bars represent standard deviations (S.D.) from three replications of the data. .... 108
- Figure 49 The calibration curve plot of various concentrations of each plant hormone and plant-growth promoting compound – (A) IAA, (B) ABA, (C) GA<sub>3</sub>, (D) SA, (E) kinetin, (F) zeatin, (G) Pip, and (H) ALA – *versus* peak area. The coefficient of determination ( $R^2$ ) values for linear regression and the LOD and LOQ values for each calibration curve was calculated and summarized in Table 9. Error bars represent standard deviations (S.D.) from three replications of the data. .... 110
- Figure 50 The peak area determined from triple-quadrupole LC/MS chromatogram representing the recovery yield of each plant hormone and plant-growth promoting compound – (A) IAA, (B) ABA, (C) GA<sub>3</sub>, (D) SA, and (E) ampicillin – passed through the technical steps including steps (1) starting reagent, (2) centrifugation, (3) filtration, (4) freeze-drying, and (5) SPE process (desalting and elution steps). Error bars represent standard deviations (S.D.) from three replications of the data ..... 116
- Figure 51 The peak area determined from triple-quadrupole LC/MS chromatogram representing the recovery yield of each plant hormone and plant-growth promoting compound – (A) IAA, (B) ABA, (C) GA<sub>3</sub>, (D) SA, (E) kinetin, (F) zeatin, (G) Pip, (H) ALA, and (I) ampicillin – passed through the desalting (DS) steps with different % (v/v) MeOH (1, 2, 3, 4, and 5% v/v). The step “200  $\mu$ M\_Hor” and “E\_100ACN” denotes the starting mixture reagent (200  $\mu$ M each) and the cartridge elution with 100% ACN, respectively. Error bars represent standard deviations (S.D.) from three replications of the data ..... 120
- Figure 52 The peak area determined from triple-quadrupole LC/MS chromatogram representing the recovery yield of each plant hormone and plant-growth promoting compound – IAA, ABA, GA<sub>3</sub>, SA, and ampicillin – passed through the individual elution (E) step with different % (v/v) ACN (20, 50, 80, and 100% v/v). The step “200  $\mu$ M\_Hor” denotes the starting mixture reagent (200  $\mu$ M each). Error bars represent standard deviations (S.D.) from three replications of the data ..... 126
- Figure 53 Quantitation of plant hormones including (A) IAA, (B) ABA, (C) SA, (D) kinetin, and (E) zeatin in unheated and heated BDL sample sets (fresh, 1-month-, 2-month-, and 3-month-storage set) by HPLC-MS/MS analysis. Error bars represent standard deviations (S.D.) from three replications of the data. .... 129

Figure 54 Green oak lettuce (*Lactuca sativa* L.) wet weight (A), dry weight (B) and canopy diameter (C) were used to test the quality of BDL samples to promote plant growth and development..... 134

Figure 55 Photographs of green oak lettuce (*Lactuca sativa* L.) treated with different conditions, (A) negative control, (B) only BDL sample, (C) positive control, and (D) the mix of BDL sample and hydroponic fertilizer..... 136





## CHAPTER 1

### INTRODUCTION

Food waste (FW), one form of the organic wastes, is a major negative factor affecting the environmental quality and a source of greenhouse gas emission. By estimation, the world population will be increased greater than 50% in 2050 and thus the demand of food and energy will be increased more than 70%. The FW have been estimated as highly accumulated as about 1.3 billion tons/year or 1.42 Kg/person/day and anticipated to increase up to 2.6 billion metric tons by year 2050 (Mahjoub & Domscheit, 2020). To eliminate the massive FW, about 1 billion dollars a year have been paid for disposal process (Melikoglu, Lin, & Webb, 2013). One of the cost-effective promising technology employed to eradicate the FW is the anaerobic digestion (AD) process, which is an oxygen free system underlying the recovery and recycling processes that accounted for 55% of organic waste treatment worldwide (Raksasat et al., 2020; Xu, Li, Ge, Yang, & Li, 2018). AD is one of the most important methods used for converting waste biomass into energy, which is a platform of the circular economy that is founded on the principles of reuse, value, recycling, and exploitation of natural cycles (Chojnacka, Moustakas, & Witek-Krowiak, 2020).

The co-digestion with animal manures derived from either pigs, cows, or poultry, can enhance the efficacy of the AD process since these manure wastes are full of potential microbes beneficial for anaerobic fermentation (Iocoli, Zabaloy, Pasdevicelli, & Gómez, 2019; Scaglia, Pognani, & Adani, 2017; Westerman & Bicudo, 2005). The AD process is divided into four stages: hydrolysis (the breakdown of macromolecules into smaller biomolecules), acidogenesis (the production of volatile fatty acids), acetogenesis (the production of acetate) and methanogenesis (the production of methane) (see details in CHAPTER 2, Figure 1), during which the microbes complete the FW co-digestion (Labatut & Pronto, 2018; Pramanik, Suja, Zain, & Pramanik, 2019; Sawyerr, Trois, Workneh, & Okudoh, 2019).

One of the major resultants obtained from the AD process is methane (CH<sub>4</sub>) biogas, which can be used as a household renewable energy source (Cheong et al., 2020)

The rest liquid, so called biogas digestate liquid (BDL), is the by-product that can be applied as an organic fertilizer as it usually contains optimal contents of plant nutrients (macronutrients such as N, P, K, Ca, Mg, and S, and micronutrients such as Zn, Fe, Mo, Mn, Cu, B, and Cl) essential for plant growth and a low abundance of toxic elements (Cd, Pb, Cr, As, and Hg) (Maathuis & Diatloff, 2013; Möller & Müller, 2012). In addition to plant nutrients, some major plant hormones such as indole-3-acetic acid (IAA) (also known as auxin), abscisic acid (ABA), and gibberellic acid (GA) (also called gibberellin A<sub>3</sub> or GA<sub>3</sub>) can be found in the BDL (Iocoli et al., 2019; Li, Guo, Pang, & Dong, 2016) and play significant roles in promoting root growth, cell division and elongation, floral induction, and plant response against biotic and abiotic stresses (Geilfus, 2019). Not only plant hormones, but also other compounds such as 5-aminolevulinic acid (ALA) can be produced by the photosynthetic bacterium *Rhodobacter sphaeroides* during the AD process and serve as an herbicide (Sasaki, Tanaka, Nishizawa, & Hayashi, 1990). Additionally, some previously reported compounds have been shown to be involved in the plant defense system (such as L-ornithine and its derivative, N<sup>δ</sup>-acetylornithine) (Adio et al., 2011; Hussein, Mekki, El-Sadek, & El Lateef, 2019) and promoting the growth of root-associated bacteria, also known as rhizobacteria (such as pipercolic acid and 2,3-butanediol) (Fatima et al., 2009; Gouffi, Bernard, & Blanco, 2000; Khalaf & Raizada, 2020; Park, Seo, Oh, Seo, & Kim, 2018; Yi et al., 2016), albeit they have not been found in the BDL.

Based on previous reports, these prompt us to analyze our BDL obtained from the animal manure-food waste anaerobic co-digestion process. Therefore, in this thesis work, we aim to quantitate the plant micro- and macronutrients by analytical methods using atomic absorption spectroscopy (AAS) and carbon-nitrogen-sulfur (CNS) analyses, and to determine those plant-growth promoting compounds, including (i) plant hormones (such as IAA, GA, ABA, jasmonic acid (JA), salicylic acid (SA), for examples) and their derivatives, (ii) plant defense compounds (such as L-ornithine, N<sup>δ</sup>-acetylornithine) and their derivatives, (iii) rhizobacterial growth promoting agents (such as pipercolic acid and 2,3-butanediol), and (iv) other plant-growth promoting compounds, in the BDL by liquid chromatography-tandem mass

spectrometry (LC-MS/MS) together with the investigation of their roles in promoting of plant growth.

### **1.1 Objective**

To quantitate plant micro- and macronutrients and determine the plant-growth promoting compounds in the BDL, and to investigate their roles in promoting of plant growth.

### **1.2 Hypothesis**

The BDL contains plant micro- and macronutrients and the plant growth-promoting compounds which are supplemental for plant growth.

### **1.3 Advantage**

The quantitative amount of plant micro- and macronutrients as well as the plant-growth promoting compounds will be used for evaluating the BDL as a qualified plant-growth supplement and as a measure of quality control of the BDL production.

### **1.4 Scope of research**

The 40 L of BDL obtained from the anaerobic co-digestion of the animal manure inoculum and FW was drained out of a 1000-L fermentation tank and then divided into two main sets, the fresh set (10 L) and the storage set (30 L). For the storage set, it was stored at ambient temperature and the aliquot of 10 L was collected at different storage times: 1, 2, and 3 months. All the samples were split into two separate aliquots. One aliquot was heated by boiling for 30 min, while the other one was not. The heated and unheated samples were analyzed by AAS and CNS analyses to quantitate plant micro- and macronutrients. All samples in each set were also be extracted by a solid-phase extraction (SPE) cartridge under optimized conditions and the compounds were then determined by LC-MS/MS. The bioassay to assess the compounds possessing the capability of promoting plant growth were carried out using appropriate plant models.

## CHAPTER 2

### LITERATURE REVIEWS

#### 2.1 Food waste

Food waste (FW) is one type of organic waste that is massively generated by food processing industries and household consumption. The high accumulation of FW can cause environmental concerns affecting communities, such as smelly odor problem, and the decomposed organic matters in FW can be potential sources of pathogenic diseases (Talan et al., 2020). It was estimated that FW generated from households and the hospitality industry accounted for 21% of total FW generated worldwide, and the eliminated FW by municipalities accounted for 30-60 % of solid urban residues (Carmona-Cabello et al., 2020). Almost 50% of the FW generated from the production stage in food processing industries was mainly from fruit and vegetables, while FW derived from cereals was abundant, with almost 50% generated from the consumer stage (Xu et al., 2018).

The FW can be divided into four groups based on the sources of the FW generated, including (1) *fruits and vegetables*, (2) *starchy foodstuffs*, (3) *meat and fish*, and (4) *non-edible products* such as bones, shells and skin, for example (Carmona-Cabello et al., 2020). FW was enriched in high contents of biomolecules (carbohydrates, proteins, lipids), minerals, and vitamins. In addition, FW can also be classified into five groups based on their physical and chemical characteristics: (1) *Physicochemical characteristics*: pH 5.1, 22.8% (w/w) dry matter (DM) and 88.2% (w/w) volatile solid (VS), (2) *Elementary composition*: carbon 45.5% (w/w) DM, hydrogen 7.0% (w/w) DM, oxygen 33.2% (w/w) DM, nitrogen 2.8% (w/w) DM, sulfur 0.4% (w/w) DM and a C/N ratio of 18.5, (3) *Biochemical characteristic (% VS)*: carbohydrates 36% (w/w), cellulose 9 % (w/w), hemicellulose 9% (w/w), protein 21% (w/w) and fats 15% (w/w), (4) *Nutritional element*: total ammonia nitrogen 731 mg/L, total Kjeldahl nitrogen 16 g/kg DM, Ca 1.6% DM, K 1.2% DM, Mg 0.2% DM, Na 2.2% DM, P 0.5% DM, Fe 482 ppm DM, Mn 62.5 ppm DM, Mo 1.2 ppm DM, and Zn 87 ppm DM, and (5) *Heavy metals*: Cd 0.3 ppm DM, Cr 28 ppm DM, Cu 23 ppm DM, Hg 0.3 ppm DM, Ni 10 ppm DM, and Pb 18 ppm DM (Fisgativa, Tremier, & Dabert, 2016).

As Thailand is an agriculture-based country and has become a “Kitchen of the World”, many agricultural FW have been anticipated to be produced. The main FW is majorly derived from cereals, especially rice, which are discharged from restaurants and household. By the nutritive index of Thai food (Department of Health, Ministry of Public Health), rice consisted of water 9.9%, protein 7%, fat 2.4%, carbohydrate 79.1%, fiber 2.5%, ash 1.6%, Ca 0.027%, P 0.25%, Fe 0.004%, and vitamin ~0.004%. The other agricultural FWs are also from protein sources like meat which consisted of water 75.8%, protein 19.6%, fat 3.3%, ash 0.9%, Ca 0.002%, and vitamin ~0.007%. Moreover, fruits and vegetables are also FW sources, which consist of water 62.6%, protein 1.1%, fat 0.2%, carbohydrate 35.4%, fiber 2.3%, ash 0.7%, Ca 0.007%, P 0.043%, Fe 0.0008%, and vitamin ~0.01%. These FW components can be important sources for the anaerobic digestion (AD) process (Talan et al., 2020; Xu et al., 2018) and also providing phenolic acids precursors for production of different value added products (Sindhu et al., 2019; Tinikul, Chenprakhon, Maenpuen, & Chaiyen, 2018).

The FW management to reduce the environmental impact has been much increasingly considered. One of the traditional disposal methods used to manage FW is the landfill method. In the U.S., 76.3 % of FW disposals were eliminated by landfill method (Xu et al., 2018). In Malaysia, landfill application can effectively reduce the wastes more than 80% due to its convenient process and low cost. However, more than 95% of carbon dioxide (CO<sub>2</sub>) caused by the organic wastes accumulated in the landfill were emitted into the atmosphere, thus causing the greenhouse effect and global warming. The other method that can eradicate the organic wastes is the AD process (Raksasat et al., 2020). Since the organic wastes, including FW, were enriched in nutrient substances such as biomolecules and minerals, they can act as good feeding sources for AD system to produce the biogas under anaerobic condition. Therefore, the FW contains components serving as valuable resources as precursors for AD process produces an organic fertilizer that contains plant nutrients and hormones that are essential for plant growth. This bio-based refinery of the FW is a platform of a sustainable and circular economy (Dahiya et al., 2018; Paritosh et al., 2017).

## 2.2 Anaerobic digestion

The anaerobic digestion (AD) is an oxygen free degradation process used to eliminate organic wastes, including FWs by anaerobic microorganisms. AD is the current technology that is used to convert organic wastes into biogas, a source of a renewable energy, and the by-products as sources of organic fertilizer for agricultures (Esposito et al., 2012). The AD technology used to eliminate the FW has potential and hopeful for sustainable and environmentally friendly management as it is a cost-effective technology for alternative energy production (Srisowmeya, Chakravarthy, & Nandhini Devi, 2020).

There are 4 stages that occur in the AD process (Figure 1). First, the “**Hydrolysis**” stage is the first step in the AD process. In this stage, the complex organic matters, such as carbohydrates, proteins, and lipids, are hydrolyzed into smaller, water-soluble compounds, such as sugars, amino acids, and long-chain fatty acids, respectively, by enzymatic processes in fermentative bacteria, such as *Bacillus*, *Proteus*, *Vibrio*, *Peptococcus*, *Clostridium*, *Micrococcus*, *Acetivibrio*, *Staphylococcus*, and *Bacteroides*. In general, the pH range at this stage is about 5.5-6.0, which is optimal for the hydrolysis process. The smaller molecules are further processed in the “**Acidogenesis**” stage where the pH is in a range of 6.0-7.0. At this stage, many acidogenic bacteria viz. *Clostridium*, *Eubacterium limosum*, *Streptococcus*, *Lactobacillus*, *Escherichia*, *Staphylococcus*, *Micrococcus*, *Bacillus*, *Sarcina*, *Veillonella*, *Pseudomonas*, *Desulfovibrio*, *Desulphuromonas*, *Desulfobacter*, and *Selenomonas* converted sugars, amino acids, and short-chain fatty acids into the volatile fatty acids (VFAs), such as propionic acid, butyric acid, and lactic acid, and alcohols. The long-chain fatty acids are not digested at this stage. The third stage is the “**Acetogenesis**” stage, where VFAs and alcohols derived from the “**Acidogenesis**” stage, the long-chain fatty acids are transformed into acetate, hydrogen (H<sub>2</sub>), and CO<sub>2</sub> by acetogenic bacteria, such as *Clostridium*, *Syntrophobacter*, and *Syntrophomonas*. This stage occurs well under pH ranges of 6.0-7.0. Acetate, H<sub>2</sub> and CO<sub>2</sub> are then transformed into CH<sub>4</sub> by methanogenic archaea in the “**Methanogenesis**” stage where the pH optimum is in a range of 6.5-7.5. For acetate transformation, the acetotrophic methanogens, such as *Methanosarcina*, *Methanospirillum*, and *Methanosaeta* are responsible for acetate conversion. While hydrogenotrophic methanogens, including

*Methanobacterium*, *Methanoplanus*, *Methanocalculus*, *Methanobrevibacter*, *Methanoculleus*, *Methanoregula*, and *Methanococcus* play roles in the condensation of H<sub>2</sub> and CO<sub>2</sub> to produce CH<sub>4</sub> (Pramanik et al., 2019).

In order to achieve an efficient AD process, seven important parameters are necessarily considered, including (i) substrate, (ii) co-digestion, (iii) pH, (iv) temperature, (v) organic loading rate (OLR), (vi) hydraulic retention time (HRT), and (vii) inoculum (Srisowmeya et al., 2020; Zhang, Su, Baeyens, & Tan, 2014). These parameters are described in brief as follows: **(I) Substrate:** FW, an efficient substrate for biogas and organic fertilizer, contains the total solid (TS) content varying between 18.1 and 30.9%, and the volatile solid (VS) content varying between 17.1 and 26.35%. The substrate to inoculum (S/I) ratio can affect the microbial metabolic pathways. The S/I ratio should be greater than 2.0 for system stability and efficiency in methane production. A low S/I ratio can result in an accumulation of organic acids and alcohols, thereby distressing the stability of the digestion system. In addition to the S/I ratio, the carbon to nitrogen (C/N) ratio is also important. The C/N ratio that is suitable for nutrient balance in the AD system is in a range of 15-30. Not only the FW substrate, the metal contents (both monovalent (M<sup>+</sup>) and divalent (M<sup>2+</sup>) metal ions), such as Na<sup>+</sup>, K<sup>+</sup>, Ca<sup>2+</sup>, Ni<sup>2+</sup>, Zn<sup>2+</sup>, and Fe<sup>2+</sup> also affect the efficiency of the AD system as these metal ions play a role as a cofactor for microbial enzymatic reaction. The recommended optimum concentration of Na<sup>+</sup>, Ca<sup>2+</sup>, and K<sup>+</sup> in the AD system should be 350, 150-300, and <400 mg/L, respectively. While the concentration of Fe<sup>2+</sup> should be 5 mg/kg FW, which is optimum for the AD process (Srisowmeya et al., 2020), **(II) Co-digestion:** Most of organic wastes treated are usually manure wastes from animal farming (such as pigs, cows and poultryes), and agricultural wastes (such as FW, municipal biosolids, and wastes from some industries). These two wastes can be digested separately in the AD system. Alternatively, the co-digestion of two or more types of wastes can enhance the efficacy of the AD system for the production of biogas and the organic fertilizer by-products (Westerman & Bicudo, 2005), **(III) pH:** It is a measure of chemical acid-base status which is used as an indicative of AD system stability. As mentioned above, the pH changes occurred during AD process are critical factors that can affect the efficiency of the AD process for production of the biogas (Pramanik et al., 2019), **(IV) Temperature:** It is an important physical

factor that can affect the AD system as it can dictate the digestion rate which depends on the microbial growth and availability. Three temperature ranges are assigned according to the microbial growth, including psychrophilic (10-30 °C), mesophilic (30-40 °C), and thermophilic (50-60 °C) conditions (J. K. Kim, Oh, Chun, & Kim, 2006; M.-S. Kim, Kim, & Yun, 2017; Sanchez, Borja, Weiland, Travieso, & Martin, 2001; Srisowmeya et al., 2020; W. Zhang et al., 2014). In general, the higher temperature can accelerate the AD process faster than the lower temperature, (V) **Organic loading rate (OLR)**: OLR is a measure of the amount of influent substrate that enters the digestion reactor per unit of time (g/L/day) (Labatut & Pronto, 2018; Srisowmeya et al., 2020; W. Zhang et al., 2014). The OLR value increased from 1 to 6 VS/L/day could reduce the methane yield about 1.73 folds. The optimum OLR for substrates like FW should be below 2.5 g VS/L/day (Srisowmeya et al., 2020; W. Zhang et al., 2014), (VI) **Hydraulic retention time (HRT)**: It is the number of days that refer to the material remaining in the AD tank. The HRT represents the growth of a microbial community and the change of the substrates to methane. The mesophilic reactor has a HRT of 14-40 days, while the thermophilic reactor is at 14-20 days (Srisowmeya et al., 2020; W. Zhang et al., 2014), (VII) **Inoculum**: It is a factor that can affect the AD process. The good quality of the inoculum should be from the anaerobic digester, which is operated under pH 7.0-8.5, VFA <1.0 g CH<sub>3</sub>COOH/L, alkalinity >3.0 g CaCO<sub>3</sub>/L, and ammonium content <2.5 g N-NH<sub>4</sub>/L. A variety of active microbial consortia are also required for good inoculum to enhance the AD process. In addition, the optimum S/I ratio is also a factor that can promote the complete AD process. It was reported that the S/I ratio of 7.5 can increase the CH<sub>4</sub> yield by about 12% (Srisowmeya et al., 2020; C. Zhang et al., 2014).



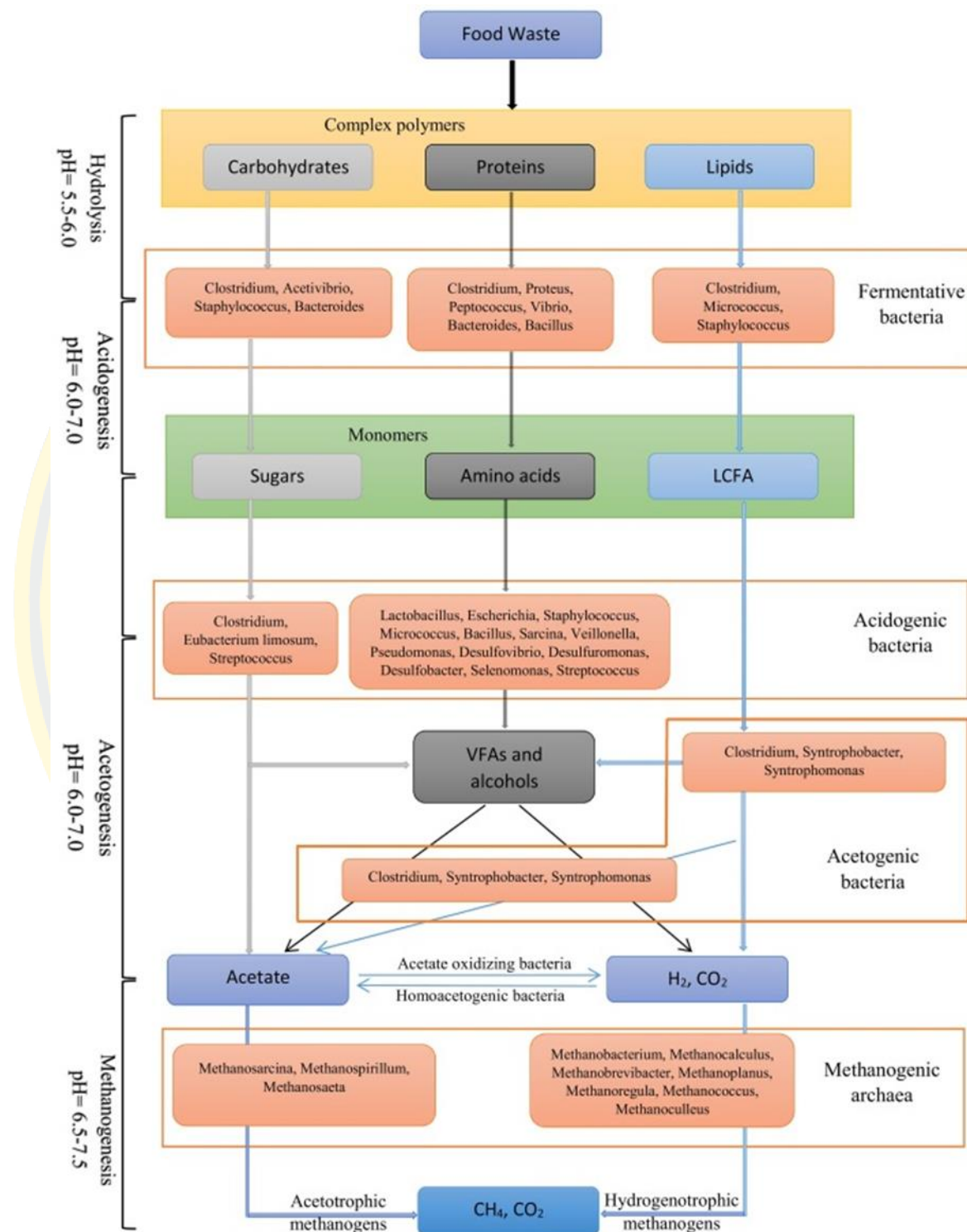


**Figure 1** The anaerobic digestion (AD) process. (reproduced from (Pramanik et al., 2019)).

### 2.3 Plant nutrients

As mentioned earlier in CHAPTER 1 plant nutrients can be classified into 2 main groups, including macronutrients and micronutrients, which are usually consisted of organic and inorganic elements that are essential for plant growth. The N, P, K, Ca, Mg, and S are macronutrients. While Fe, Mn, Cu, Zn, B, Mo, and Cl are of micronutrients. These elements can be derived from soil minerals or organic fertilizers obtained from AD.

For the macronutrients, nitrogen plays significant roles as a part of the chlorophyll molecule and ingredients of several vitamins and in promoting the green color of plant. Usually, plants need nitrogen in ranges of 1.25-1.75 % to promote the growth. The nitrogen content is also used to determine the C/N ratio, which is a key parameter to indicate the energy source and nutrients in the AD system. When the carbon substance is greater than nitrogen, it could cause the changes in the microorganism's community in the system and affects the AD process (Liang, Yuan, Yang, & Meng, 2017). Phosphorus functions to develop the root, seed, and fruit and initiation of flowering. Plants need phosphorus in a range of 0.15-0.25 %. While potassium plays a role in controlling the opening and closing of leaf stomata. In photosynthesis, potassium assists in the balance of electrical charges at the site of ATP production. Plants need potassium with a range of 1-1.5 %. For Ca and S, plants need them about 0.1-0.2 % to promote cell division, syntheses of chlorophyll component, amino acids, and vitamins, and enhance the growth of roots and seeds. For the micronutrients, they help synthesize auxin, chlorophyll, and starch. They also help regulate the digestion of sugar in plants by performing as a part of enzymes that play a role in the regulation of plant growth and is necessary for the conversion of carbohydrate. In addition, they help develop the plant reproductive systems. The micronutrients are needed very few for plant growth (Osman, 2013; Uchida, 2000).

During the AD process, the degradation of proteins and the mineralization of the organic nitrogen is the primary source of the digestate nitrogen. At least 50% of the digestate nitrogen occurs as ammonium nitrogen ( $\text{NH}_4^+\text{-N}$ ) form, which may be directly absorbed by the plant and plays a crucial role in plant growth. Among the digestates obtained from the AD of three livestock manures (chicken, cattle, and pig), the digestate from the AD of chicken manure contains about 2-folds higher total

nitrogen concentration (2893 mg/l) than that of the fermentation of the cattle and pig manures (1115 and 1103 mg/l, respectively). Similarly, the potassium content of the chicken manure digestate (1961 mg/l) is also higher than that of the pig and cattle manure digestates (1520 and 1216 mg/l, respectively). In contrast, the total phosphorus content of the cattle manure digestate (352 mg/l) is slightly higher than that of the chicken and pig manure digestates (244 and 226 mg/l, respectively) (S. Wu & Dong, 2020). From this data, it suggests that the AD process of manure wastes of the monogastric animals (such as chicken and swine) yields higher contents of AD metabolites and nutrients than that of the ruminants (cattle), which can be used as an organic fertilizer for plant growth, development, and production, as well as their ability to withstand diseases (Lu et al., 2019).

Not only are essential elements to be analyzed, but the elements with their potential toxicity, such as As, Cd, Cr, Pb, Ni, Zn, Cu, and Hg, are also being concerned because these elements can be polluted in many agricultural soils, thus affecting plant productivity (Burló, Guijarro, Carbonell-Barrachina, Valero, & Martínez-Sánchez, 1999). The limited concentrations of heavy metals in soil are regulated and issued by several countries, as listed in Table 1 (S. Wu & Dong, 2020).

**Table 1** The limits of heavy metal in soil issued by several countries

	<b>Cd</b>	<b>Pb</b>	<b>Hg</b>	<b>Ni</b>	<b>Cr</b>	<b>As</b>	<b>Zn</b>	<b>Cu</b>
<b>EU recommendations</b>	20	750	16	300	1000	nr	2500	1000
<b>EU recommendations starting 2015</b>	5	500	5	200	600	nr	2000	800
<b>EU recommendations starting 2015</b>	2	300	2	100	600	nr	1500	600
<b>UK</b>	1.5	200	1	50	100	nr	400	200
<b>Finland</b>	1.5	100	1	100	300	25	1500	300
<b>USA</b>	85	840	57	420	nr	75	7500	4300
<b>Italy, fertilizer</b>	1.5	140	1.5	100	nr	nr	500	230
<b>Turkey</b>	10	1200	25	400	1200	nr	4000	1750
<b>China, in acid soil (pH &lt;6.5)</b>	5	300	5	100	600	75	500	250
<b>China, in alkali soil (pH ≥6.5)</b>	20	1000	15	200	1000	75	1000	500
<b>Sweden</b>	2	100	2.5	50	100	nr	800	600

Heavy metal unit: mg/kg DM; nr, no record.

## 2.4 Plant hormones

Plant hormones are endogenous chemical molecules, including 9 species: Auxin (also called indole-3-acetic acid, IAA), abscisic acid (ABA), gibberellic acid (also called gibberellin, GA), cytokinin (CK), ethylene (ET), jasmonic acid (JA), salicylic acid (SA), brassinosteroids (BRs), and strigolactone (SL) (Yang et al., 2019). These hormones are accountable for growth regulation, advancement, and generative processes as well as responsible for acclimation of plant against environmental stimulus (Dilworth, Riley, & Stennett, 2017). Each hormone functions through the binding with their corresponding receptors located at different sites of plant cells (Figure 2), except for SA and SL, in which their receptors are not known (Santner & Estelle, 2009). The details of each plant hormone and its molecular and physiological action are discussed in brief below.

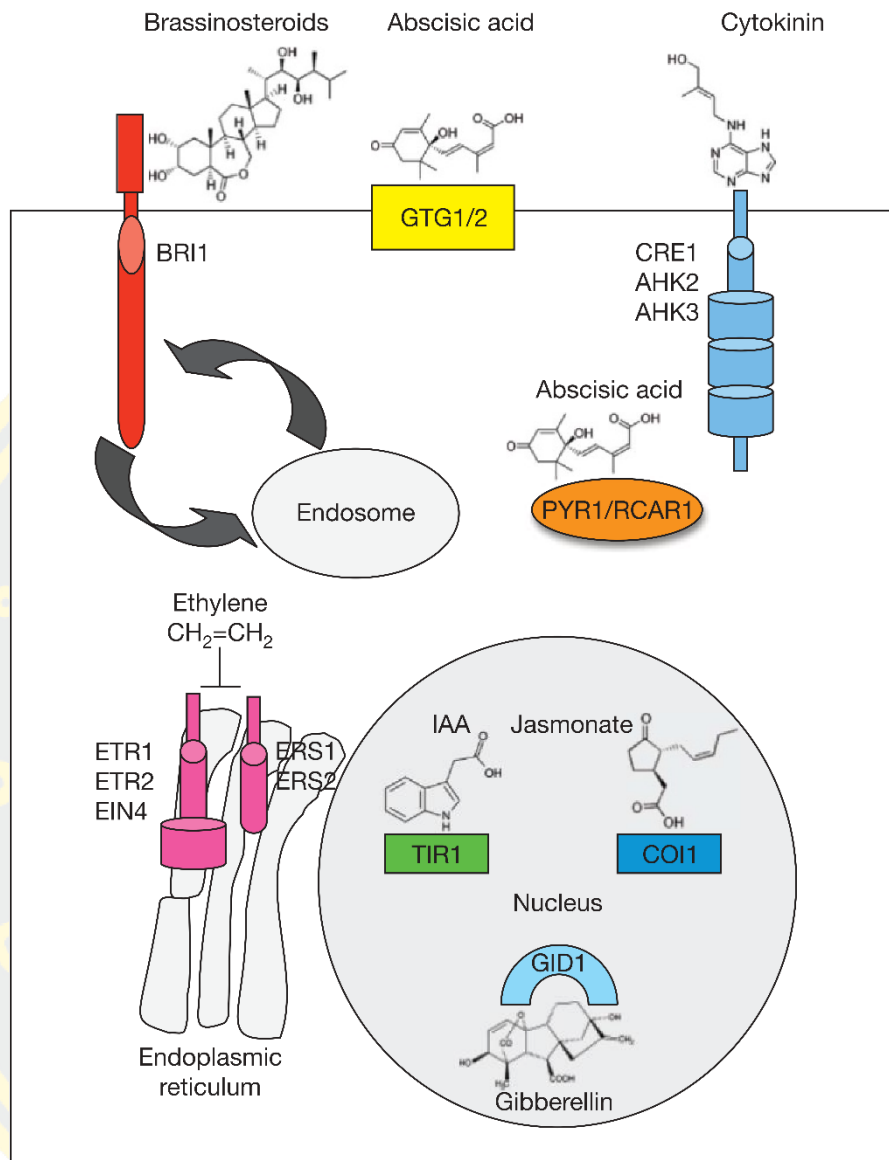


**Figure 2** Location of each plant hormone binding with their receptors. (reproduced from (Santner & Estelle, 2009)).

### 2.4.1 Indole-3-acetic acid (IAA)

IAA, also known as auxin, is a tryptophan-like essential plant hormone (Figure 3A), which plays a major role in plant growth and regulation (X. Han, Zeng, Bartocci, Fantozzi, & Yan, 2018). IAA is essential for plant growth and regulation, and could help stimulate stem elongation, cell division, root growth, ethylene production, and fruit development (Cox, Brandl, de Moraes, Gunasekera, & Teplitski, 2018). It is the first plant hormone that was identified and synthesized in chloroplasts. It can be generated from tryptophan *via* either indole-3-acetamide (IAM) or indole-3-pyruvic acid (IPA) pathway (Duca, Lorv, Patten, Rose, & Glick, 2014; Spaepen & Vanderleyden). In the IAM pathway (Figure 3B), tryptophan is first converted into IAM by tryptophan monooxygenase and then to IAA by IAM hydrolase. In other ways, IAM can also be generated from the enzymatic cascade of oxidoreductase, acetaldoxime dehydratase, and nitrile hydratase reactions to convert tryptophan into indole-3-acetaldoxime (IAOx), IAOx into indole-3-acetonitrile (IAN), and IAN into IAM, respectively. While in the IPA pathway (Figure 3C), the amino transferase catalyzes the conversion of tryptophan into IPA, which is further converted into indole-3-acetaldehyde (IAAld) and IAA, respectively, by decarboxylase and aldehyde dehydrogenase, respectively (Duca et al., 2014; Spaepen & Vanderleyden).

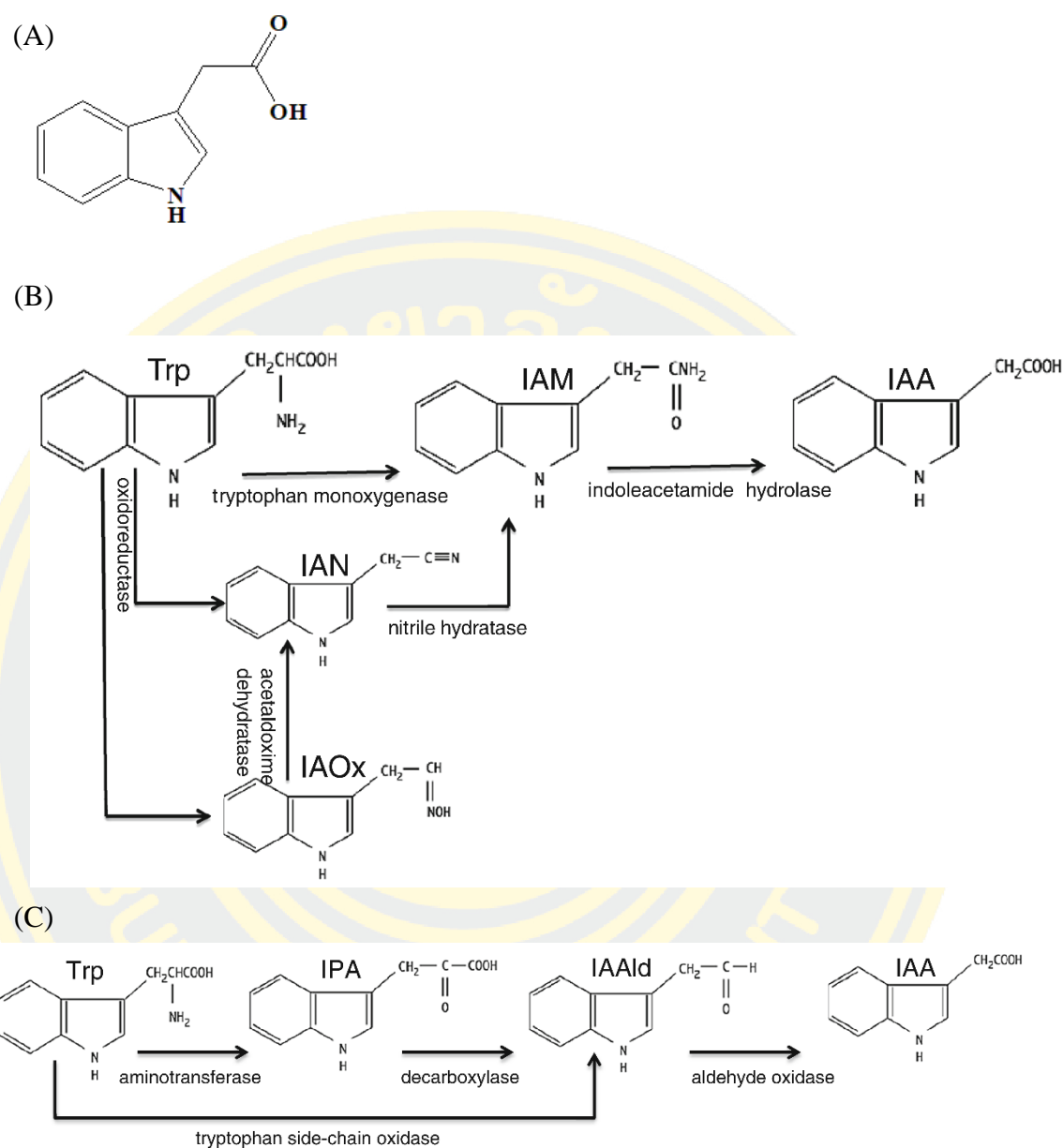


**Figure 3** Structure and biosynthetic pathways of indole-3-acetic acid (IAA). (A) The chemical structure of IAA. The biosynthetic pathway of IAA via (B) indole-3-acetamide (IAM) and (C) indole-3-pyruvic acid (IPA). (reproduced from (X. Han et al., 2018)).



Auxin is generated and dispersed throughout the plant *via* a complex cell-to-cell transport system. It is accumulated at the primordium of leaves to initiate the shoot of apical meristem. The direction of auxin transport is determined by the asymmetric localization of transport proteins residing within cells. The auxin/indole-3-acetic acid (Aux/IAA) proteins and the auxin response factors (ARFs) are the transcription factors that regulate the transcription of auxin-responsive genes and their functions are depended on the cellular level of auxin. At low levels of auxin (Figure 4, panel a), the Aux/IAA proteins bind to the DNA bound ARFs and then recruit a co-repressor TOPLESS (TPL) to form the protein complexes that repress the transcription of auxin-responsive genes. When auxin is present at high levels, it binds to the protein complex SCF (Skp, Cullin, F-box containing complex, a multi-protein E3 ubiquitin ligase complex) (Figure 4, panel b) and enhances the binding affinity of the protein complex SCF and Aux/IAs, thus promoting ubiquitination and degradation of Aux/IAs. This allows the transcription of auxin-responsive genes, which occurs through the transcriptional activation by the DNA bound ARFs (Chapman & Estelle, 2009; H. Han, Zhang, & Sun, 2009; Santner, Calderon-Villalobos, & Estelle, 2009).

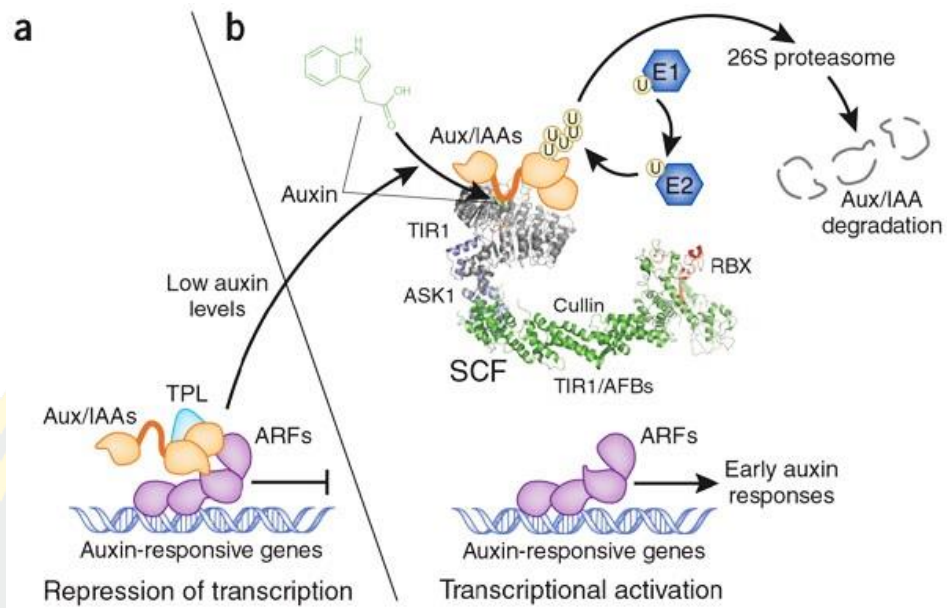


**Figure 4** The transcription of auxin-responsive genes regulated by protein/transcription factors upon the cellular levels of auxin. (reproduced from (Santner et al., 2009)).

### 2.4.2 Abscisic acid (ABA)

ABA is a plant hormone in which its chemical structure possesses the cyclohexenone moiety (Figure 5A). It can be synthesized *via* the multi-step enzymatic conversion of zeaxanthin, a type of carotenoids, through cascade intermediates (Figure 5B) (Ma et al., 2018). ABA plays a role in the inhibition of seed germination and budding. It also functions in embryo maturation, floral induction, cell division, elongation, and response to biotic and abiotic stresses. The ABA content in plants could be increased dramatically under stressful environmental conditions, such as water shortages, high salinity, and temperature extremes, which stimulate the stress-tolerance responses, thus promoting plants adaptation to survive under these harsh conditions.

The molecular action of ABA to respond to environmental stresses occurs *via* the molecular interactions of several protein complexes (Figure 6). In brief, when plant cells face environmental stresses such as drought, cold, and salinity, the ABA content is increasingly accumulated. The accumulated ABA binds and activates the regulatory components of the ABA receptors, thus resulting in downstream signaling cascade to inhibit type 2C protein phosphatases (PP2Cs), which allows the Snf1-related protein kinases 2 (SnRK2s) activation through autophosphorylation. The active SnRK2s phosphorylate the ion channel proteins, SLAC1 and KAT1, which reside in guard cells to mediate the closure of the stomata in order to reduce water loss. The active SnRK2s also activate the other related proteins through phosphorylation, so as to arrest seed germination and mediate the expression of the responsive genes to produce the corresponding proteins that help stabilize the structure of plant cell membrane (Ng, Melcher, Teh, & Xu, 2014).

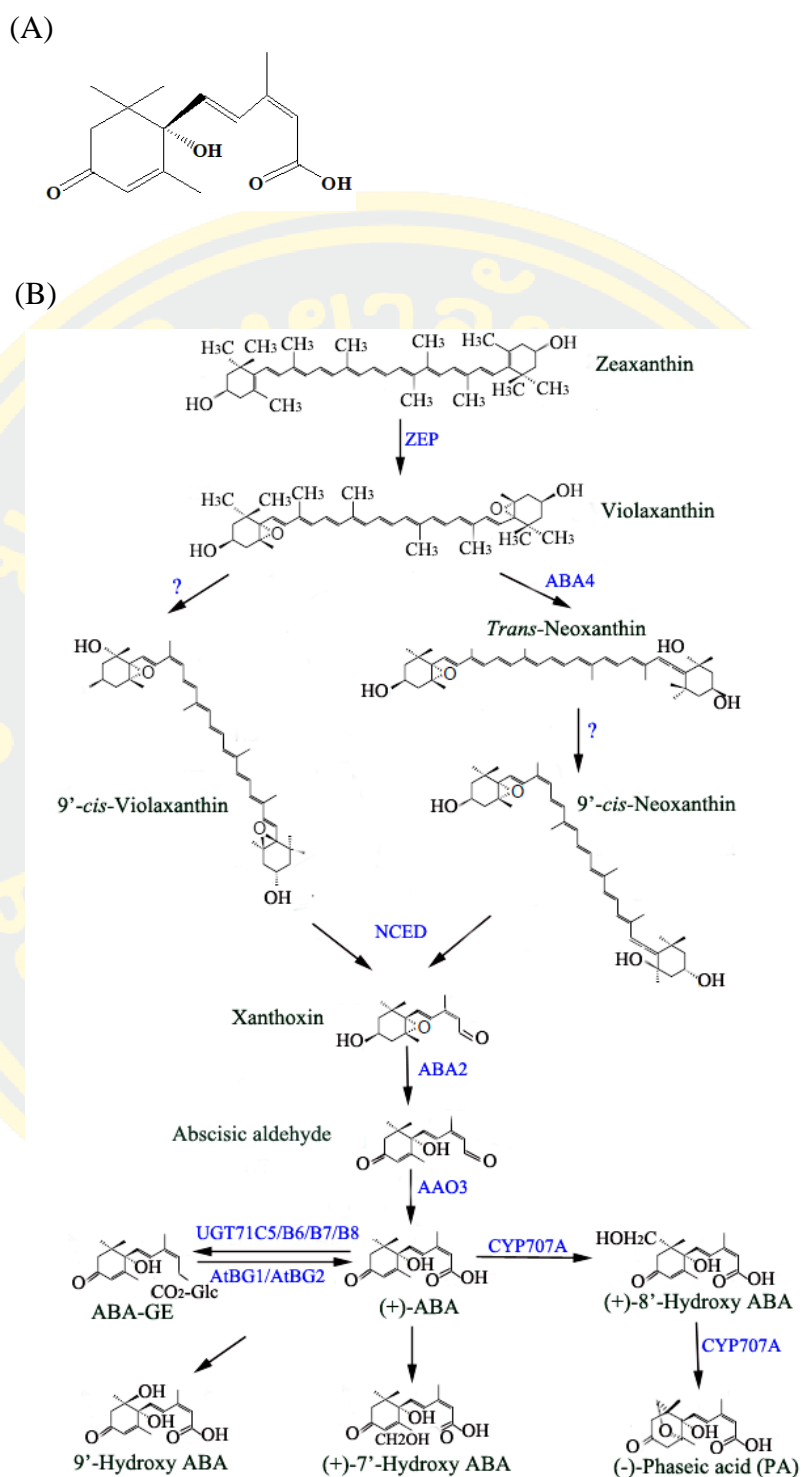


**Figure 5** Structure and biosynthetic pathways of abscisic acid (ABA). (A) The chemical structure of ABA. (B) The biosynthesis of ABA via multi-step enzymatic conversion of zeaxanthin. (reproduced and modified from (X. Han et al., 2018)).

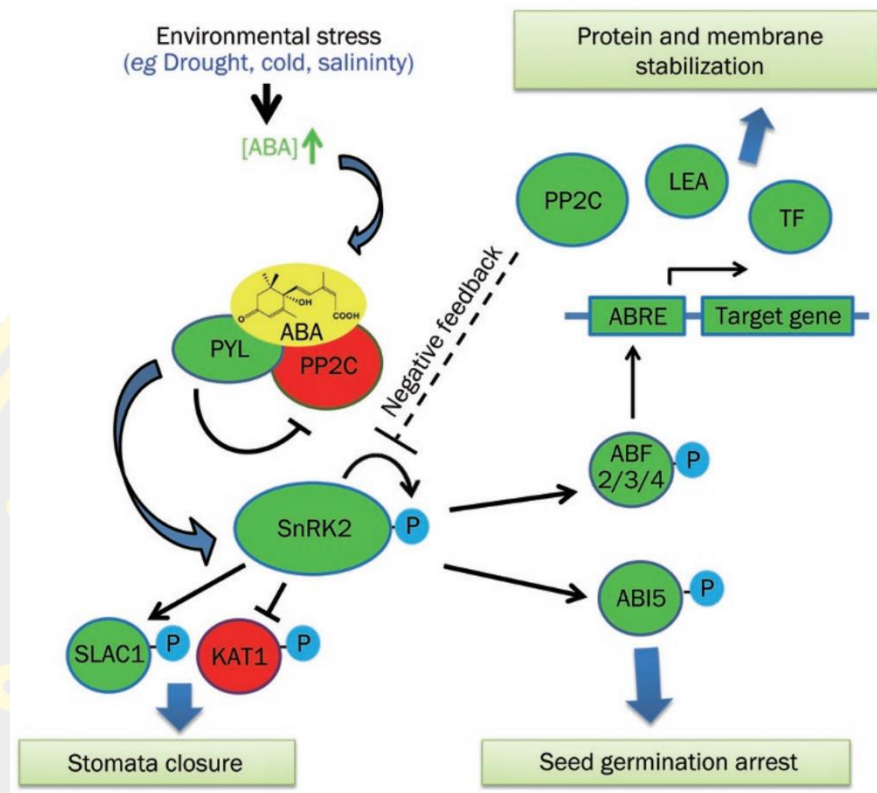


**Figure 6** Role of ABA in abiotic stress response via cascade phosphorylation process.  
(reproduced from (Ng et al., 2014)).

### 2.4.3 Gibberellic acid (GA)

Gibberellic acid (GA) is also known as gibberellin. It is a plant hormone that plays role in seed germination, stem elongation, and floral induction. The most active GA include GA<sub>1</sub>, GA<sub>3</sub>, GA<sub>4</sub>, GA<sub>5</sub>, GA<sub>6</sub>, and GA<sub>7</sub> (Figure 7) (X. Han et al., 2018). Among these GAs, the most common GA found in plants is GA<sub>3</sub> (Tian et al., 2017). GA<sub>3</sub> is not stable and can be transformed into different forms as shown in Figure 8 under aqueous solution at different pHs, temperatures, and reaction times (Camara et al., 2018). The biosynthesis of GA derivatives can occur through a multi-step enzymatic transformation of geranylgeranyl diphosphate (GGDP) (Camara et al., 2018). Other than regulating plant growth, GA also increases the activity of plant enzymes, such as  $\alpha$ -amylase, proteinase, ribonuclease,  $\beta$ -glucanase, and pentosanases, to promote plant development (Dilworth et al., 2017).

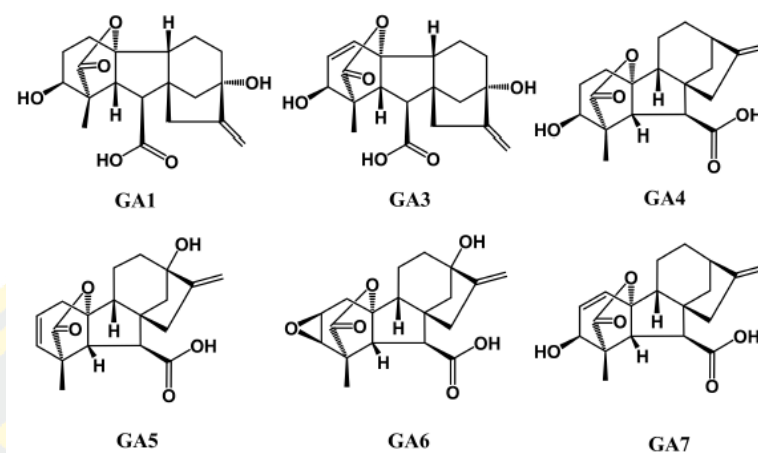


**Figure 7** Structure of gibberellic acid derivatives.  
(reproduced from (X. Han et al., 2018)).

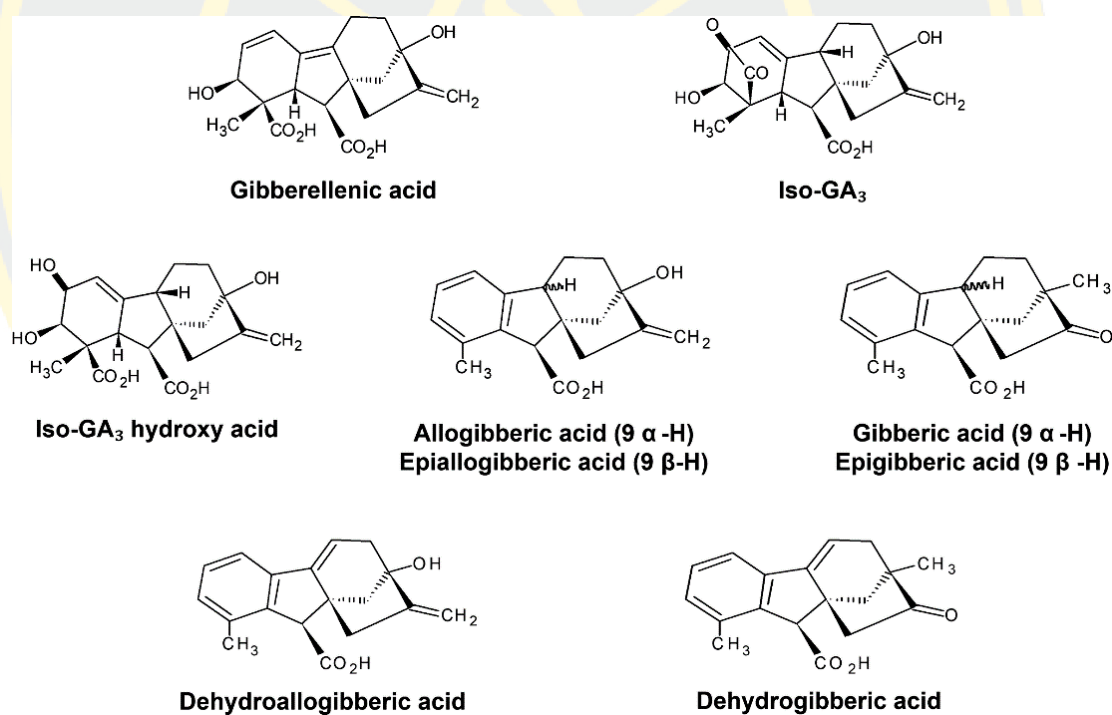


**Figure 8** Decomposition of GA<sub>3</sub> into different forms under aqueous solution at different pHs, temperatures or reaction times.  
(reproduced from (Camara et al., 2018)).

Similar to the Aux/IAA and ARF protein factors in response to auxin, the DELLA and PIF3/4 protein factors' responses to the GA concentration levels, which affect the expression of the GA-responsive genes (Figure 9). At low levels of GA, DELLA binds to transcription PIF3/4, causing no transcription of the GA-responsive genes. In contrast, at high levels of GA, the GA binds its receptor GID1 to form a complex, which can bind to DELLA. Similar to the response towards auxin, the binding complexes formed can recruit the protein complex SCF to bind and mediate the ubiquitination of DELLA, thus promotes the degradation of DELLA and allowing the transcription factor PIF3/4 activates the transcription of the GA-responsive genes to encode the corresponding functional proteins (Santner & Estelle, 2009).



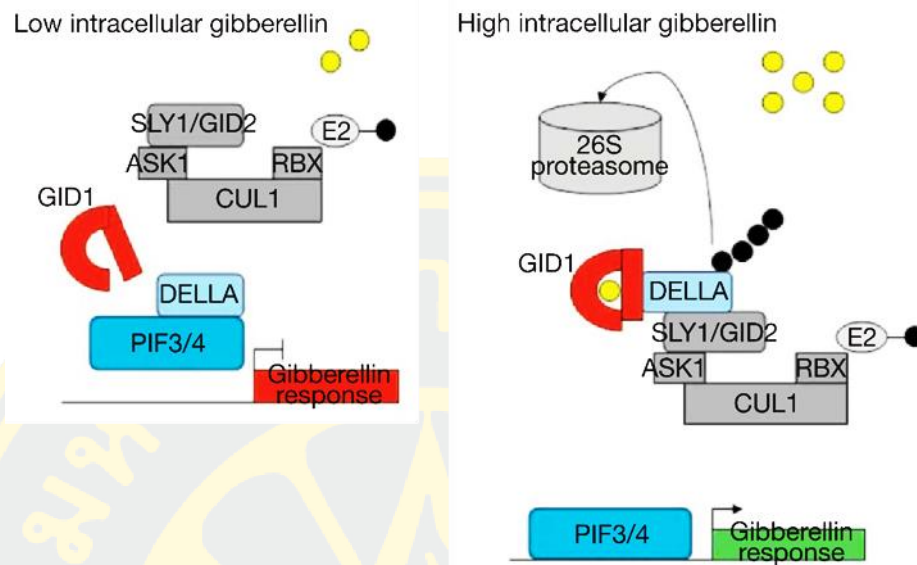


**Figure 9** The transcription of gibberellin-responsive genes regulated by protein/transcription factors upon the cellular levels of gibberellin. (Santner & Estelle, 2009).

#### 2.4.4 Cytokinin (CK)

CK is a plant hormone that possesses the adenine core structure, which can be diverse in different forms upon the modification by isoprene and aromatic groups at the C<sub>6</sub>-NH<sub>2</sub> moiety of the adenine core (Figure 10) (Sakakibara, 2005). Among CK derivatives, zeatin, which is a major form of CK, is found the most (Sakakibara, 2005). CK is found ubiquitously in root tips, the apical meristem region of the plant, and immature leaves and seeds. The major site of CK synthesis is found in root tips (Dilworth et al., 2017). Cytokinin functions to control cell proliferation, cell cycle progression, and cell and plastid development (Andrabi et al., 2018). The CK synthesis in higher plants is initiated by the conjugation of adenine nucleotide with dimethylallyl diphosphate (DMAPP) derived from mevalonate (MVA) and methylerythritol phosphate (MEP) pathways, which are catalyzed by adenosine phosphate-isopentenyltransferase (IPT) (Figure 11) and occurred through a multi-step enzymatic processes (Figure 12) (Yamaguchi et al., 2010).

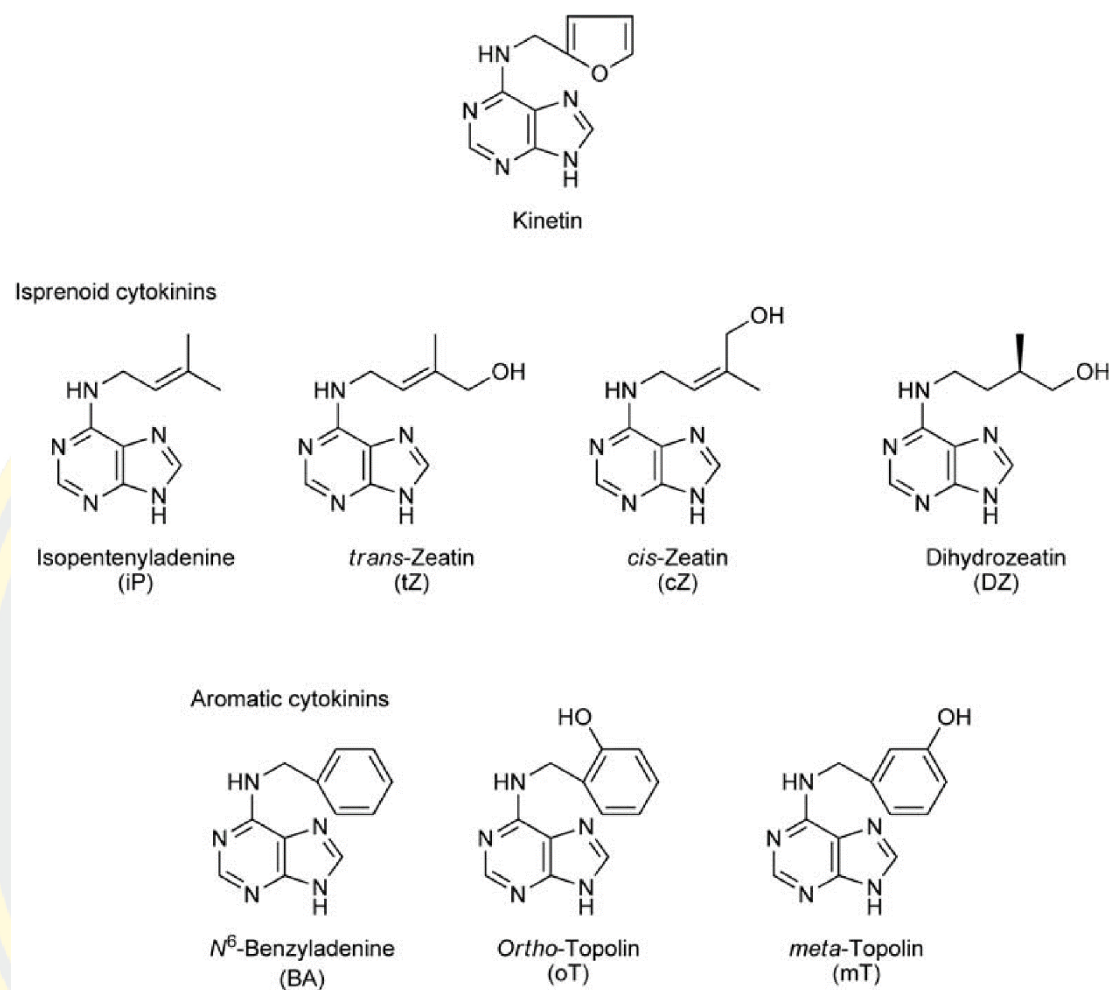


**Figure 10** The chemical structures of cytokinin derivatives (reproduced from (Dilworth et al., 2017)).

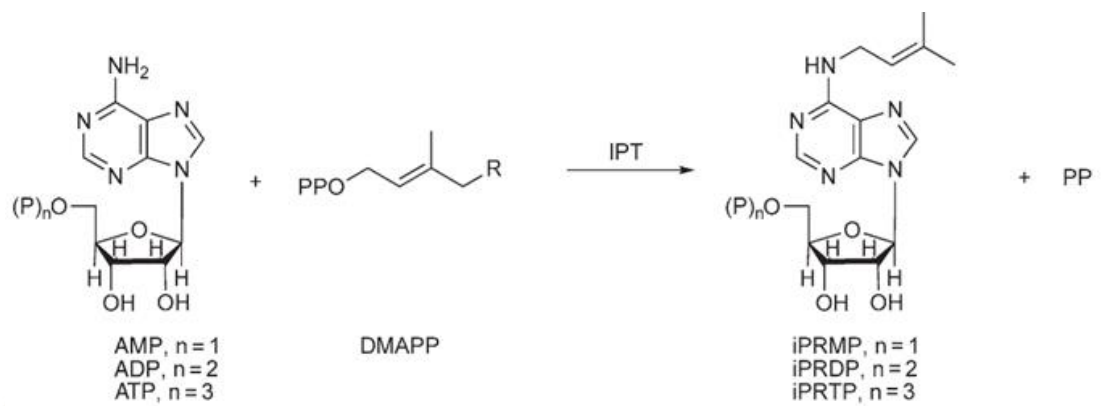


**Figure 11** The reaction of adenosine phosphate-isopentenyltransferase (IPT) that catalyzes the isopentane transfer to nucleotide, yielding the nucleotide-isopentene linkage, which is a CK precursor.

(reproduced from (Yamaguchi et al., 2010))

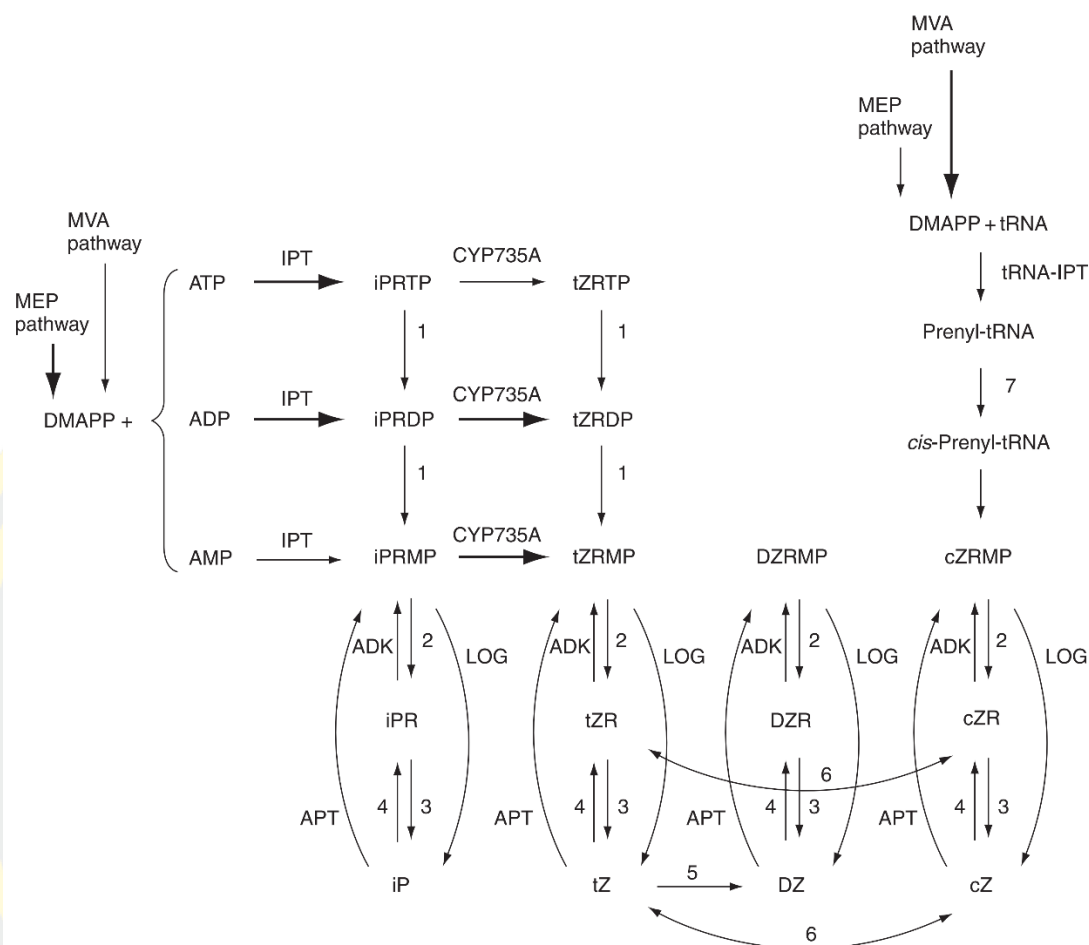


**Figure 12** The proposed model for biosynthesis of CK derivatives from DMAPP derived from MVA and MEP pathways in higher plants via multi-step enzymatic processes. Some key enzymes involved in biosynthesis such as adenosine phosphate-isopentenyltransferase (IPT) catalyzing the linkage of isopentene and nucleotide, cytochrome P450 mono monooxygenase (CYP735A) catalyzing the hydroxylation of isopentane moiety, and cytokinin riboside 5'-monophosphate phosphoribohydrolase (LOG) catalyzing the removal of the nucleotide moiety via hydrolysis process. (reproduced from (Yamaguchi et al., 2010))

CK mediates growth and development of plant cells through the regulatory networks of protein complexes inside the cell. CK does not directly enter plant cell, but it transduces the signals instead *via* the binding with its plasma membrane receptor connecting with the authentic histidine kinases (AHKs) that mediate the histidine phosphorylation of the protein complexes (Figure 13). The phosphoryl group is then transferred to a histidine phosphotransfer protein (HPt) catalyzed by authentic histidine phosphotransferases (AHPs). The phosphorylated HPt delocalizes into the nucleus and then transfer the phosphoryl group to the Type-B response regulators (RRs), thus promoting the transcription of the cytokinin-responsive genes (Gujjar & Supaibulwatana, 2019; Werner & Schmülling, 2009).

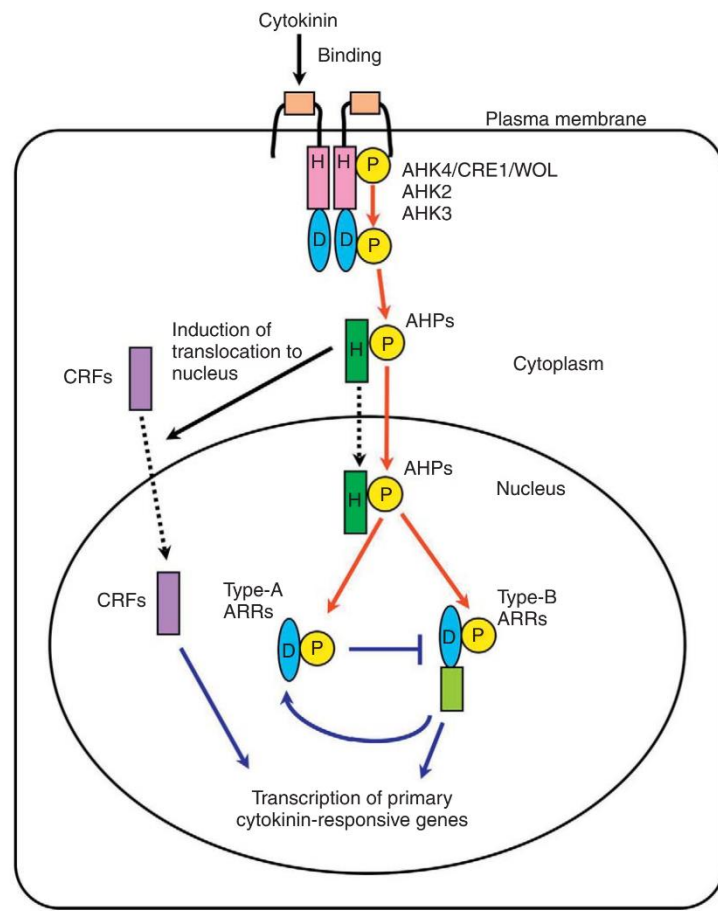
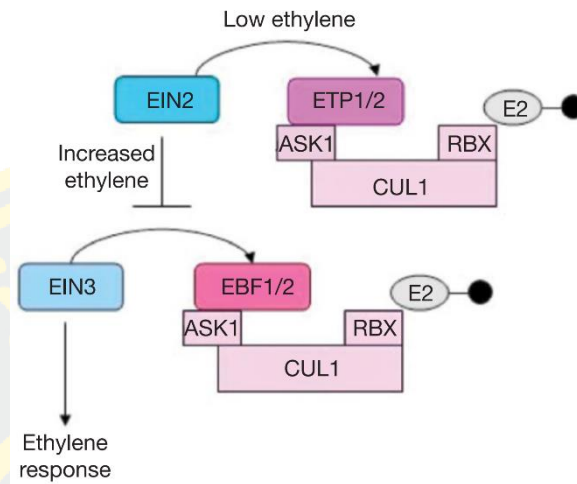


**Figure 13** The CK molecular action by signaling transduction *via* the phosphotransfer process.  
(reproduced from (Yamaguchi et al., 2010).

#### 2.4.5 Ethylene (ET)

ET is a small gaseous plant hormone with simple chemical constituents ( $\text{CH}_2=\text{CH}_2$ ). It functions to accelerate fruit maturing processes and inhibits stem elongation. Moreover, it also boosts cell growth/expansion and regulates the stages of flower formation and sex expression. Ethylene gas can be synthesized from auxin mediated by red light. The production rate of ethylene could be dependent on the concentration of IAA. In agricultural industries, ethylene is usually used to accelerate the ripening of post-harvested fruits (Dilworth et al., 2017). The mode of action of ET occurs within plant cells through binding with its receptors located in endoplasmic reticulum (Figure 2) and is dependent on the regulated protein turnovers and ET concentrations (Figure 14). When ET is low, the level of the SCF protein complex is high, which can promote the degradation of the transcriptional regulators EIN2 and EIN3, resulting in no activation of transcription of ET-responsive genes. While at a high concentration of ET, the level of the SCF protein complex is decreased, thereby increasing the EIN2 level. The accumulated EIN2 can inhibit the degradation of EIN3, thus allowing EIN3 to activate the transcription process (Santner & Estelle, 2009).

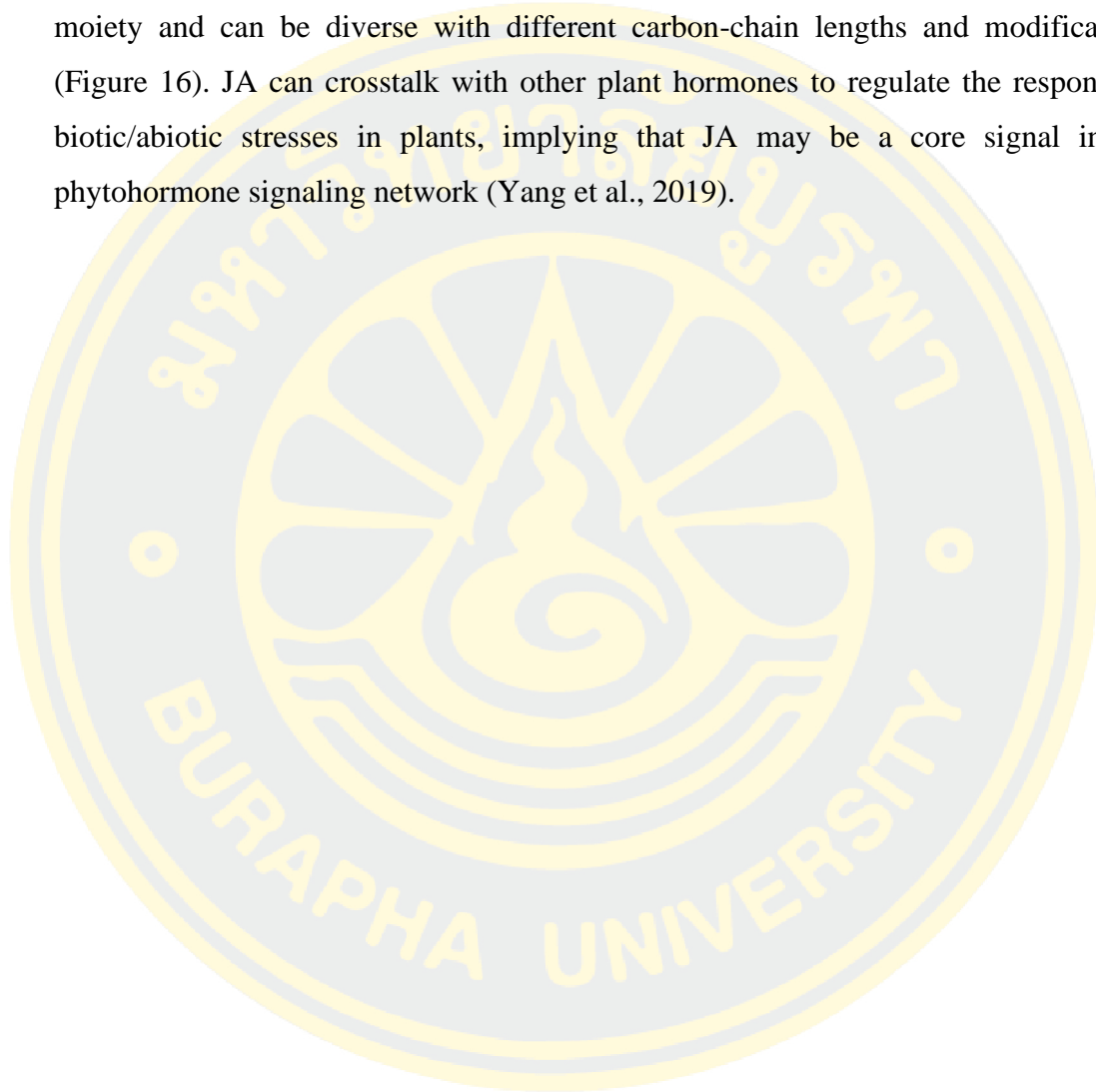


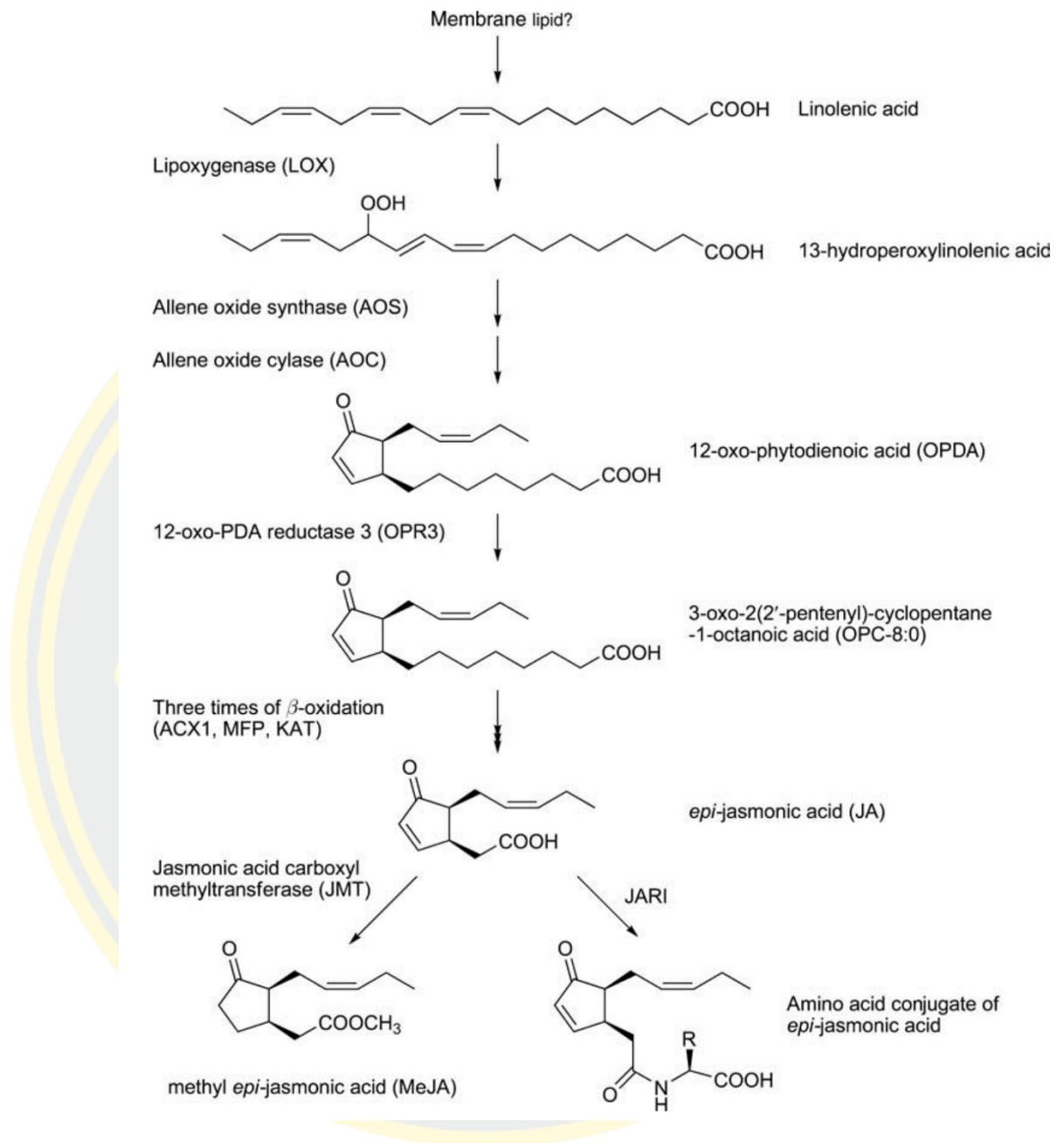


**Figure 14** The mode of action of ET towards transcription of ET-responsive genes through the regulated protein turnovers and ET concentrations. (reproduced from (Santner & Estelle, 2009).

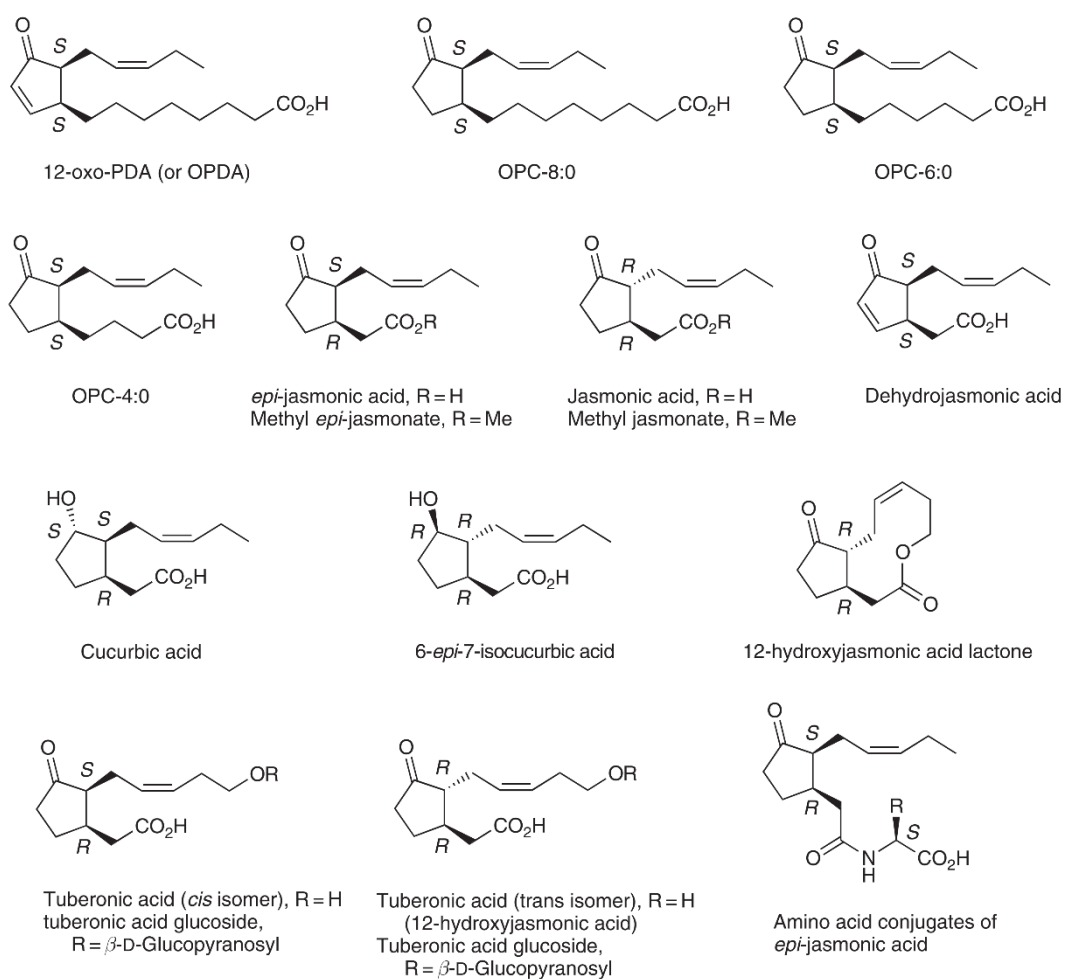
#### **2.4.6 Jasmonic acid (JA)**

JA is an amphiphilic molecule which is derived from linolenic acid and endogenous growth-regulating substances found in higher plants (Figure 15) (Geilfus, 2019). Its chemical structure also contains the cyclopentanone/cyclopentenone ring moiety and can be diverse with different carbon-chain lengths and modifications (Figure 16). JA can crosstalk with other plant hormones to regulate the response to biotic/abiotic stresses in plants, implying that JA may be a core signal in the phytohormone signaling network (Yang et al., 2019).



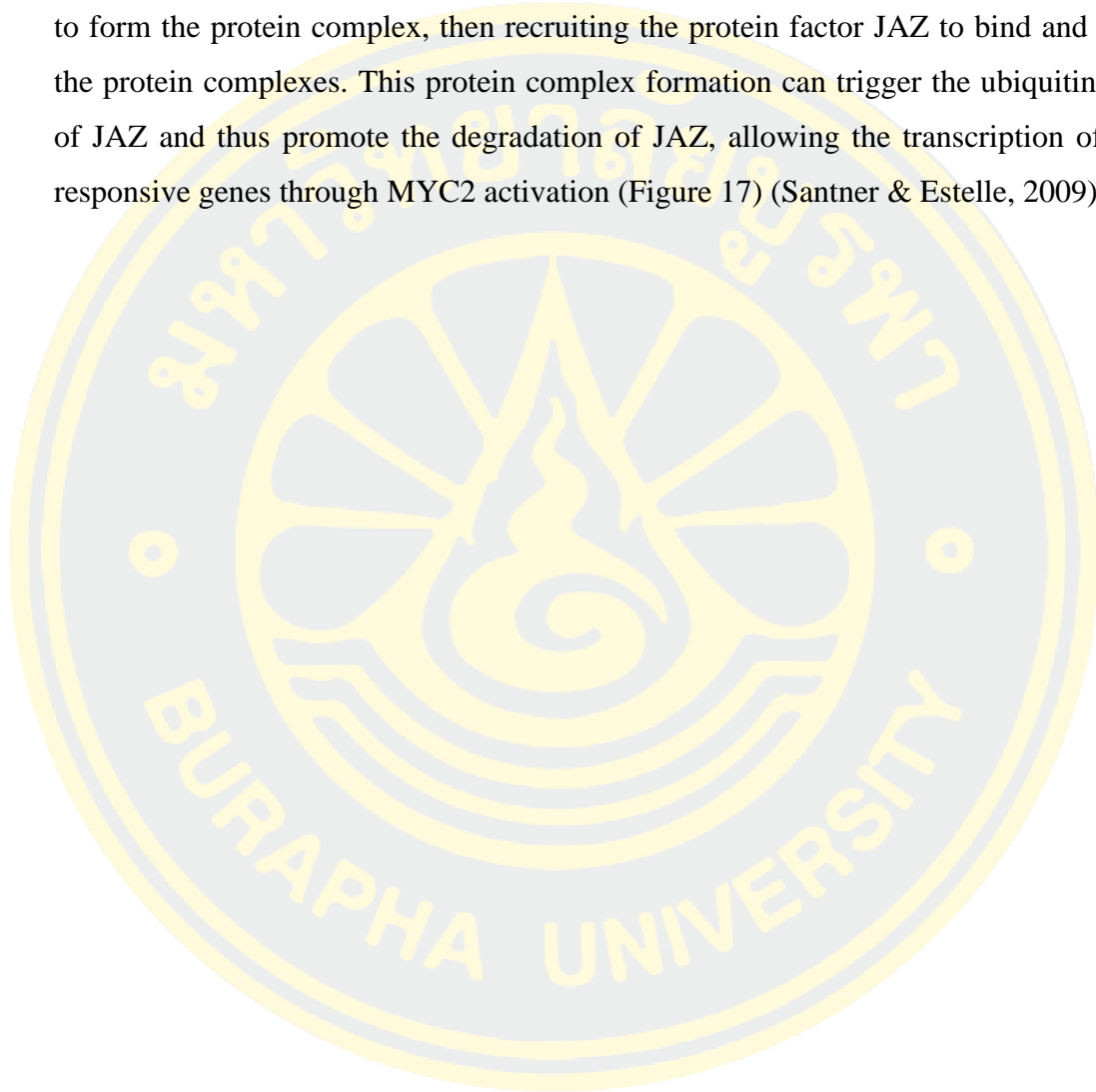


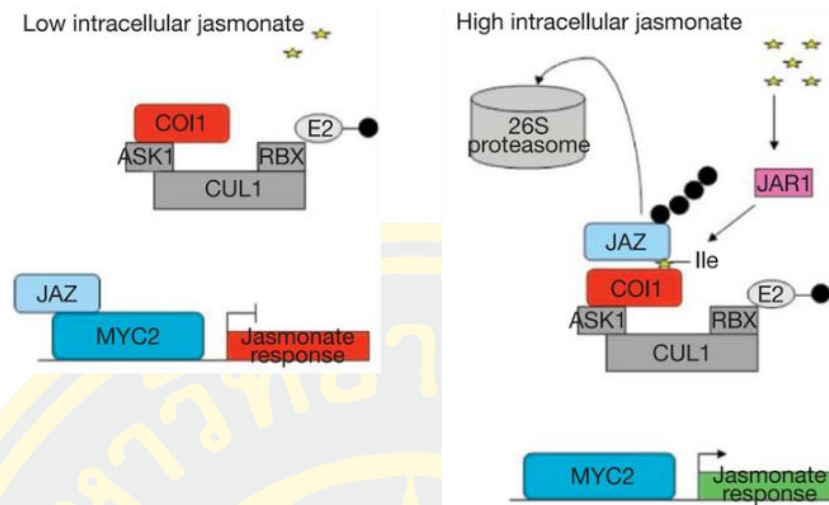
**Figure 15** The biosynthetic pathway of JA derivatives.  
(reproduced from (Yamaguchi et al., 2010)).



**Figure 16** The chemical structures of JA derivatives.  
(reproduced from (Geilfus, 2019; Yamaguchi et al., 2010)).

Similar to the response to hormones IAA and GA, the response of plant towards JA is concentration dependent. At low levels of JA, the protein factor JAZ binds to the transcriptional factor MYC2, thus inactivating the transcription of JA-responsive genes. In contrast, at high levels of JA, the protein factor COI1 binds to JA to form the protein complex, then recruiting the protein factor JAZ to bind and form the protein complexes. This protein complex formation can trigger the ubiquitination of JAZ and thus promote the degradation of JAZ, allowing the transcription of JA-responsive genes through MYC2 activation (Figure 17) (Santner & Estelle, 2009).

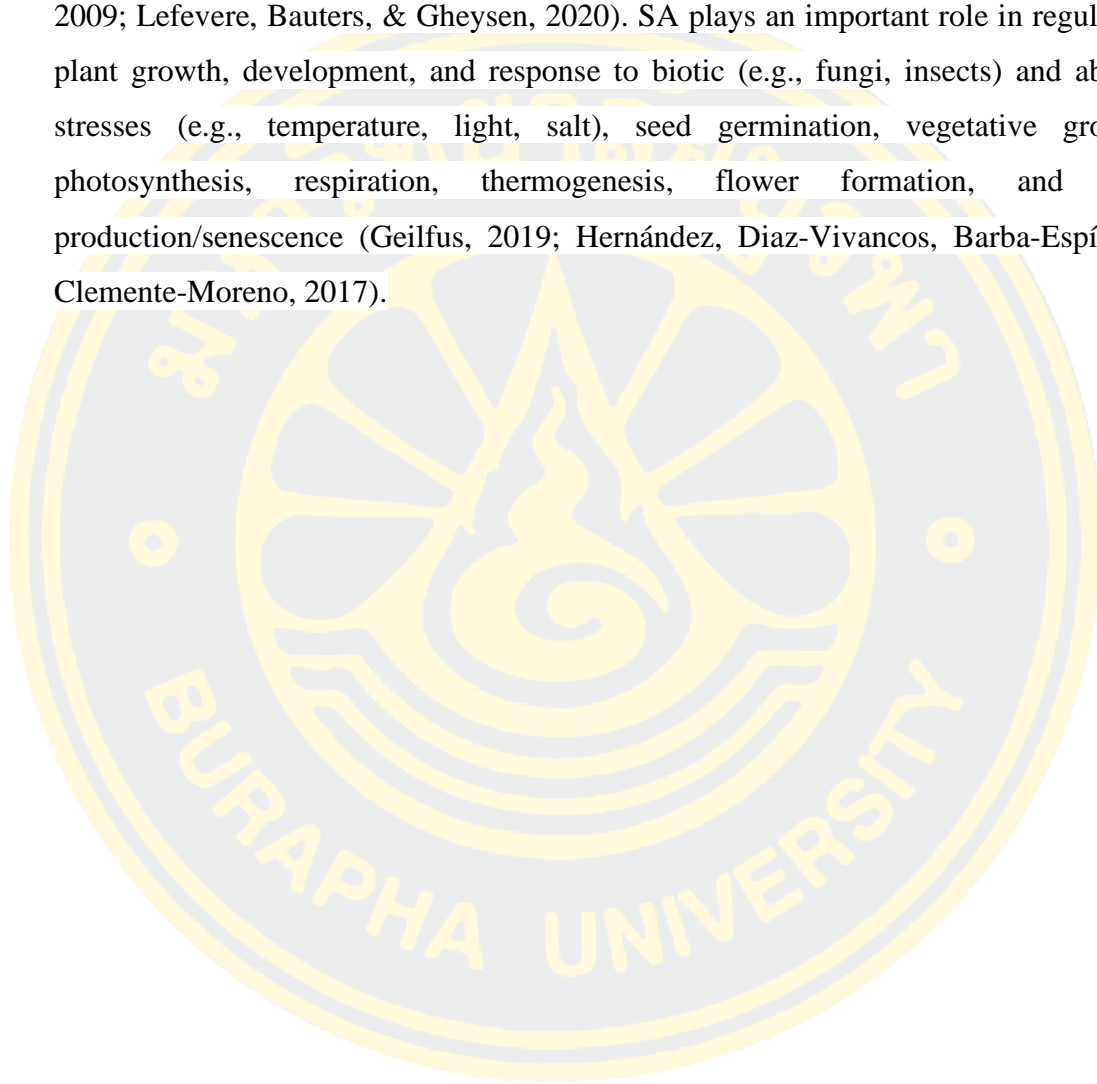


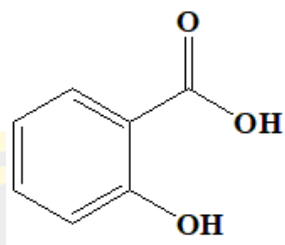


**Figure 17** The transcription of JA-responsive genes regulated by protein/transcription factors upon the cellular levels of JA. (reproduced from (Santner & Estelle, 2009))

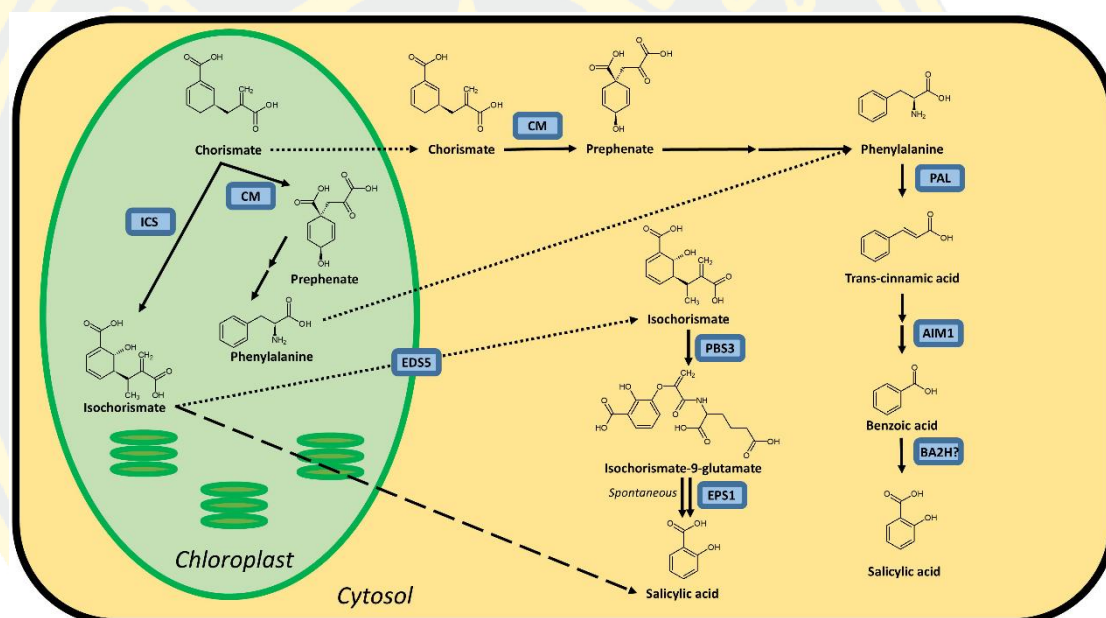
#### **2.4.7 Salicylic acid (SA)**

SA is a phenolic acid-derived plant hormone (Figure 18), which is majorly synthesized from chorismate-derived phenylalanine by phenylalanine ammonia lyase (PAL) and other cascade enzymes (Figure 19) (Chen, Zheng, Huang, Lai, & Fan, 2009; Lefevere, Bauters, & Gheysen, 2020). SA plays an important role in regulating plant growth, development, and response to biotic (e.g., fungi, insects) and abiotic stresses (e.g., temperature, light, salt), seed germination, vegetative growth, photosynthesis, respiration, thermogenesis, flower formation, and seed production/senescence (Geilfus, 2019; Hernández, Diaz-Vivancos, Barba-Espín, & Clemente-Moreno, 2017).





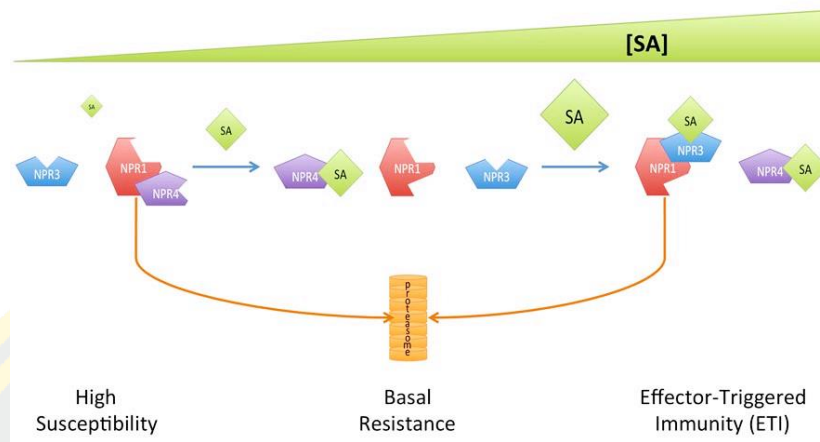
**Figure 18** Structure of salicylic acid (SA).  
(reproduced from (Geilfus, 2019)).



**Figure 19** Biosynthetic pathway of SA from chorismite-derived phenylalanine.  
(reproduced from (Lefevere et al., 2020)).



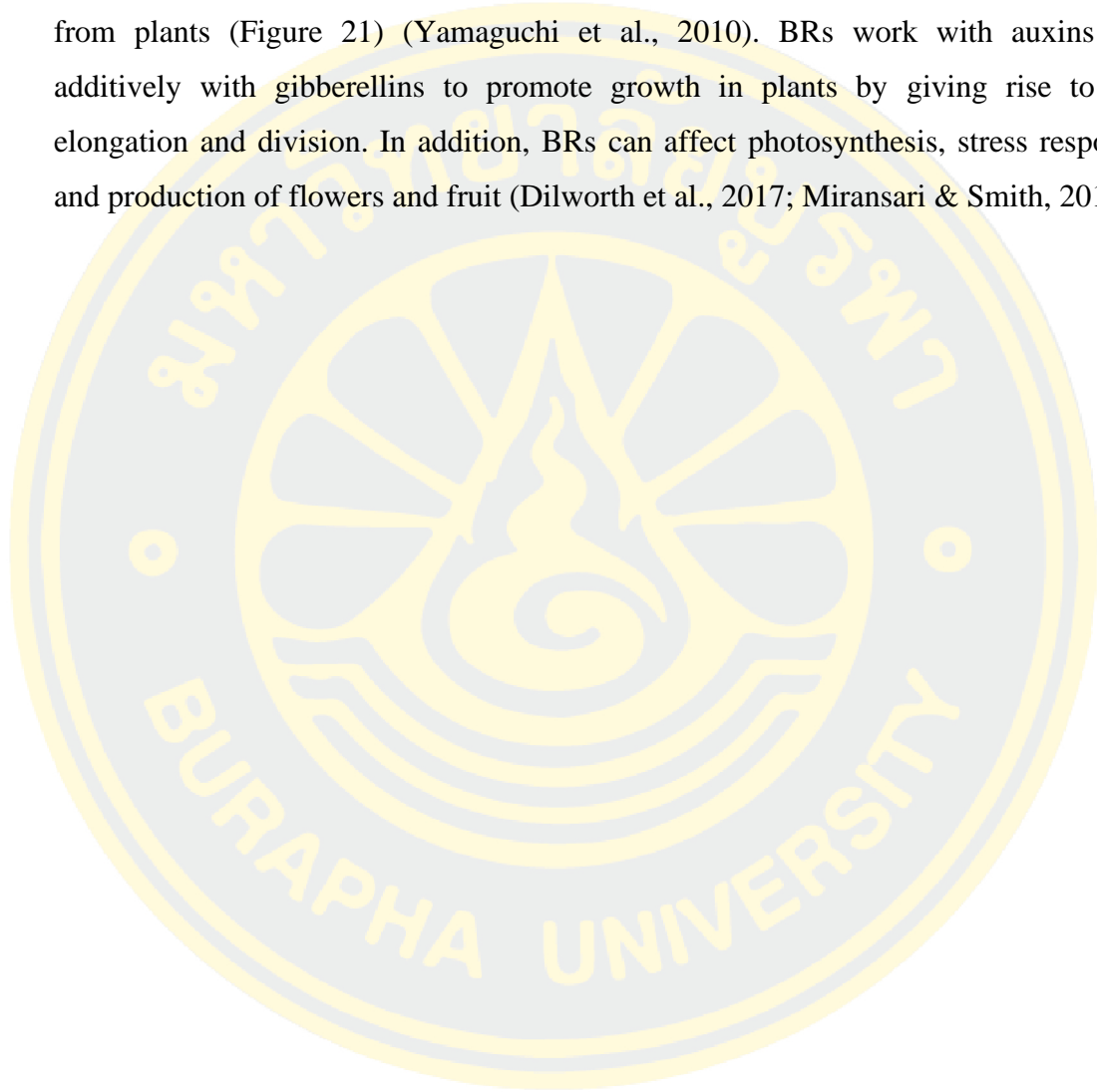
SA is well-known for its significant roles in plant-defense response, including basal resistance, effector triggered immunity (ETI, alternatively called as resistance gene-mediated resistance), and systemic acquired resistance (SAR). The mode of action of SA in response to plant-pathogen interactions could involve the binding interactions with the non-expressor of pathogenesis-related (NPR) transcription co-activators (the protein factors involved in inducing the transcription of the defense gene), such as NPR1, NPR3, and NPR4 (Moreau, Tian, & Klessig, 2012). The different levels of SA could affect the binding interactions between SA and NPR transcription co-activators and the consequent plant-defense response. At low SA levels, NPR1 binds to NPR4 to form a binding complex that is targeted for degradation in proteasomes. Plant cells are highly susceptible to pathogen infection. But when SA is gradually increased after pathogen infection, SA could interrupt the NPR1-NPR4 binding complex to form the SA-NPR4 binding complex instead, thereby liberating NPR1 which can now activate the transcription of the defense gene. Under this SA levels, plant cells possess the basal resistance towards the pathogen infection. If the SA levels are present at very high concentrations, the binding complex of SA and NPR4 occurs with the concomitant formation of the binding complex of SA and NPR3. The binding complex of SA-NPR3 could promote its interaction with NPR1 to form a ternary complex of SA-NPR3-NPR1, thus leading to NPR1 degradation in the proteasome. With this SA condition, plant cells possess the effector-triggered immunity to tackle the pathogen infection (Figure 20) (Kumar, 2014; Moreau et al., 2012; Pieterse & Van Loon, 1999).

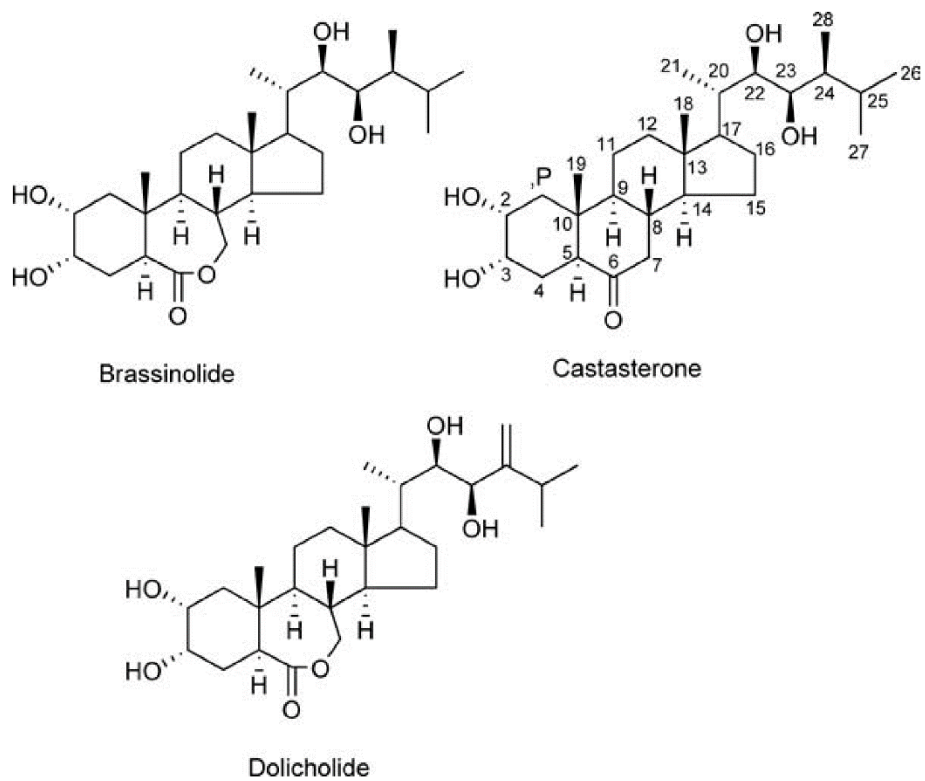


**Figure 20** Different levels of SA in binding with the NPR transcription co-activators in response to pathogen infection. (reproduced from (Moreau et al., 2012)).

#### **2.4.8 Brassinosteroids (BRs)**

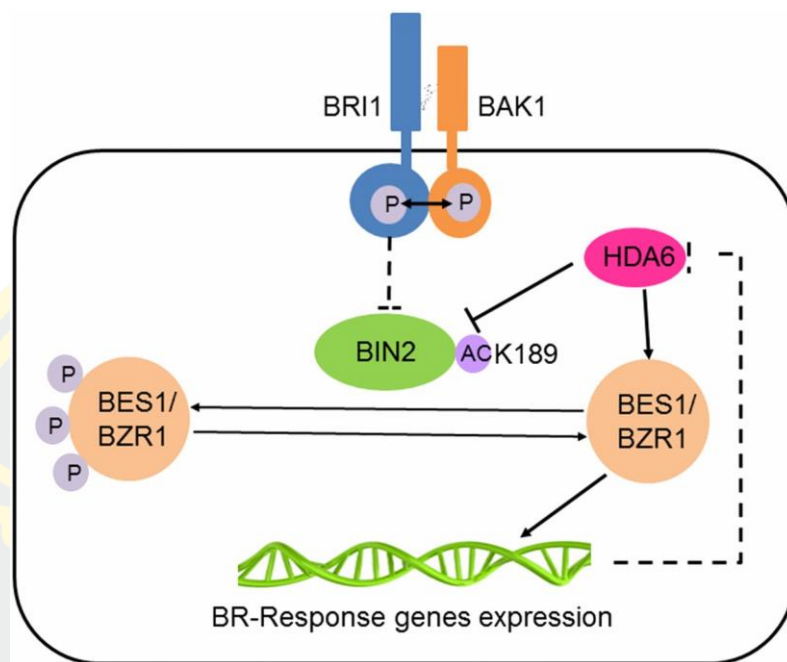
BRs are lipophilic, naturally occurring polyhydroxy steroidal hormones in which three BRs, including brassinolide, castasterone, and dolicholide, were isolated from plants (Figure 21) (Yamaguchi et al., 2010). BRs work with auxins and additively with gibberellins to promote growth in plants by giving rise to cell elongation and division. In addition, BRs can affect photosynthesis, stress response, and production of flowers and fruit (Dilworth et al., 2017; Miransari & Smith, 2014).





**Figure 21** The chemical structures of three BRs isolated in plants. (reproduced from (Yamaguchi et al., 2010)).

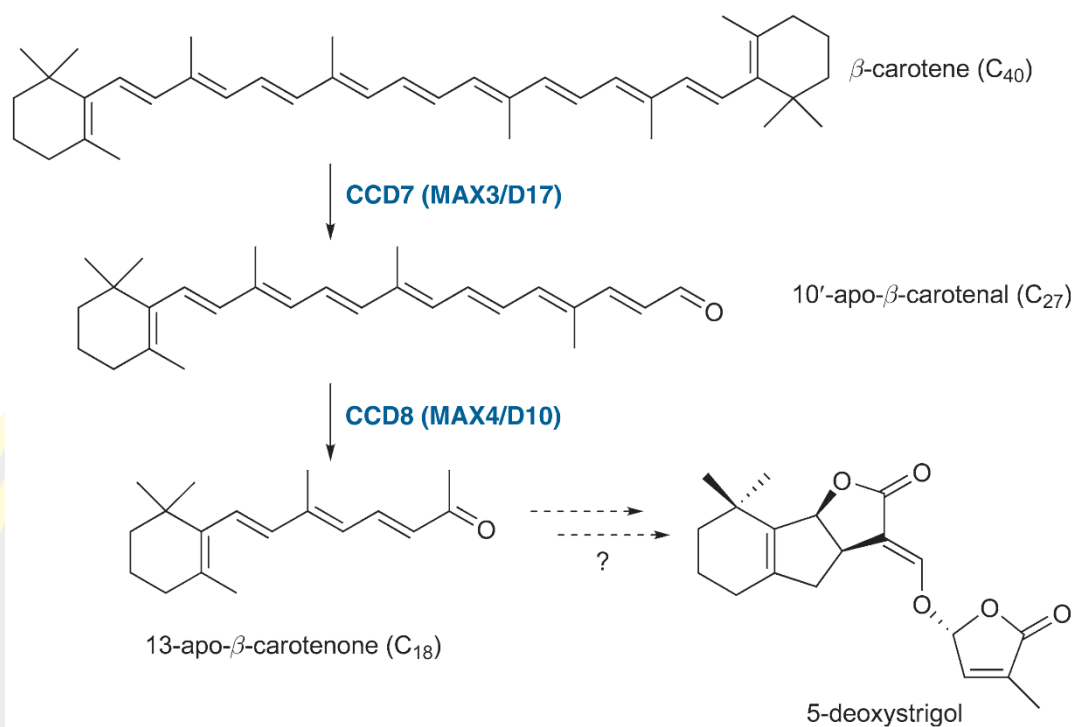
The mode of action of BRs in the regulation of the BRs-responsive gene expression occurs through the BR signaling pathway as BRs could not enter the plant cells, but they bind to their receptors located on the plant cell membrane instead (Figure 2). Upstream BR signaling is controlled by phosphorylation/dephosphorylation and acetylation/deacetylation of the key negative regulator BR-INSENSITIVE 2 (BIN2). The phosphorylated and acetylated forms of BIN2 has higher activity to phosphorylate the downstream transcription factors (BES1 and BZR1) to inhibit BR signaling. To allow BR signaling to occur, the histone deacetylase HDA6 catalyzes the removal of the acetyl moiety on the Lys189 site of BIN2, thereby inhibiting BIN2 activity and hence promoting BR signaling to activate the expression of BR-responsive genes (Figure 22) (Hao, Wang, Qiao, Leng, & Wang, 2016).



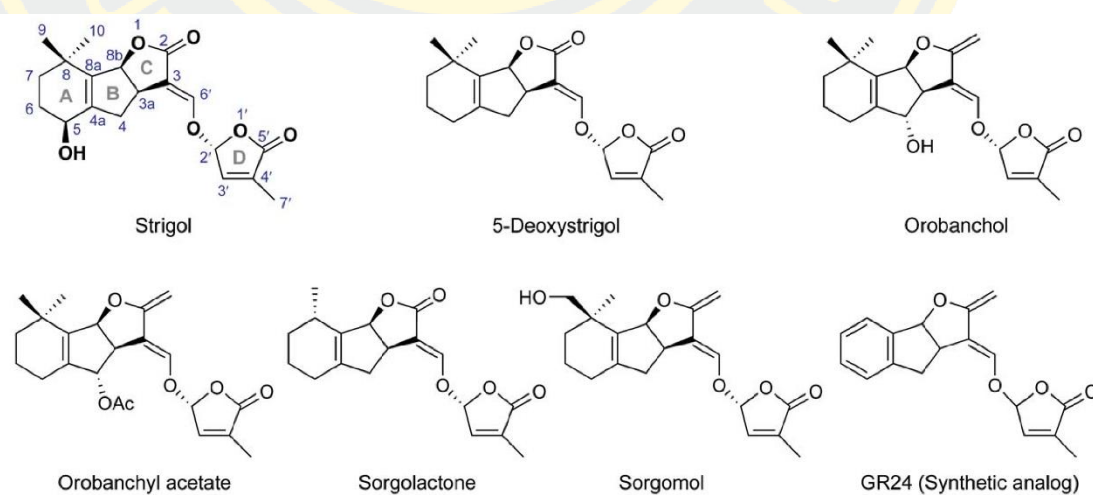
**Figure 22** The BR signaling pathway controlled by phosphorylation/dephosphorylation and acetylation/deacetylation of the key negative regulator BR-INSENSITIVE 2 (BIN2).  
(reproduced from (Hao et al., 2016)).

#### **2.4.9 Strigolactones (SLs)**

SLs are carotenoid-derived plant terpenes (Figure 23) which function in the rhizosphere and in plant (Yoneyama, Xie, Yoneyama, & Takeuchi, 2009). SLs contain a terpenoid lactone carrying a unique four-ring structure. Several strigol-related compounds, including 5-deoxystrigol, orobanchol, orobanchyl acetate, sorgolactone, sorgomol, and GR24 (Figure 24), have been identified as germination stimulants of parasite seeds in root secreted substances of various plant species (Dilworth et al., 2017; Yamaguchi et al., 2010). SLs serve as endogenous hormones involved in the control of plant development and as components of root secreted substances which promote symbiotic interactions between plants and soil microbes (Dilworth et al., 2017; Yamaguchi et al., 2010).



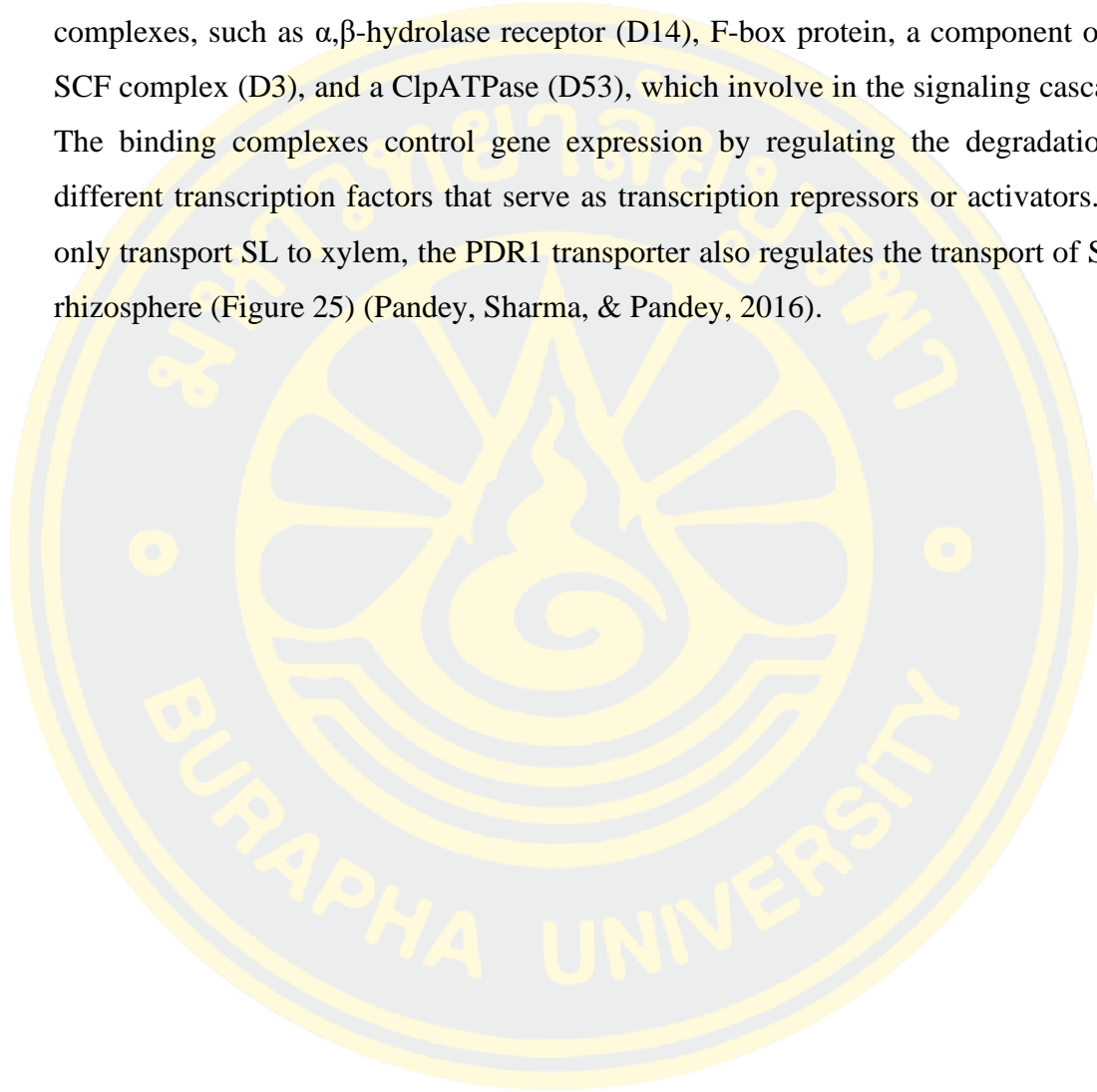
**Figure 23** The possible pathway to synthesize SL via oxidative cleavage of  $\beta$ -carotene catalyzed by carotenoid-cleavage dioxygenases, CCD7 and CCD8. (reproduced from (Santner & Estelle, 2009)).



**Figure 24** Structure of SL derivatives. (reproduced from (Yamaguchi et al., 2010)).



The mode of action of SL in response to plant stress and development occurs through the binding of SL (produced within plant cells and transported to the xylem *via* PDR1 membrane-bound transporter) with the membrane-bound protein receptor complexes, such as  $\alpha$ , $\beta$ -hydrolase receptor (D14), F-box protein, a component of the SCF complex (D3), and a ClpATPase (D53), which involve in the signaling cascades. The binding complexes control gene expression by regulating the degradation of different transcription factors that serve as transcription repressors or activators. Not only transport SL to xylem, the PDR1 transporter also regulates the transport of SL to rhizosphere (Figure 25) (Pandey, Sharma, & Pandey, 2016).



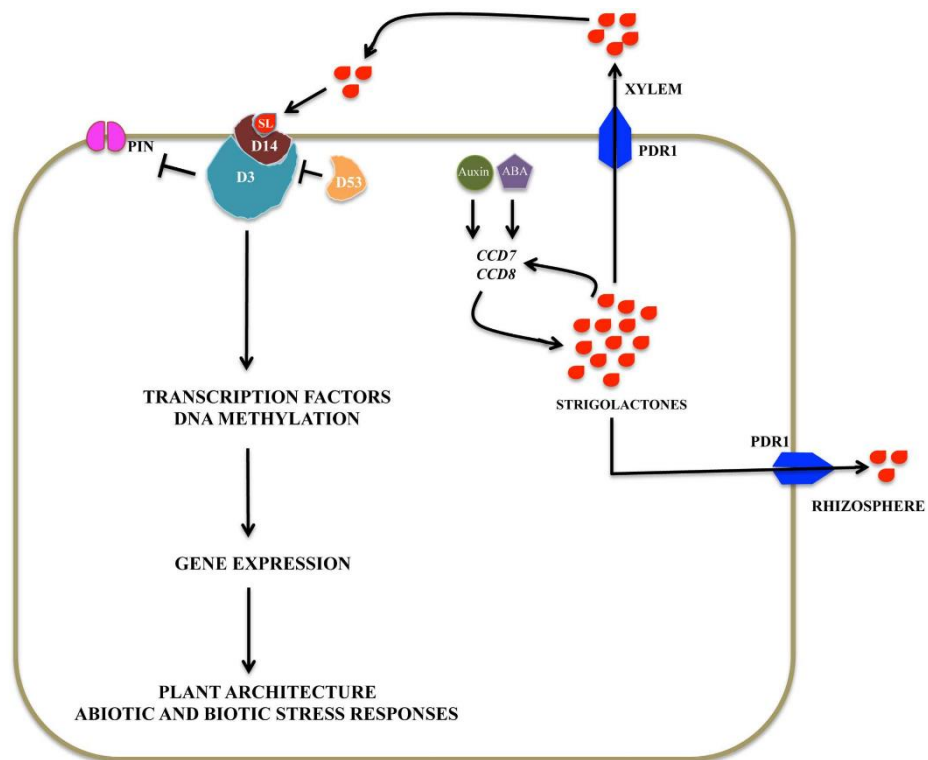


**Figure 25** The SL signaling pathway to regulate the expression of the SL-responsive genes to response plant stress and development. (reproduced from (Pandey et al., 2016)).

In recent years, seven plant hormones, including IAA, SA, ABA, JA, GA<sub>3</sub>, *trans*-zeatin (t-Z), and *trans*-zeatin riboside (t-ZR), have been successfully detected by LC-MS/MS under well optimized conditions (H.-x. WANG, WANG, WANG, & DING, 2020). To achieve good analysis, the study showed that a scan mode, either negative or positive, is necessarily fine-tuned for each hormone and depends on individual chemical properties. In addition, the fragmentor voltage (FV) and collision energy (CE) are also indispensably adjusted to gain the highest abundant intensity of product ions (Table 2). The full scan of precursor ions of authentic hormone in a mixture solution showed that GA<sub>3</sub>, ABA, JA, and SA were detected in a negative ion mode (Figure 26), while t-Z, t-ZR, and IAA had high abundance in a positive ion mode (Figure 27).

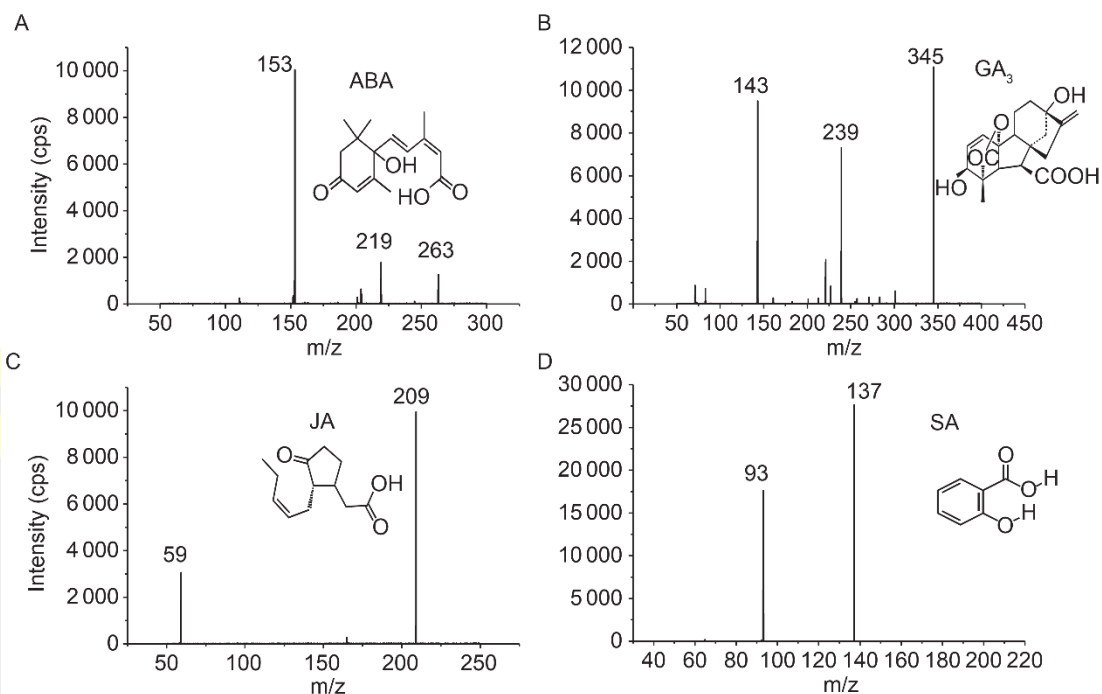


**Figure 26** Fragmentation patterns of authentic compounds, ABA (A), GA<sub>3</sub> (B), JA (C), and SA (D), analyzed in a negative mode of LC-MS/MS. (reproduced from (H.-x. WANG et al., 2020)).

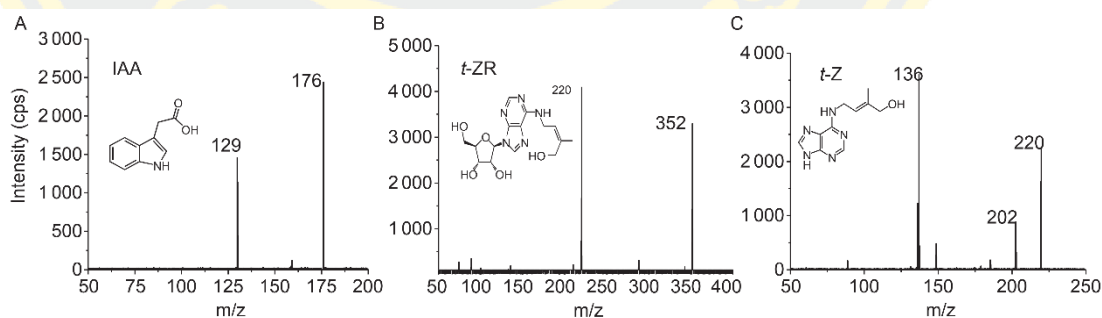


**Figure 27** Fragmentation patterns of authentic compounds, IAA (A), t-ZR (B), and t-Z (C), analyzed in a positive mode of LC-MS/MS. (reproduced from (H.-x. WANG et al., 2020)).

**Table 2** The established parameters for quantitative analysis of plant hormones by LC-MS/MS.

<b>Plant hormone</b>	<b>Scan mode</b>	<b>Precursor ion (m/z)</b>	<b>Product ion (m/z)</b>	<b>Fragmentor voltage (V)</b>	<b>Collision Energy (eV)</b>
t-Z	+	352	220	110	15
t-ZR	+	220	136	92	15
IAA	+	176	130	68	12
GA <sub>3</sub>	–	345	143	120	25
ABA	–	263	153	85	5
JA	–	209	59	60	10
SA	–	137	93	65	15

Data from (H.-x. WANG et al., 2020).

## 2.5 Other compounds involving in plant growth/development

In this section, other compounds that are not categorized as plant hormones (such as pipercolic acid, 5-aminolevulinic acid, L-ornithine, and 2,3-butanediol) but involve in plant growth/development, have also been described in brief below.

### 2.5.1 Pipercolic acid (Pip)

Pip is a non-protein amino acid (Figure 28), which can be biosynthesized *via* lysine catabolism. Accumulation of Pip in plant depends on bacterial pathogen infection and relates to systemic acquired resistance (SAR), a defense system against bacteria pathogens in plants. Pip can increase the level of free radicals including nitric oxide (NO), reactive oxygen species (ROS), and glycerol-3-phosphate (G3P), thus rendering plants more resistant to bacterial pathogen infection (Hartmann et al., 2017; C. Wang et al., 2018).

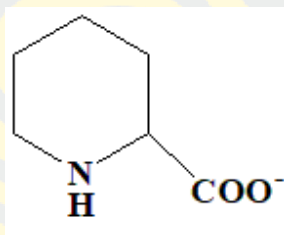


**Figure 28** The chemical structure of Pip (reproduced from (Servillo et al., 2012)).

Plants and animals have evolved immune systems to defend themselves against infections because they live in an environment that is potentially hazardous microorganisms. Local activation of immunity in plants typically leads to SAR to recurrent pathogen infections in distal tissues. Several mutations causing SAR deficiency have been found in genes responsible for producing Pip from lysine. One previously found that Pip-induced SAR is dependent on a functioning flavin-dependent monooxygenase 1 (FMO1) gene, whose mutation has no effect on Pip accumulation during infection. The hydroxylation of Pip to N-hydroxypipelic acid (NHP), the downstream metabolic SAR mediator, is carried out by FMO1. Local pathogen infection in plants causes SAR in distal tissues, which protects against future pathogen infections. A three-step biochemical mechanism produces NHP after infection: The Lys aminotransferase ALD1 transforms L-Lys to 2,3-dehydropipelic acid (2,3-DP), which is then reduced to Pip by the reductase SARD4. The monooxygenase FMO1 then N-hydroxylates Pip to produce NHP. Another essential regulator of SAR is the plant hormone SA, which inhibits the negative conversion of Pip to NHP (Figure 29) (Shan & He, 2018).

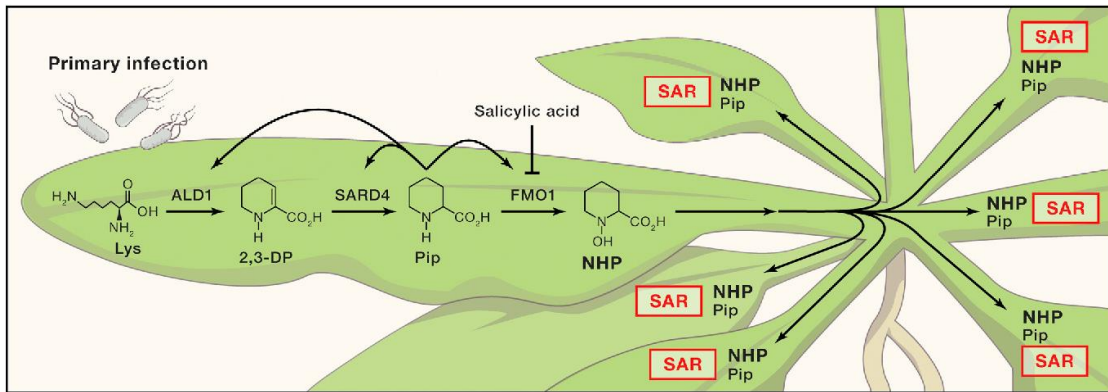


**Figure 29** The biosynthesis of Pip in response to pathogen infection. (reproduced from (Shan & He, 2018)).



### 2.5.2 5-Aminolevulinic acid (ALA)

ALA is a non-protein amino acid (Figure 30), which is an essential growth regulator in higher plants. It is primarily responsible for enhancing photosynthesis, decreasing the effects of abiotic stresses, and enhancing plant biomass and fruit quality under normal growth conditions in higher plants, such as rice, strawberry and peach. In roots, ALA functions to relieve damage caused by water stress by promoting the increased activities of lactate dehydrogenase (LDH) and alcohol dehydrogenase (ADH). In addition, ALA can also act as a precursor in the biosynthesis pathway of all tetrapyrroles, such as chlorophyll, heme, and siroheme (Y. Wu et al., 2018; Y. Wu, Liao, Dawuda, Hu, & Yu, 2019). ALA can be formed during the AD process by the photosynthetic bacterium *Rhodobacter sphaeroides* and serves as an herbicide (Sasaki et al., 1990).

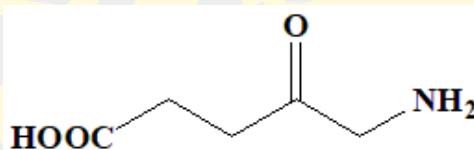


**Figure 30** The chemical structure of ALA.  
(reproduced from (Kanto et al., 2013)).

### 2.5.3 L-Ornithine (Orn)

Orn is a polyamine compound (Figure 31) that is mainly derived from L-glutamate in plants. It is an intermediate found in arginine biosynthesis. It was found that L-ornithine can increase tolerance towards drought in sugar beet plants (Hussein et al., 2019; Shargool, Jain, & McKay, 1988). Its derivative, *N*<sup>δ</sup>-acetylornithine, which was identified as a jasmonic acid-induced metabolite in *Arabidopsis* and plays a role in plant defense system (Adio et al., 2011).

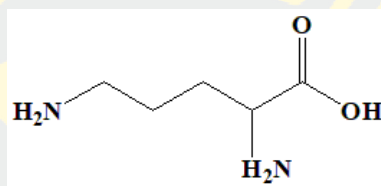


**Figure 31** The chemical structure of Orn.

(reproduced from (LoGiudice, Le, Abuan, Leizorek, & Roberts, 2018)).

#### 2.5.4 2,3-Butanediol (2,3-BD)

2,3-BD is the volatile compound that gives rise to the induced systemic resistance in plants (Yi et al., 2016). 2,3-BD can be produced by certain strains of root-associated bacteria (rhizobacteria), including *Paenibacillus polymyxa*, multiple *Klebsiella* species, *Bacillus licheniformis*, and *Bacillus amyloliquefaciens* (Park et al., 2018). 2,3-BD with different specific stereoisomers, (+)-2*S*,3*S*; (-)-2*R*,3*R* and meso-2,3 (Figure 32), can also be produced by acetoin biotransformation in *Aspergillus foetidus*, *Penicillium citrinum*, *Saccharomyces carlbergensis*, *Pichia fermentans*, and *Rhodotrula glutinis* (Javidnia, Faghih-Mirzaei, Miri, Attaroshan, & Zomorodian, 2016). 2,3-BD can induce SAR in the plant immune response *via* ROS homeostasis and pathogenesis-related (PR) gene expression. It could effectively enhance SAR by down-regulating the ROS gene and concomitant with up-regulating the ROS detoxification and PR protein expression (Park et al., 2018).

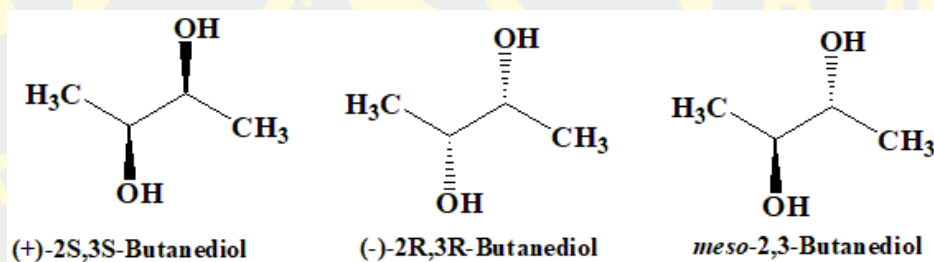


**Figure 32** The chemical structure of 2,3-BD with difference specific stereoisomer. (reproduced from (Javidnia et al., 2016))

## **2.6 Bioactive compounds detected in the biogas digestate liquid derived from the anaerobic digestion system**

Some previous reports have demonstrated that some plant hormones, such as GA<sub>3</sub>, IAA, and ABA can be detected in the biogas digestate liquid (BDL) derived from the anaerobic co-digestion systems (Li et al., 2016; Scaglia, Pognani, & Adani, 2015; Scaglia et al., 2017). In the separate anaerobic digestion of three animal manure feedstocks from chicken, dairy, and pig, the lab-scale results showed that three plant hormones, GA<sub>3</sub>, IAA, and ABA, can be quantitatively detected by HPLC-UV technique and their concentrations were 16, 22, and 35 mg/L, respectively, higher than the original manure (Li et al., 2016). It was found that these three plant hormones in BDL were sensitive differently towards different temperatures, 4, 20, and 37 °C (Li et al., 2016). At 4 °C, GA<sub>3</sub> and ABA were rather stable at about 100% for 88 days, while IAA was gradually decreased and remained only about 75%. At 20 °C, it was found that ABA was slightly decreased about 5% for 88 days, while IAA was decreased about 50% for 88 days. In contrast, GA<sub>3</sub> was sharply decreased about 75% after 20 days. While at 37 °C, GA<sub>3</sub> drastically decreased by about 75% after about 10 days. IAA and ABA remained at about 20% and 80% for 88 days. These indicated that GA<sub>3</sub> is much sensitive to high temperatures than IAA and ABA (Li et al., 2016).

The analysis of the dissolved organic matters in a digestate form (DOM<sub>d</sub>) derived from anaerobic co-digestion of pig slurry and pruning-garden waste mixture showed that only the auxin-like compounds were found in DOM<sub>d</sub> detected by GC/MS technique. DOM<sub>d</sub> can exhibit auxin-like properties in promoting the hypocotyl and root lengths of germinated cucumber seed. It was hypothesized that the presence of auxin-like compounds could result from the anaerobic digestion of aromatic amino acids that provide the auxin-like active molecules (Scaglia et al., 2015). The other anaerobic co-digestion of pig slurry and different types of wastes (e.g. biomass, municipal and food industry wastes), also showed that DOMs obtained from different anaerobic co-digestion systems provide different concentrations of auxin-active forms, IAA and hydroxyphenylacetic acid, and auxin-like molecules, fatty acids, amino acids, and carboxylic acids, as detected by GC/MS technique (Scaglia et al., 2017).

In addition, bioactive digestate compounds, such as amino acids (L-arginine, L-ornithine, L-cysteine, and L-aspartate), hormones (L-adrenaline, 19-hydroxy androstenedione, and estrone), alkaloids (tryptamine and N-methyltyramine), and vitamin B5, were detected in various types of manures and digestates. After the AD of pig manure, the levels of alkaloids, such as tryptamine, serotonin, and IAA, increased. Similarly, by the AD of chicken manure, the concentration of alkaloids, such as tryptamine, N-methyltyramine, and serotonin, can be enhanced (Lu et al., 2019).

Table 3 summarizes the quantitative amounts of bioactive compounds, such as GA<sub>3</sub>, IAA, ABA, and TAA (total amino acid) in anaerobic digestates. The IAA level of digestates is higher than that of the original feedstock. Chicken manure (collected directly from the liquid outlet of the digester) had the highest GA concentration in digestates. The IAA and TAA contents of chicken manure (concentrated liquid digestate) was rather greater than that of cattle manure and pig manure. Pig manure (collected directly from the liquid outlet of the digester) had a higher average ABA content than cattle manure and chicken manure (S. Wu & Dong, 2020).

**Table 3** Bioactive substances in anaerobic digestates.

Feedstock	GA <sub>3</sub> (mg/l)	IAA (mg/l)	ABA (mg/l)	TAA (mg/l)
Chicken manure <sup>a</sup>	44.83 ± 1.68	36.84 ± 0.23	13.23 ± 9.15	-
Pig manure <sup>a</sup>	16.37 ± 2.16	21.17 ± 2.02	35.59 ± 3.42	-
Cattle manure <sup>a</sup>	38.53 ± 1.40	17.38 ± 2.31	23.53 ± 2.27	-
Chicken manure <sup>b</sup>	-	27,900	-	4,940

Data from (S. Wu & Dong, 2020). <sup>a</sup>The sample was collected directly from the liquid outlet of the digester. <sup>b</sup>The sample was present as the concentrated liquid digestate.

Furthermore, the presence of bioactive and antimicrobial compounds formed during anaerobic digestion, it has been shown to reduce pathogenic fungus growth when slurry is applied to land. The bioactive chemicals found in BDL include 1,2-benzenedicarboxylic acid, butyl 2-methylpropyl ester (54.9%), and 9-octadecenamide (*Z*)-(2.51%) were detected in the EA extract, as well as tetrahydro-2-furanmethanamine (1.32%), cyclic octatomic sulfur (1.17%), squalene (4.06%), and cholestan3-ol (9.06%) were detected in the DM extract. All were conducted using GC/MS. Bioactive substances were extracted using ultrasound-assisted extraction with three solvents: ethyl acetate (EA), dichloromethane (DM), and *n*-butanol (NB). The EA extract inhibited *Fusarium oxysporum* by about 84%. The digestate with a dilution to 15, 20, or 25% could reduce growth of *Rhizoctonia solani* by over 70% in only 24h. The presence of numerous bioactive components in digested slurry suggests that, in addition to its action as an organic fertilizer, it may also contribute to the control of phytopathogens when applied to land (Lu et al., 2020).

## 2.7 Hydroponic assay

In order to assess the capability of BDL samples promote plant growth/development, the bioassay is being performed using the plant model. Upon plant hormones and hormone-like active compounds detected, the appropriate bioassay has been demonstrated. The previous reports demonstrated that seed germination and root elongation measurements are the easy-to-assay methods used for evaluation the BDL as a potential plant biostimulant/plant growth supplement (Iocoli et al., 2019; Li et al., 2016; Scaglia et al., 2015). Lettuce (*Lactuca sativa L.*) can be used as the plant model by measuring different growth parameters including the wet and dry weight of leaves, dry weight of roots and leaves number (Iocoli et al., 2019; Li et al., 2016). The different systems of the hydroponic assay have been described in brief below.

Hydroponics is a soilless plant cultivation technique that use mineral nutrient solutions with or without the addition of an inert support, such as gravel, vermiculite, rockwool, peat moss, saw dust, coir dust, and coconut fiber, for examples. Most hydroponic systems are setup with the automatic control system used to treat water, nutrients, and photoperiod according to plant needs. The hydroponic systems are preferred in plant cultivation due to their efficient management of resources and food production (Phibunwatthanawong & Riddech, 2019; Sharma, Acharya, Kumar, Singh, & Chaurasia, 2018). The previous reports demonstrated that the digestate fertilizer obtained from biogas production can be used as a nutrient supplement for soilless vegetable culture, which represents the combination of food production and organic waste management. In addition, high crop yields can be achieved by soilless production and is feasible even with no availability of crop land (Pelayo Lind et al., 2021).

Hydroponics systems are classified into five different types including (i) wick, (ii) drip, (iii) ebb-flow, (iv) deep-water culture and (v) nutrient-film technique (NFT) systems (Sharma et al., 2018). For the wick system, it is the most basic hydroponic system due to no requirement of mechanical works, such as electricity, a pump, or aerators. In this system, plants are cultivated in an absorbent matrix, such as coco coir, vermiculite, or perlite, with a nylon wick connecting the root area with a

nutritional solution storage tank. This technique is suitable for plants, herbs, and spices with small sizes, but not for plants that require a massive water (Figure 33) (Sharma et al., 2018).

For the latter type, the ebb-flow system is the hydroponic system that works on flood and drain techniques (Figure 34). A nutrient solution contained inside the reservoir tank is pumped into the grow tray until its level is at a specified volume, which is kept for a certain time to allow the absorption of nutrients and moisture by plants. If a nutrient solution is at an excess level, the overflow compartment would help reduce the excess volume by draining a nutrient solution back into the reservoir tank. This hydroponic system is applicable for growing different kinds of crops, however, the problems with root rot, algae blooms, and mold can occur (Sharma et al., 2018).

For the drip system (Figure 35), it is one of the popular hydroponic techniques to be used in plant growing at both home and commercial scales. By this technique, the nutrient solution inside the reservoir is delivered to the individual plant root by dripping the solution into the root in an appropriate proportion. The flow-rate speed of the nutrient solution dripping is controlled by the absorbent medium used (Sharma et al., 2018).

For a deep-water culture technique (Figure 36), plant roots are immersed in nutrient-rich water with aeration. As there is flow of water in this system, the oxygen and nutrient concentrations, salinity, and pH should be carefully monitored. The change of these physicochemical parameters could promote the growth of algae and mold quickly in the reservoir. This technique is suitable for larger plants that produce fruits, such as cucumbers and tomatoes, which grow in this environment (Sharma et al., 2018).

For the nutrient film technique (NFT) system (Figure 37), this technique is set up to get rid of the problem that occurred in the ebb-flow system. In this system, water or nutrient solution circulates throughout the system and enters the growing tray *via* a water pump. The system is designed to have a slight slope to allow the nutritional solution flows through the roots and turns back into the reservoir. Many



leafy greens such as lettuce may be easily grown by this technique, which is also the most extensively used technique on a commercial scale (Sharma et al., 2018).

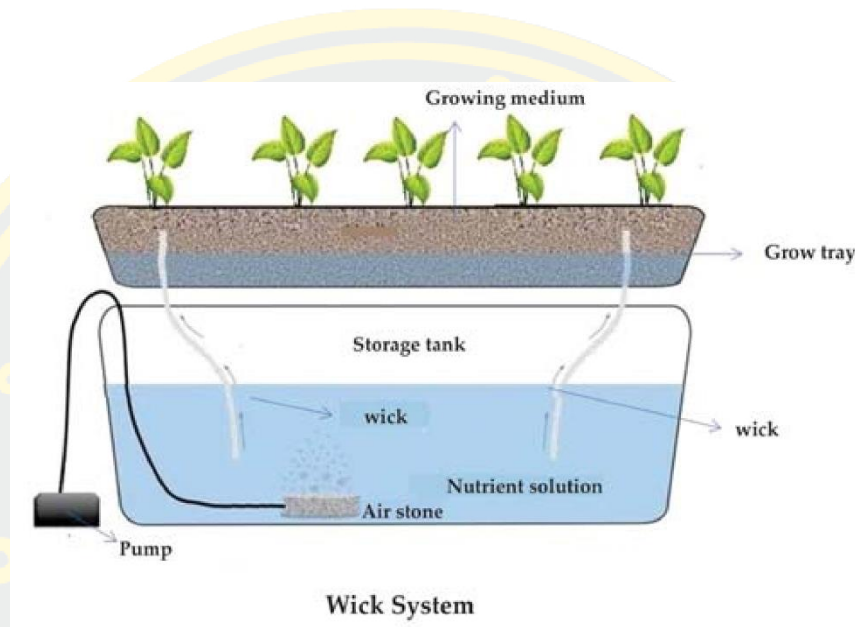


**Figure 33** The wick system of hydroponic assay (reproduced from (Sharma et al., 2018))

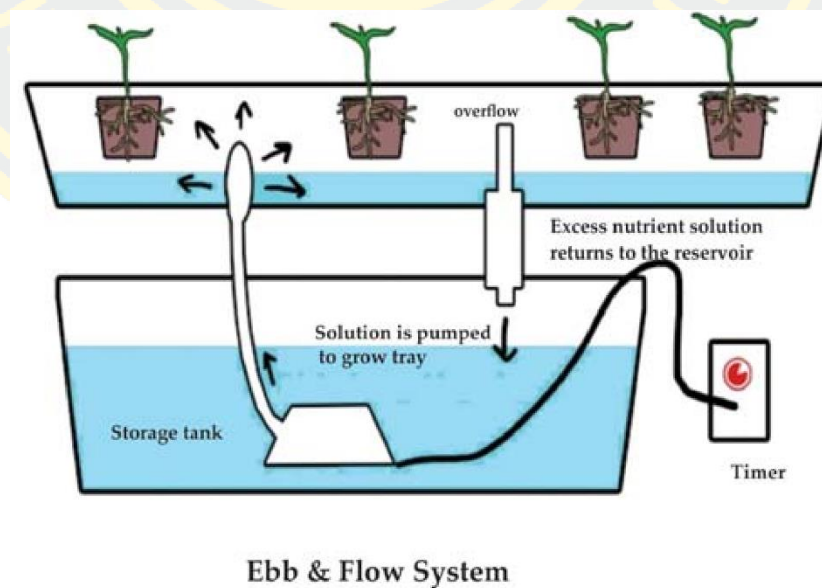
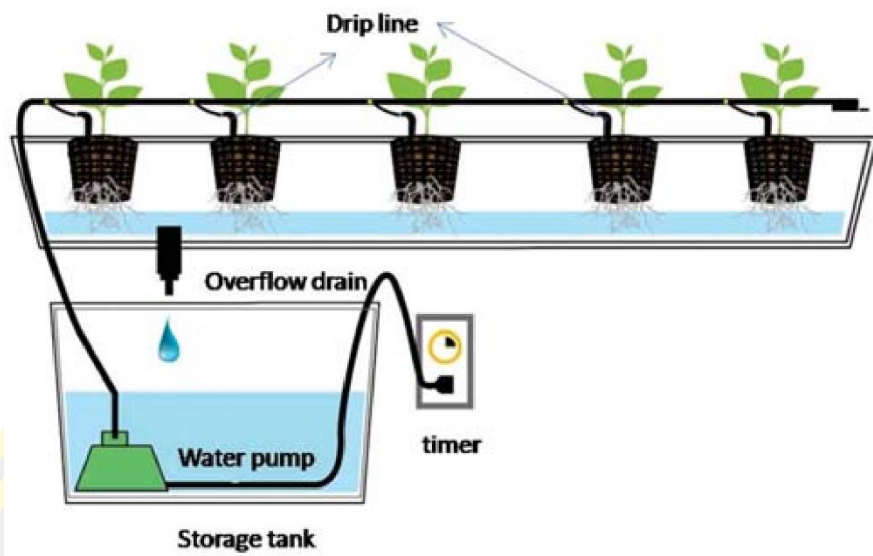
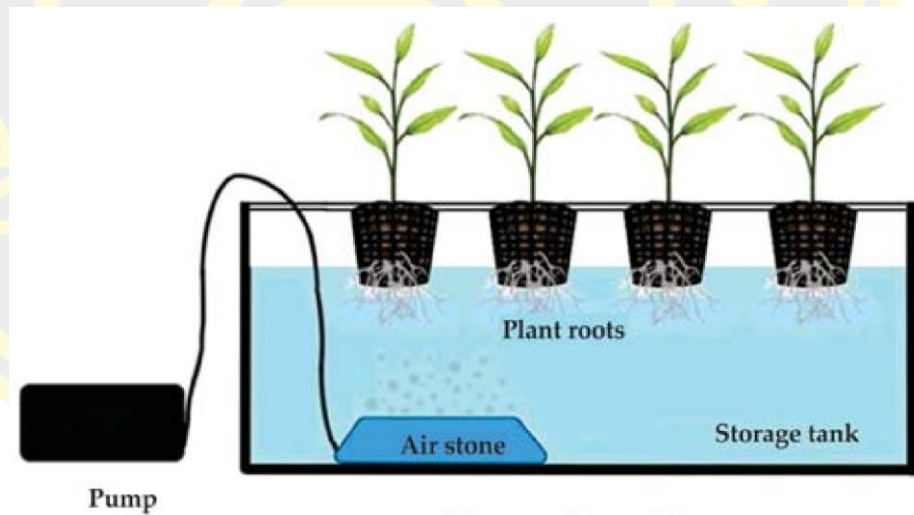


**Figure 34** The ebb-flow system of hydroponic assay (reproduced from (Sharma et al., 2018))



Drip system

**Figure 35** The drip system of hydroponic assay (reproduced from (Sharma et al., 2018))



Deep water culture

**Figure 36** The deep-water culture of hydroponic assay (reproduced from (Sharma et al., 2018))

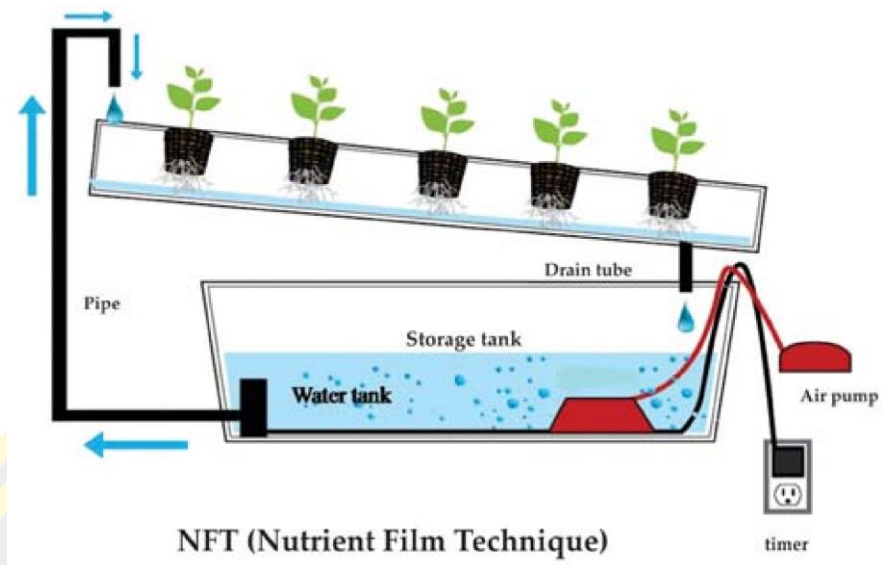


**Figure 37** The nutrient film technique system of hydroponic assay (reproduced from (Sharma et al., 2018))

## CHAPTER 3

### RESEARCH METHODOLOGY

#### 3.1 Chemicals and instruments

All chemicals used in this work are of analytical and HPLC grades with the highest purity and quality. Indole-3-acetic acid (IAA), abscisic acid (ABA), gibberellic acid ( $GA_3$ ), 5-aminolevulinic acid (ALA), pipecolic acid (Pip), zeatin, jasmonic acid (JA), salicylic acid (SA), kinetin, and L-ornithine were purchased from Sigma-Aldrich, USA. Methanol (MeOH), formic acid (FA), and acetonitrile (ACN) were purchased from Honeywell, USA. All metal standards (1000 ppm) were purchased from Perkin Elmer Pure. EDTA and coal (LECO Certified Reference Materials) were used as a reference for determining N and S content, respectively.

Sample separation and clarification were carried out by high-speed centrifuges (Thermo scientific, USA), plant hormones and hormone-like active compounds were analyzed by Agilent 6470 Triple-Quadrupole LC/MS (QqQ) (Agilent Technologies, USA). Plant nutrients, micro- and macronutrients, were analyzed by PinAAcle 900F atomic absorption spectrometer (AAS) (PerkinElmer, USA). The biogas digestate liquid (BDL) sample extraction was carried out by Sep-Pak  $C_{18}$  cartridge Solid Phase Extraction (SPE) (Waters Corporation, USA). The extracted sample was made as a powder by freeze-dryer (Alpha 2-4 LDplus, CHRIST, Germany). The carbon and nitrogen content in BDL samples was analyzed by CNS 628 series elemental analyzer (LECO corporation, USA). The pH and salinity were monitored by a pH meter (Mettler Toledo, USA) and an electrical conductivity meter (HORIBA, Japan), respectively.

### **3.2 Acquirement of biogas digestate liquid (BDL)**

Before acquiring BDL, a 1000-L fermentation containing 700 L of animal manure inoculum co-digested with the real food waste (RFW), operated under the C-ROS (Cash Return from ZeroWaste and Segregation of Trash) project of the School of Bimolecular Science and Engineering (BSE) at Vidyasirimedhi Institute of Technology (VISTEC), was carried out under proper anaerobic conditions, in that the  $O_2$  content should be in a range of 0.1-0.2% (v/v) or less and  $CH_4$  should be more than 50% (v/v). 40 L of the fermentation liquid was drained and collected, then assigned as “biogas digestate liquid (BDL). After the BDL drainage, about 40 kg of the RFW slurry was added into the fermentation tank to maintain the next round of fermentation process. The collected BDL was handled properly for further analyses (see the next section).

### **3.3 BDL sample handlings**

As shown in Figure 38, the collected BDL was split into two main sets, the fresh set (10 L) and storage set (30 L). For the storage set, it was stored at ambient temperature and each aliquot of 10 L was collected at different storage times: 1, 2, and 3 months. All of samples – fresh and storage samples – were divided into two separate aliquots. One aliquot was heated by boiling for 30 min, while another one was not. The heated and unheated aliquots of all samples were measured for pH and conductivity and kept at  $-20\text{ }^\circ\text{C}$  until analyzed.

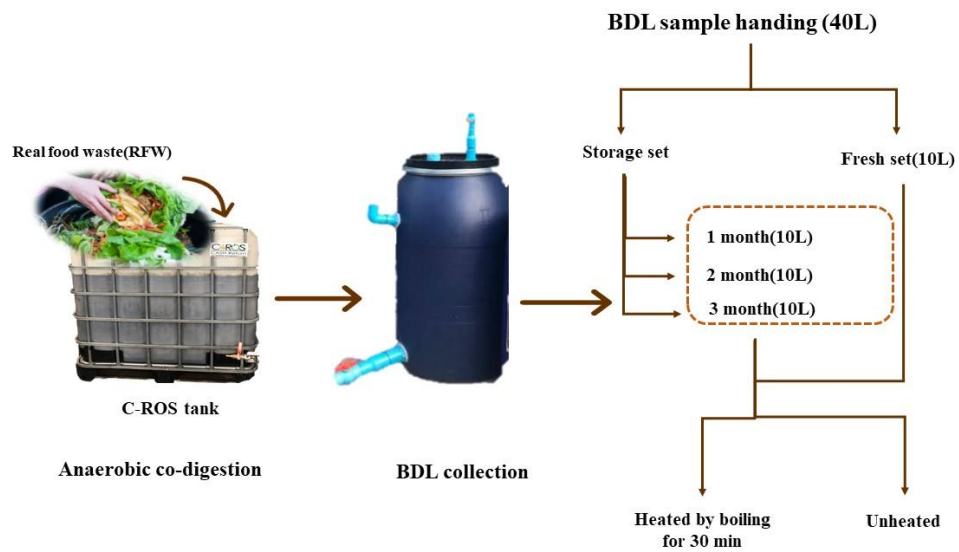


**Figure 38** The overview summary of a schematic representation for production of BDL and BDL sample handlings.

### 3.4 Metal analysis of heated and unheated BDL samples

For metal analysis, the metal treatment process was required and carried out by the standard protocol described in the American Society for Testing and Materials (ASTM; designation number D1971-16). In principle, the sample was digested with mineral acids and heated at atmospheric pressure. 100 ml of each sample was added with 0.5 ml of the concentrated HNO<sub>3</sub> (63% (w/w)) and 5 ml of the concentrated HCl (37% (w/w)). Then, heating the sample on a hot plate at 80 °C in a fume hood and avoid sample boiling until the sample volume is reduced to 20 ml. After that, the acidified sample was centrifuged at 4,000 rpm for 30 min and the supernatant was added with 2% (v/v) HNO<sub>3</sub> to obtain the final volume of 100 ml and then stored at 4 °C until analyzed. Before applying the digested sample to the AAS apparatus, the digested sample was necessarily filtered by a 0.22 μm syringe filter to remove the small particulates.

The conditions used in the AAS analysis were described as follows: light sources generating the particular wavelength for detection of each type of element was the hollow cathode lamp (HCL) for analysis of K, Fe, Zn, Mo, Mn, Mg, Cd, Cr, and Cu and the electrodeless discharge lamp (EDL) for analysis of P, Pb, Hg, and As. The source of energy for free-atom production is heated by an air/acetylene flame used for analyzing K, Fe, Zn, Mg, Mn, Cd, Cr, Cu, and Pb while nitrous oxide/acetylene flame used for analyzing P and Mo. The sample flow rate was set at 8.8 ml/min. The burner type was also appropriately used. For air/acetylene flames, the stainless steel burner should be placed, while nitrous oxide/acetylene flame should be compatible with the titanium burner (Paul, Pandey, Ramesh, & Meena, 2017).

### 3.5 CNS analysis of heated and unheated BDL samples

For analysis of carbon, nitrogen, and sulfur, the samples were not required for pretreatment. The sample was directly placed in a nickel boat liner that resided within the oven. The sample was then heated sequentially at 950 °C in a primary furnace, then 850 °C in a secondary furnace for nitrogen and carbon analysis, respectively. For sulfur analysis, a temperature of 1,350 °C was applied. During the combustion process, the 99.99% O<sub>2</sub> gas was applied to oxidize C, S, and N and the corresponding detectable gases such as CO<sub>2</sub>, SO<sub>2</sub>, and NO<sub>x</sub>, respectively, were formed and analyzed. The gases were detected by the infra-red (IR) and thermal

conductivity (TC) cells. The non-dispersive IR (NDIR) cell was used for the detection of CO<sub>2</sub> and SO<sub>2</sub> for determination of carbon and sulfur, while a TC cell was used to detect NO<sub>x</sub> for quantitation of nitrogen. EDTA and coal were used as a reference to determine nitrogen and sulfur content, respectively.

### **3.6 The condition optimization for LC-MS/MS analysis of authentic plant hormones and plant-growth promoting compounds**

The solution of each authentic plant hormone and plant-growth promoting compound, including indole 3 acetic acid (IAA), abscisic acid (ABA), gibberellic acid (GA<sub>3</sub>), jasmonic acid (JA), salicylic acid (SA), kinetin, zeatin, 5-aminolevulinic acid (ALA), and pipecolic acid (Pip), were prepared at a selected concentration (IAA, 100 μM; ABA, 50 μM; GA<sub>3</sub>, 50 μM; JA, 1,830 μM; SA, 50 μM; kinetin, 33 μM; zeatin, 64 μM; ALA, 100 μM; and Pip, 100 μM) and injected into a ZORBAX Eclipse Plus C<sub>18</sub> column (5 μm, 4.6 x 250 mm, Agilent Technologies) pre-equilibrated with a solvent mixture of 70% Solvent A (Milli-Q<sup>®</sup> Type I ultrapure water) and 30% Solvent B (MeOH) in negative mode. The column flow rate was operated at 0.6 ml/min. After loading the solution, the column was treated with the gradient change of Solvent B from 30% to 100% within 6 min. The column was maintained with 100% Solvent B for more 4 min and then turned back to 30% Solvent B within 6 min. The optimized LC condition is summarized in Table 4. In positive mode, the system is pre-equilibrated with a solvent mixture of 100% Solvent A (Milli-Q<sup>®</sup> Type I ultrapure water) and 0% Solvent B (MeOH). The flow rate of the column was set at 0.4 ml/min. After loading the solution, the column was treated with the gradient change of Solvent B from 0% to 60% within 10 min. The column was maintained with 60% Solvent B for more 2 min and then Solvent B from 60% to 100% within 15 min. For another 5 min, the column was maintained with 100% Solvent B. Finally, it turned back to 0% solvent B within 22 min. After that, the eluent obtained from the column was ionized by electrospray ionization (ESI) before transmitting into the QqQ analyzer. The condition of the source parameter for QqQ was optimized as shown in Table 5. In addition, there was also an optimization of the mass conditions such as product ion, fragmentor voltage, and collision energy to get the best signal for plant hormone analysis. The retention time (RT) of each compound separated was then analyzed.



**Table 4** The optimized distribution of Solvents A and B for compound separation in C<sub>18</sub> column chromatography and MS/MS analysis with negative and positive modes.

Mode	Time (min)	% Solvent A	% Solvent B
Negative	0	70	30
	6	0	100
	10	0	100
	16	70	30
Positive	0	100	0
	2	100	0
	10	40	60
	12	40	60
	15	0	100
	20	0	100
	22	100	0

**Table 5** The optimized conditions of source parameters for QqQ analyzer.

Parameters	Setup
Gas temp	300 °C
Gas flow	7 ml/min
Nebulizer	45 psi
Sheath Gas Temp	300 °C
Sheath Gas Flow	12 l/min
Capillary	3500 V
Nozzle Voltage	500 V

### **3.7 Determination of the optimal internal standard for LC-MS/MS analysis**

The internal standard (IS) is usually used to validate the method used, therefore in this section, we determine the optimal IS for LC-MS/MS analysis of plant hormones and plant-growth promoting compounds.

In this work, isopropyl  $\beta$ -D-1-thiogalactopyranoside (IPTG) (allolactose analogue and synthetic inducer which is not found in nature) and ampicillin (antibiotic) were chosen to be examined because they are anticipated to be not appeared in the BDL. Ampicillin and IPTG were prepared at a concentration of 50  $\mu$ M and 100  $\mu$ M, respectively, and filtered by a 0.22  $\mu$ m syringe filter to remove the small particulates before subjection into a ZORBAX Eclipse Plus C<sub>18</sub> column (5  $\mu$ m, 4.6 x 250 mm, Agilent Technologies). The LC separation and MS/MS analysis of ampicillin and IPTG was carried out under the optimized conditions shown in Tables 4 and 5. The RT, signal abundance, and peak area of IPTG and ampicillin were analyzed to gain the best IS for LC-MS/MS analysis of plant hormones and plant-growth promoting compounds.

### **3.8 Determination of limit of detection (LOD) and limit of quantitation (LOQ) from the calibration curve plot of each authentic plant hormone and plant-growth promoting compound**

LOD and LOQ are important for method validation. LOD is the lowest concentration of analyte in samples that can be detected, while LOQ represents the lowest concentration of analyte that can be analyzed in the quantitative measurement. The LOD and LOQ can be determined from the standard deviation (SD) of the response and the slope of the linear equation. Therefore, the LOD and LOQ can be calculated from Equations 1 and 2, respectively (Shrivastava & Gupta, 2011).

To determine LOD and LOQ from the calibration curve of each authentic plant hormone and plant-growth promoting compound, different concentration ranges of each compound, including IAA (125, 250, 500, and 1000  $\mu$ M), ABA (62.5, 125, 500, and 1000 nM), GA<sub>3</sub> (39.0625, 78.125, 156.25, 312.5, 625, and 2,500 nM), SA (1.56, 3.12, 6.25, and 25.00  $\mu$ M), kinetin (62.5, 125, 500, 1,000, and 4,000 nM), zeatin (7.80, 15.60, 31.25, 62.50, 125, 250, 500, and 1,000 nM), ALA (7.80, 15.60, 31.25, 62.5, and 250  $\mu$ M), and Pip (7.80, 31.25, 62.50, and 250  $\mu$ M), were prepared in 50 mM sodium phosphate buffer, pH 7.0 and filtered by a 0.22  $\mu$ m syringe filter

before subsection into an LC-MS/MS system operated under optimal setup conditions as shown in Tables 4 and 5. The calibration curve of each compound was constructed and LOD and LOQ were then calculated from the SD value of the response and the slope of the linear equation using Equations 1 and 2, respectively.

$$LOD = \frac{3SD}{Slope} \quad \text{Eq. 1}$$

$$LOQ = \frac{10SD}{Slope} \quad \text{Eq. 2}$$

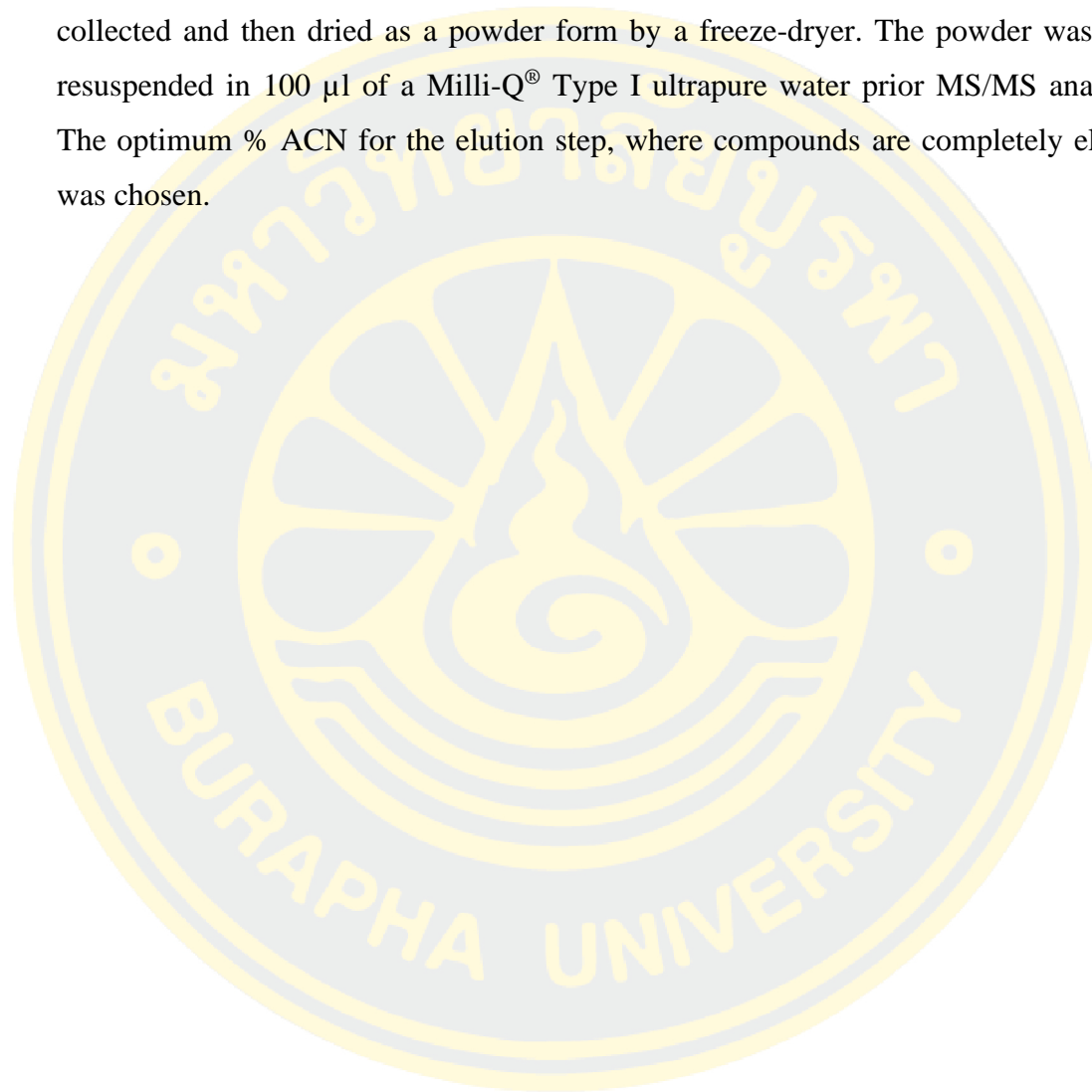
### 3.9 Optimization of the extraction method for future separating plant hormones and plant-growth promoting compounds from the BDL samples

To optimize the method suited for extraction of plant hormones and plant-growth promoting compounds in the BDL samples, the solid-phase extraction (SPE) technique was the method of choice used for separation. All the authentic plant hormones and plant-growth promoting compounds, including IAA, ABA, GA<sub>3</sub>, SA, kinetin, zeatin, ALA, and Pip, were used for optimization of the SPE conditions, such as washing/desalting and elution steps, before carrying out with the real BDL samples. The overview of the SPE workflow was summarized in Figure 39 shown below.

Three replicates of a mixture solution of authentic compounds (200 μM each) prepared in 50 mM sodium phosphate buffer (pH 7.0) were mixed thoroughly with a selected IS, ampicillin (1 mM). Each of the mixture solution was filtered by a 0.22 μm syringe filter and 1 ml of the filtrate solution was loaded onto the Sep-Pak C<sub>18</sub> cartridge (360 mg sorbent/cartridge, 55-105 μm, WAT051910) pre-activated by 100% MeOH (3 ml) and pre-equilibrated with a Milli-Q<sup>®</sup> Type I ultrapure water (2 ml). Since salt contents can potentially perturb mass ionization, the washing/desalting steps were therefore optimized. After loading the mixture solution, the cartridge was washed with Milli-Q<sup>®</sup> Type I ultrapure water (1 ml) and then desalted with 4 ml of each varying % MeOH (1, 2, 3, 4, and 5%). The washed and desalted solutions were separately collected and analyzed by LC-MS/MS to monitor the corresponding *m/z* of

each compound. The optimum % MeOH for the desalting step, where no compounds were detected, was chosen for further experiments.

To optimize the elution condition, the cartridge was stepwise eluted with 1 ml of each varying % ACN (20, 50, 80, and 100%). Each of the eluted fractions was collected and then dried as a powder form by a freeze-dryer. The powder was then resuspended in 100  $\mu$ l of a Milli-Q<sup>®</sup> Type I ultrapure water prior MS/MS analysis. The optimum % ACN for the elution step, where compounds are completely eluted, was chosen.



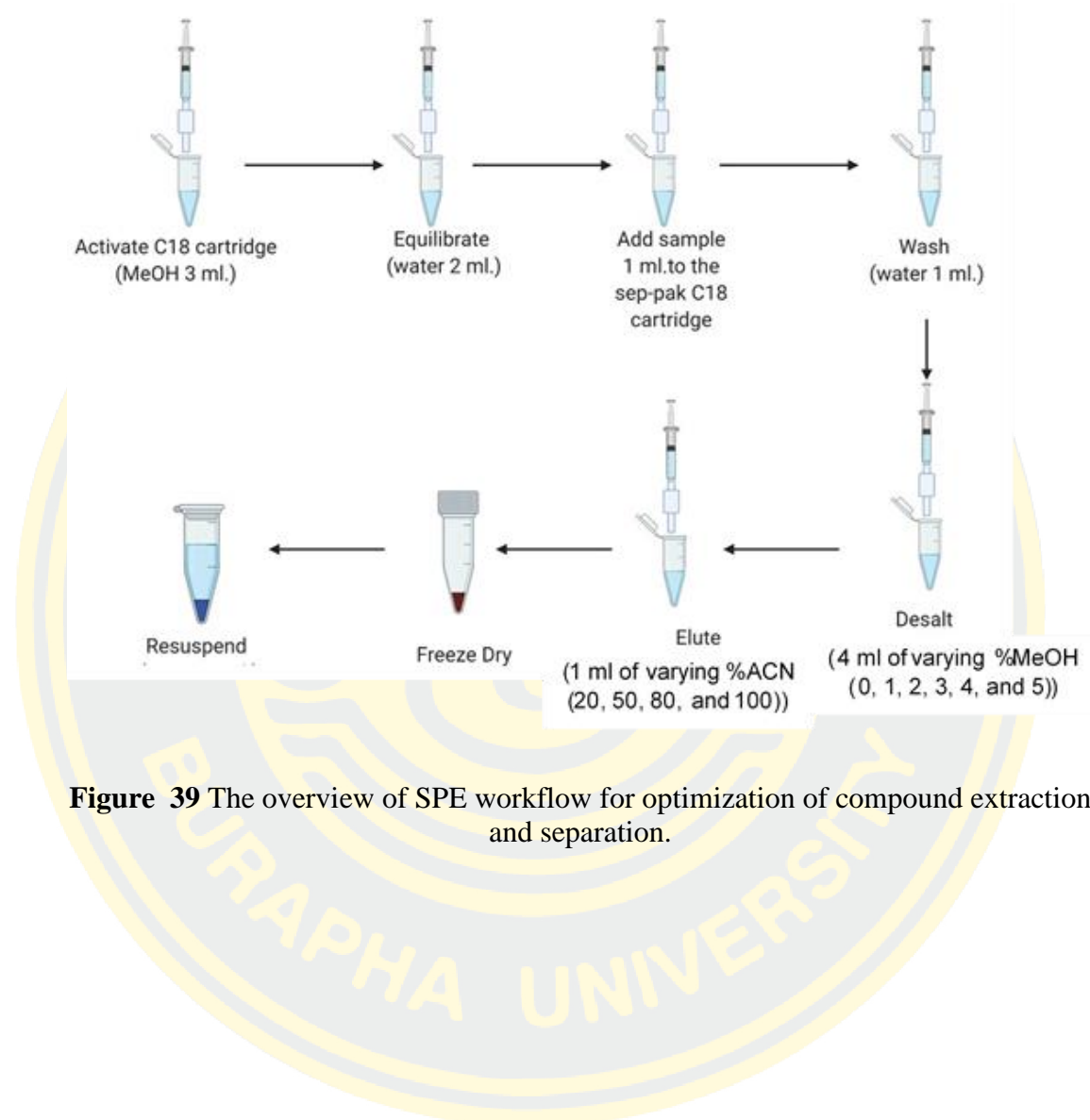


**Figure 39** The overview of SPE workflow for optimization of compound extraction and separation.

### **3.10 Quantitation of plant hormones and plant-growth promoting compounds in heated and unheated BDL samples**

In this section, plant hormones and plant-growth promoting compounds in heated and unheated BDL samples from the fresh and storage sets were extracted by SPE method and quantitated by LC-MS/MS. As the BDL samples are colloidal, therefore the clarification steps are needed before loading samples onto the Sep-Pak C<sub>18</sub> cartridge.

Three replicates of each BDL sample (10 ml) were mixed thoroughly with 50  $\mu$ M ampicillin (IS) and then clarified by low-speed centrifugation at 4,000 rpm for 50 min to separate the large particles. Each of the supernatant was further clarified by ultrafiltration using a 0.22  $\mu$ m membrane filter unit to remove the small particles. The filtrate was then dried by the freeze-dryer and the filtrate powder was resuspended with 1 ml of a Milli-Q<sup>®</sup> Type I ultrapure water prior subjection into SPE apparatus (Figure 39). Plant hormones and plant-growth promoting compounds of each BDL sample were detected and quantitated by the optimized LC-MS/MS conditions (Tables 4 and 5) as follows: IAA, ABA, GA<sub>3</sub>, JA, SA, and zeatin were detected in a negative mode, while kinetin, ALA, and Pip were detected in a positive mode. The scheme represented for the extraction of plant hormones and plant-growth promoting compounds in the BDL samples are shown in Figure 40. The concentration of each compound was then determined from the calibration curve of each compound.

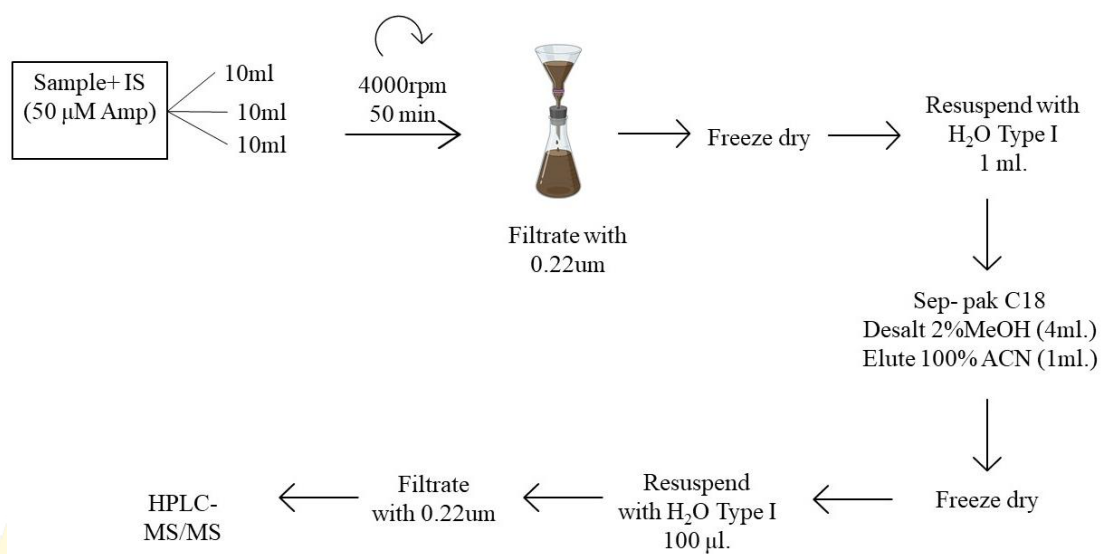


**Figure 40** The scheme represents the workflow of extraction of plant hormones and plant-growth promoting compounds from the BDL samples.

### 3.11 Temperature effect on plant hormone stability

The previous report demonstrated that major plant hormones derived from the anaerobic digestion systems were sensitive to high temperatures (Li et al., 2016). It was found that GA<sub>3</sub> was degraded at 20 and 37 °C within 20 days. IAA concentration was decreased by 70.5% at 37 °C, while ABA concentration was likely unchanged along 90 days at 4 and 20 °C. The data indicated that these major plant hormones are not tolerant to high temperatures (Li et al., 2016).

As the BDL samples in this research work were also handled under heated condition, therefore, we tested if the heating temperatures may affect plant hormone stability. Three replicates of a mixture solution of authentic compounds (200 µM each) were prepared in 2 ml of 50 mM sodium phosphate buffer (pH 7.0) and contained in 15-ml plastic test tubes. The test tubes were placed in the water bath heated at either 40 °C (a moderate high temperature commonly used for rotary evaporation) or 100 °C (a boiling temperature used for heating BDL samples) for 30 min (an incubation time that is equivalent to the time for heating BDL samples). During heating process, the solution temperature in the test tubes was monitored and recorded. After vaporization, the remaining volume of solution was measured and a buffer was added up to 2 ml before analyzing with LC-MS/MS. The amount of each compound in the heated solution was quantitated and then compared with the unheated one.

### 3.12 Hydroponic assay

To evaluate the capability of BDL samples in promoting plant growth and development, the hydroponic assay using green oak lettuce (*Lactuca sativa L.*) as a plant model was carried out by the deep-water culture system (see Figure 36) in the foam boxes (38.8 × 53.8 × 20.7 cm) placed under a homemade greenhouse with different treated conditions, including negative control (tap water), positive control (~170X-diluted hydroponic fertilizer, 120 ml/ 20 l), only 20X-diluted BDL sample, and a mixture of 20X-diluted BDL samples and ~170X-diluted hydroponic fertilizer. The BDL samples tested in this experiment were the heated and unheated BDL samples of fresh, 1-month-storage, 2-month-storage, and 3-month-storage sets. It



should be noted that one greenhouse can accommodate eight foam boxes, in which each of them can be filled with 12 pots (Figure 41A).

Before performing the hydroponic assay, the seedling of green oak lettuce seeds (imported from the Netherlands under the brand VIZIR, Batch. 6122799; Expiry date: August, 2022) was conducted by cultivating seeds inside the tap-water wet sponge to allow seed germination in the dark for 3 days. After germination period, the sponge harboring the germinated seed was moved outside to allow the light reaction occurred and the sprout with 2-3 leaves was present until day 10-14 (Figure 41B). Then, the sponge harboring the germinated seed was placed inside the planting pot buried in the foam box filled with 20 l of each tested solution, thus allowing the roots to completely soak (Figure 41C). About 45 days, the green oak lettuce was ready for harvest and the growth parameters, such as wet and dry weights (root, leaves, and whole body), height (whole body, excepting for root), and width (canopy size) were measured.

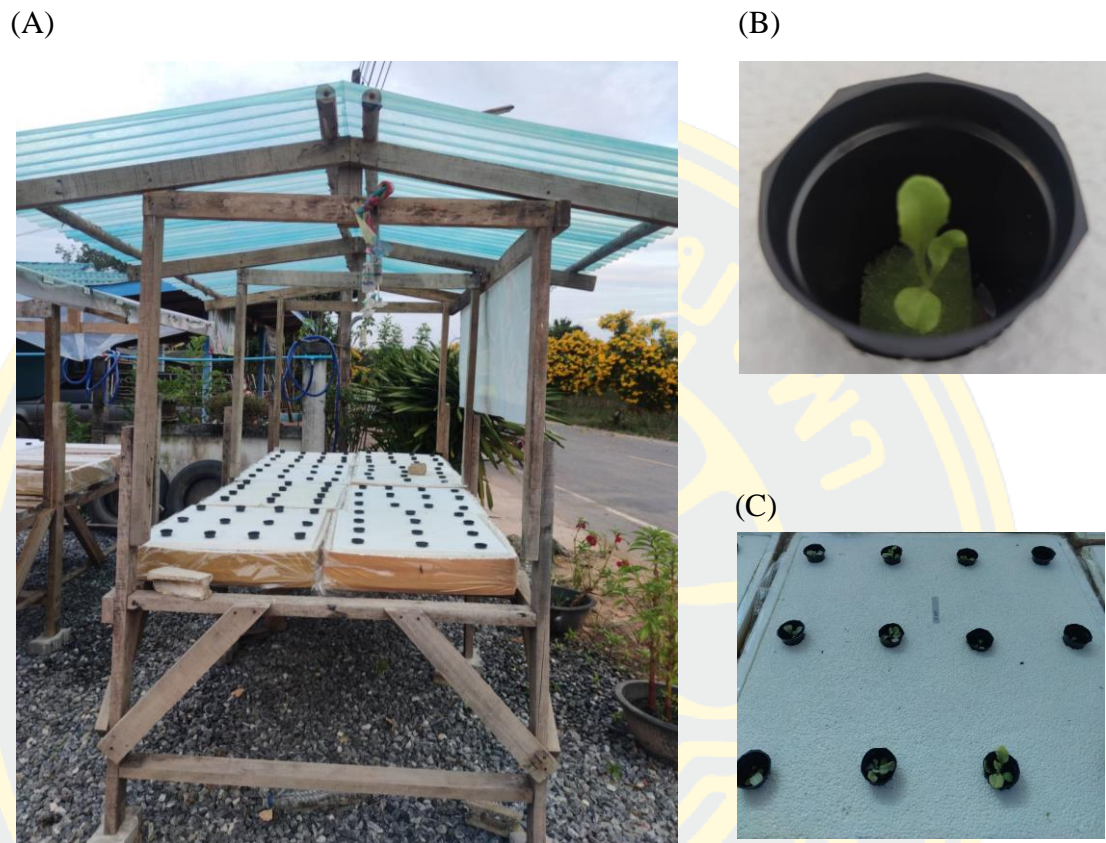


**Figure 41** The planting of green oak lettuce in the deep-water culture system of the hydroponic assay. (A) The greenhouse applied for the hydroponic assay. (B) Seed germination of green oak lettuce inside the tap-water wet sponge. (C) The planting pots were placed on foam boxes filled with tested solution.

## CHAPTER 4

### RESULTS

#### 4.1 The basic physicochemical properties of BDL samples

Since some physicochemical properties (*i.e.*, acid-base and salinity) could affect plant growth, the unheated and heated BDL samples of the fresh, 1-month-, 2-month-, and 3-month-storage sets, were measured for basic physicochemical properties before applying them further to plant-growth experiments. Each BDL sample was measured for pH and electrical conductivity (EC) under ambient temperature. The results showed that the pH values of all unheated and heated BDL sample sets were similar in a range of pH 8-9 (Table 6), indicating that BDL samples were mild alkaline. The EC values measured were also in the same range of 10-13 mS/cm, which was equivalent to the EC of industrial waste water (~10 mS/cm) and much higher than that of the tap water (0.05-0.8 mS/cm) (Fondriest Environmental, Inc. "Conductivity, Salinity and Total Dissolved Solids." Fundamentals of Environmental Measurements. 3 Mar 2014.). The data suggest that all of the BDL samples contain high abundances of salt contents, which may contribute to the mild alkaline property. It should be noted that both physicochemical parameters measured (both pH and EC values) were not significantly different over the storage period, suggesting that the fresh BDL samples (unheated and heated sets) could be ready for field application. However, high salt contents have been still concerned.

**Table 6** The pH and electrical conductivity of unheated and heated BDL sample sets.

<b>BDL sample set</b>	<b>Treatment condition</b>	<b>pH</b>	<b>Electrical conductivity (EC) (mS/cm)</b>
Fresh	Unheated	8.03	13.56
	Heated*	8.69	11.18
1-Month storage	Unheated	8.21	13.27
	Heated*	9.10	10.40
2-Month storage	Unheated	8.57	13.18
	Heated*	8.86	10.46
3-Month storage	Unheated	8.31	13.21
	Heated*	8.77	10.64

\*The BDL samples were heated at 100 °C for 30 min to eradicate some plant and human pathogens.

## 4.2 Plant nutrients and toxic elements

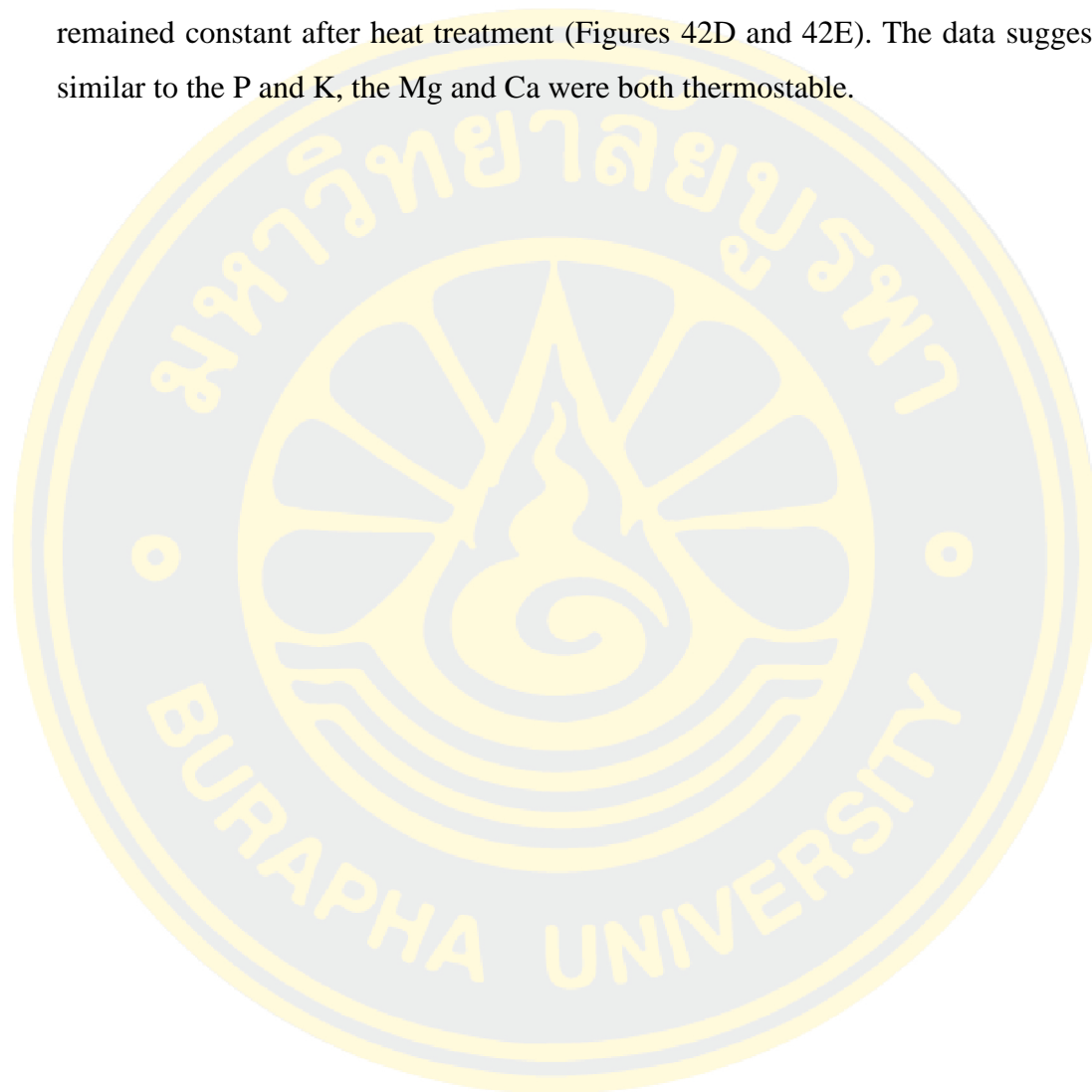
### 4.2.1 Macronutrients

As the macronutrients are vital for plant growth and development, each BDL sample set was therefore analyzed by analytical techniques to quantify the macronutrients including N, P, K, Ca, and Mg. Only N content was analyzed by the CNS analyzer using EDTA as a standard. While other macronutrients were analyzed by AAS and the concentration of each macronutrient was determined from the calibration curve plot of standard element concentration *versus* absorbance at a particular wavelength (Appendix). For each of the BDL sample set (fresh, 1-month-, 2-month-, and 3-month-storage set), the macronutrient contents detected in unheated and heated samples were compared.

For the N contents, the results obtained from CNS analysis showed that the N concentrations of all unheated BDL samples (fresh, 1-month-, 2-month-, and 3-month-storage set) were higher than those of all the heated BDL samples (Figure 42A). In unheated BDL samples, the N concentration in the fresh set was determined as high as 1,320.52 mg/l and slightly decreased ~30% to 868 mg/l after storage for 3 months (Table 7). The data indicate that the N contents of unheated BDL samples were decreased as the storage time increased. However, after heat treatment, the N contents in all of the heated BDL sample sets, largely decreased as compared to unheated BDL sample sets. This could be due to the loss of the volatile N (such as  $\text{NH}_4\text{-N}$ ) during heat treatment.

The AAS analysis at absorbance 213.55 nm showed that the P contents in unheated BDL sample sets were increased up to as high as about 500,000 mg/l (Table 7) as the storage time increased to 3 months (Figure 42B). It was hypothesized that during storage period, some biological processes occurred and could enhance synthesis of the P-containing compounds. The data also suggest that the P was rather stable overheat, thus making the P contents were not changed after heat treatment. In addition to the P, the K, which is a key macronutrient, was also analyzed by AAS at absorbance 766.49 nm. The results shown in Figure 42C indicated that the K contents measured in all of unheated and heated BDL sample sets were rather unchanged (2,111-2,796 mg/l) (Table 7). The data suggest that the K contents were steady over the storage period without any loss and extra and were also thermostable.

For the measurement of the Mg and Ca contents, the absorbance at 285.21 and 422.67 nm, respectively, were measured. The results indicated that in an unheated BDL sample sets, the Mg and Ca contents were slightly decreased (from 65 to 45 mg/l and 67 to 50 mg/l, respectively) over the storage time (Table 7) and were likely remained constant after heat treatment (Figures 42D and 42E). The data suggest that similar to the P and K, the Mg and Ca were both thermostable.



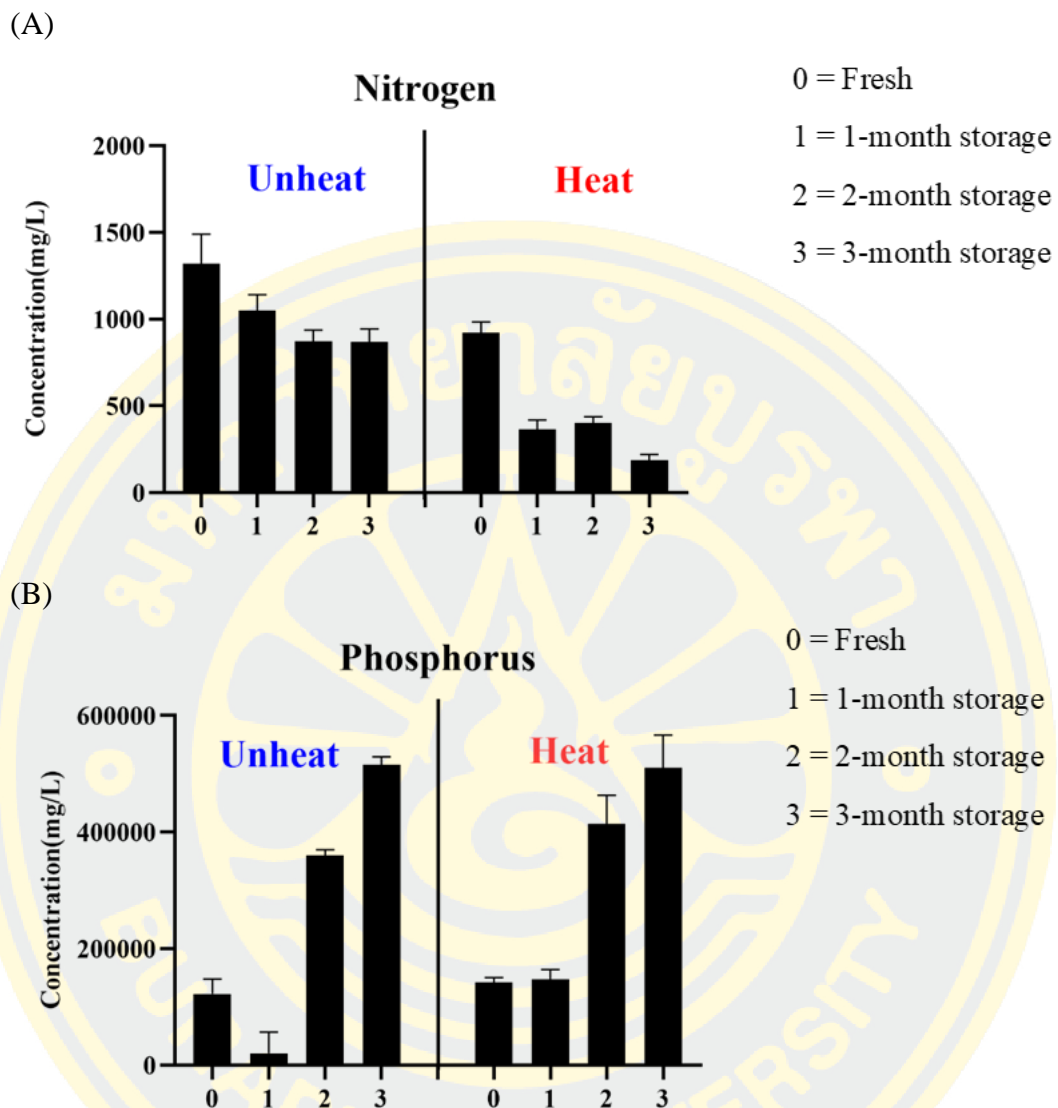
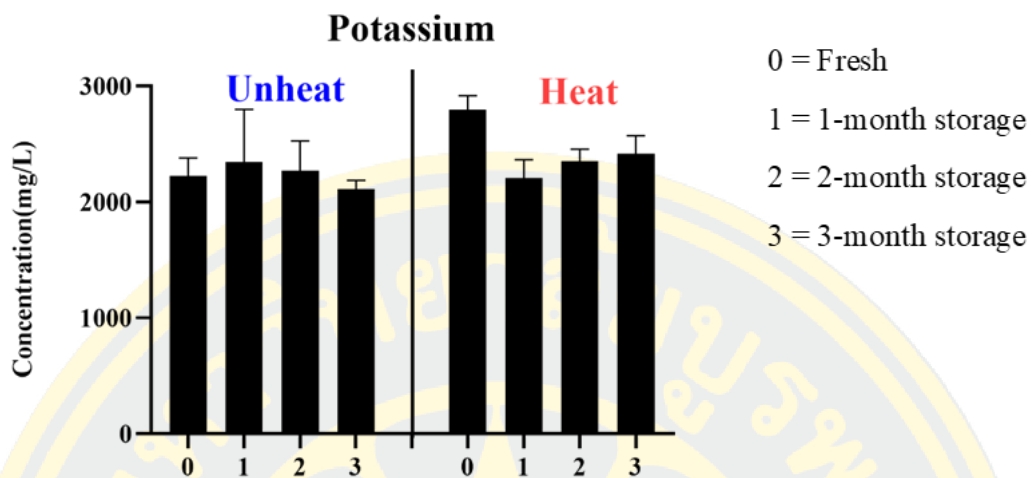


**Figure 42** Quantitation of macronutrients (N, P, K, Mg, and Ca) in each of unheated and heated BDL sample set (fresh, 1-month-, 2-month-, and 3-month-storage set). The N contents were analyzed by CNS analyzer (A), while the P (B), K (C), Mg (D), and Ca (E) contents were analyzed by AAS technique. Error bars represent standard deviations (S.D.) from three replications of the data. All concentrations of macronutrients determined were summarized in Table 7.

(C)



(D)

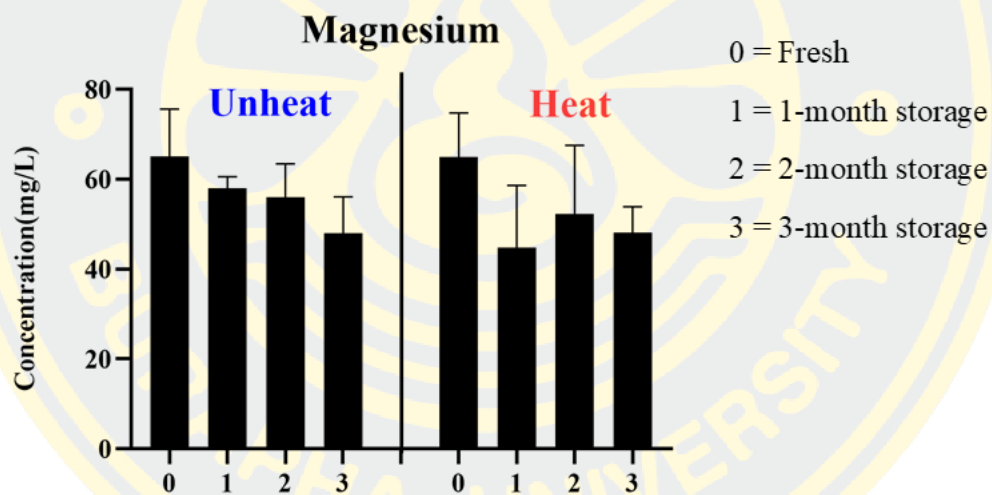


**Figure 42 (continued)** Quantitation of macronutrients (N, P, K, Mg, and Ca) in each of unheated and heated BDL sample set (fresh, 1-month-, 2-month-, and 3-month-storage set). The N contents were analyzed by CNS analyzer (A), while the P (B), K (C), Mg (D), and Ca (E) contents were analyzed by AAS technique. Error bars represent standard deviations (S.D.) from three replications of the data. All concentrations of macronutrients determined were summarized in Table 7.



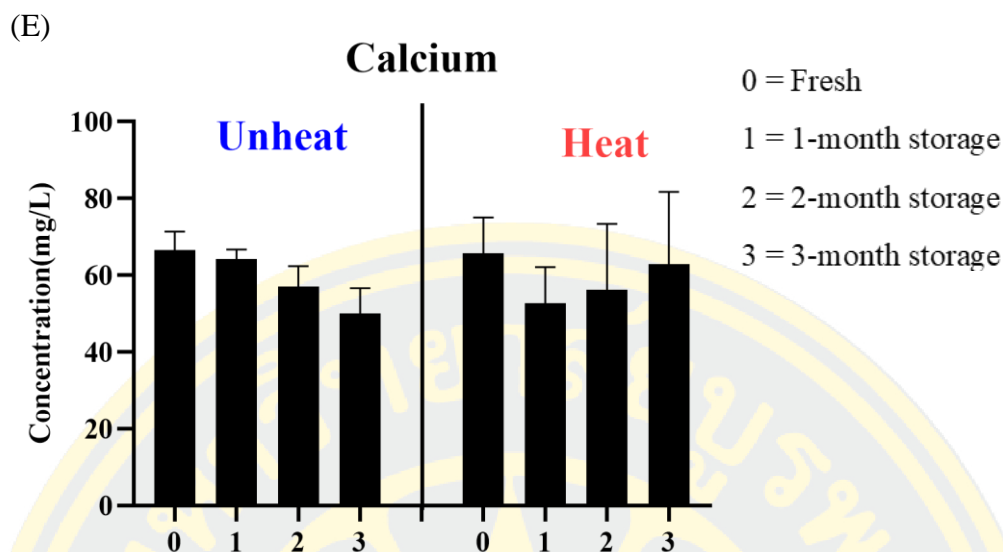


**Figure 42 (continued)** Quantitation of macronutrients (N, P, K, Mg, and Ca) in each of unheated and heated BDL sample set (fresh, 1-month-, 2-month-, and 3-month-storage set). The N contents were analyzed by CNS analyzer (A), while the P (B), K (C), Mg (D), and Ca (E) contents were analyzed by AAS technique. Error bars represent standard deviations (S.D.) from three replications of the data. All concentrations of macronutrients determined were summarized in Table 7.

#### 4.2.2 Micronutrients

As the micronutrients, including Fe, Cu, Zn, Mn, and Mo are involved in synthesis of crucial substances such as auxin, chlorophyll, and starch during plant growth, therefore their contents in unheated and heated BDL sample sets (fresh, 1-month-, 2-month-, and 3-month-storage set) were quantitatively analyzed by AAS technique. For the AAS measurement, Fe, Cu, Zn, Mn, and Mo were monitored absorption signal at 248.33, 324.75, 213.86, 279.48, and 313.26 nm, respectively. Each micronutrient concentration was determined from the calibration curve plot of standard metal concentration *versus* absorbance at a particular wavelength (Appendix). The results shown in Figure 43 and Table 7 indicate that all micronutrients – Fe (Figure 43A), Cu (Figure 43B), Zn (Figure 43C), Mn (Figure 43D), and Mo (Figure 43E) – measured in all of unheated and heated BDL sample sets were likely unchanged (~3, ~200, ~0.9, ~0.3, and ~0.13 mg/l, respectively) (Table 7). The data suggest that all of the micronutrients were found to be steady over the storage period without any loss and extra and were also heat-resistant.

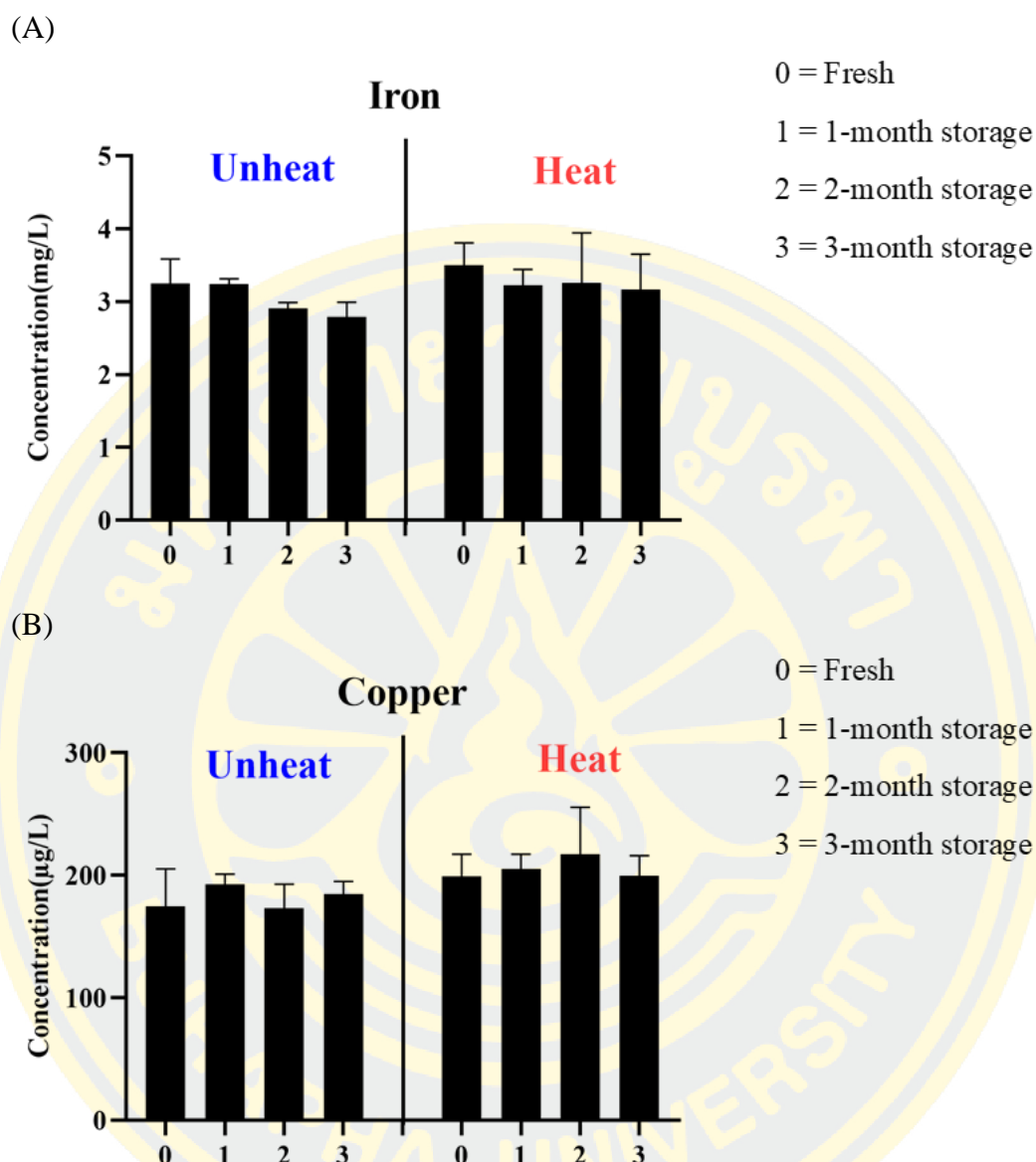
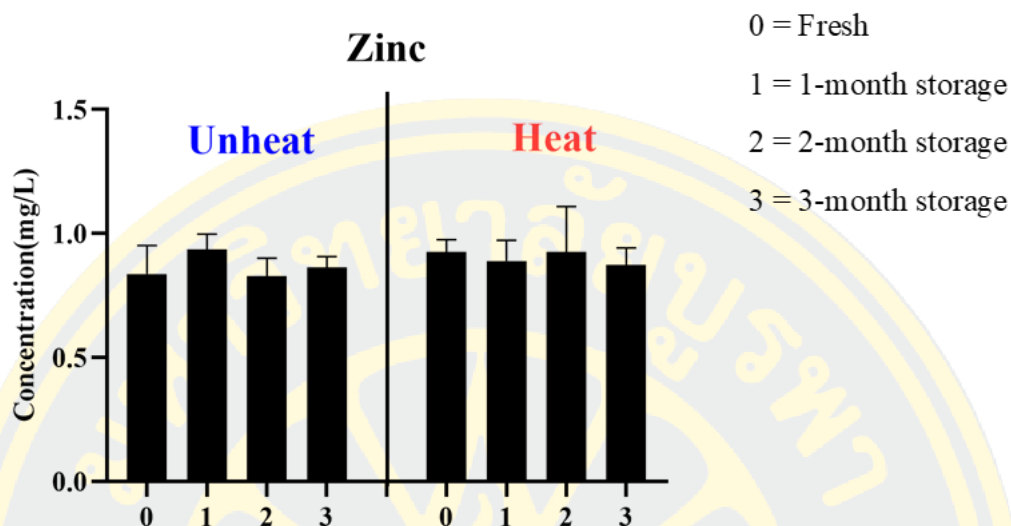


**Figure 43** Quantitation of micronutrients (Fe, Cu, Zn, Mn, and Mo) in each of unheated and heated BDL sample set (fresh, 1-month-, 2-month-, and 3-month-storage set). All of the micronutrients, Fe (A), Cu (B), Zn (C), Mn (D), and Mo (E), were analyzed by AAS technique. Error bars represent standard deviations (S.D.) from three replications of the data. All concentrations of micronutrients determined were summarized in Table 7.

(C)



(D)

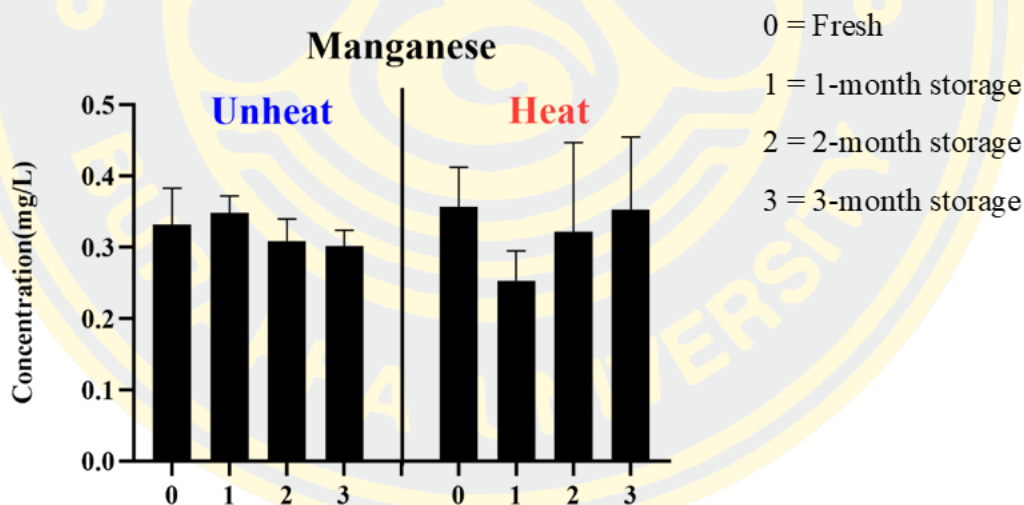


**Figure 43 (continued)** Quantitation of micronutrients (Fe, Cu, Zn, Mn, and Mo) in each of unheated and heated BDL sample set (fresh, 1-month-, 2-month-, and 3-month-storage set). All of the micronutrients, Fe (A), Cu (B), Zn (C), Mn (D), and Mo (E), were analyzed by AAS technique. Error bars represent standard deviations (S.D.) from three replications of the data. All concentrations of micronutrients determined were summarized in Table 7.

(E)

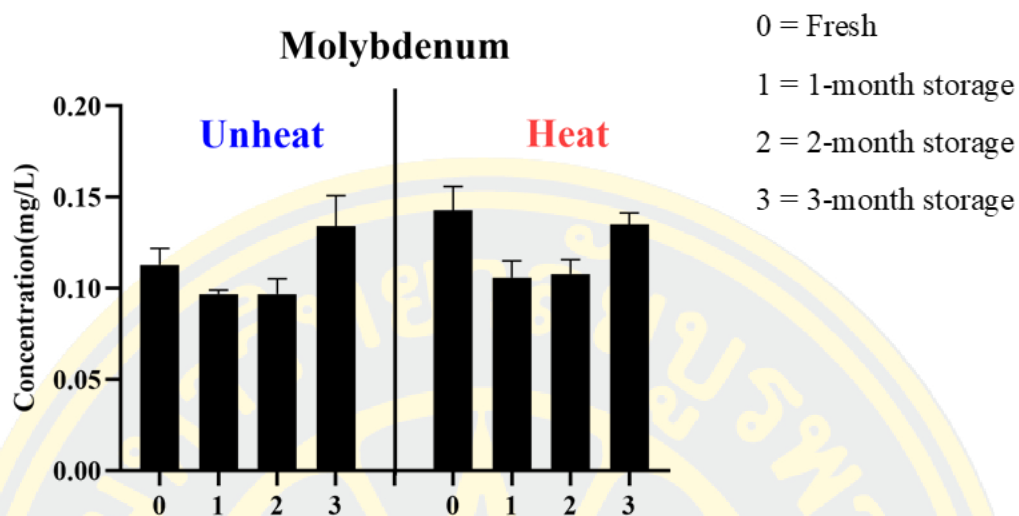


**Figure 43 (continued)** Quantitation of micronutrients (Fe, Cu, Zn, Mn, and Mo) in each of unheated and heated BDL sample set (fresh, 1-month-, 2-month-, and 3-month-storage set). All of the micronutrients, Fe (A), Cu (B), Zn (C), Mn (D), and Mo (E), were analyzed by AAS technique. Error bars represent standard deviations (S.D.) from three replications of the data. All concentrations of micronutrients determined were summarized in Table 7.

### 4.2.3 Toxic elements

According to the regulations by the Department of Agriculture (DOA) of Thailand, the toxic elements potentially affecting plant growth were As, Pb, Cd, and Cr. The quantity of these elements must be controlled to not exceed the value determined by DOA. Therefore, these toxic elements (As, Pb, Cd, and Cr) in all of unheated and heated BDL samples sets (fresh, 1-month-, 2-month-, and 3-month-storage set) were monitored and analyzed by AAS at absorbance 193.7, 283.31, 228.8 and 357.87 nm, respectively. The concentration of each toxic element was determined from the calibration curve plot of a standard element *versus* absorbance at a particular wavelength (Appendix). The results showed that all the toxic elements in all of the unheated and heated BDL sample sets were detected at very low concentrations (Figure 44 and Table 7). The As contents were found about 40  $\mu\text{g/l}$  in all of unheated and heated BDL samples sets, excepting the 3-month-storage set that detected only a half (Figure 44A). This suggests that the As could be reasonably lowered upon storage time increased. In contrast, the Pb contents in all of the heated BDL sample sets were unexpectedly increased about twice ( $\sim 40 \mu\text{g/l}$ ) as compared to those of unheated BDL sample sets ( $\sim 20 \mu\text{g/l}$ ) (Figure 44B). For measurement of the Cd (Figure 44C) and Cr (Figure 44D) contents, the results showed that both metals measured in all of unheated and heated BDL sample sets were likely unchanged ( $\sim 9$  and  $\sim 25 \mu\text{g/l}$ , respectively), suggesting that these metals were found to be steady over the storage period without any loss and extra.

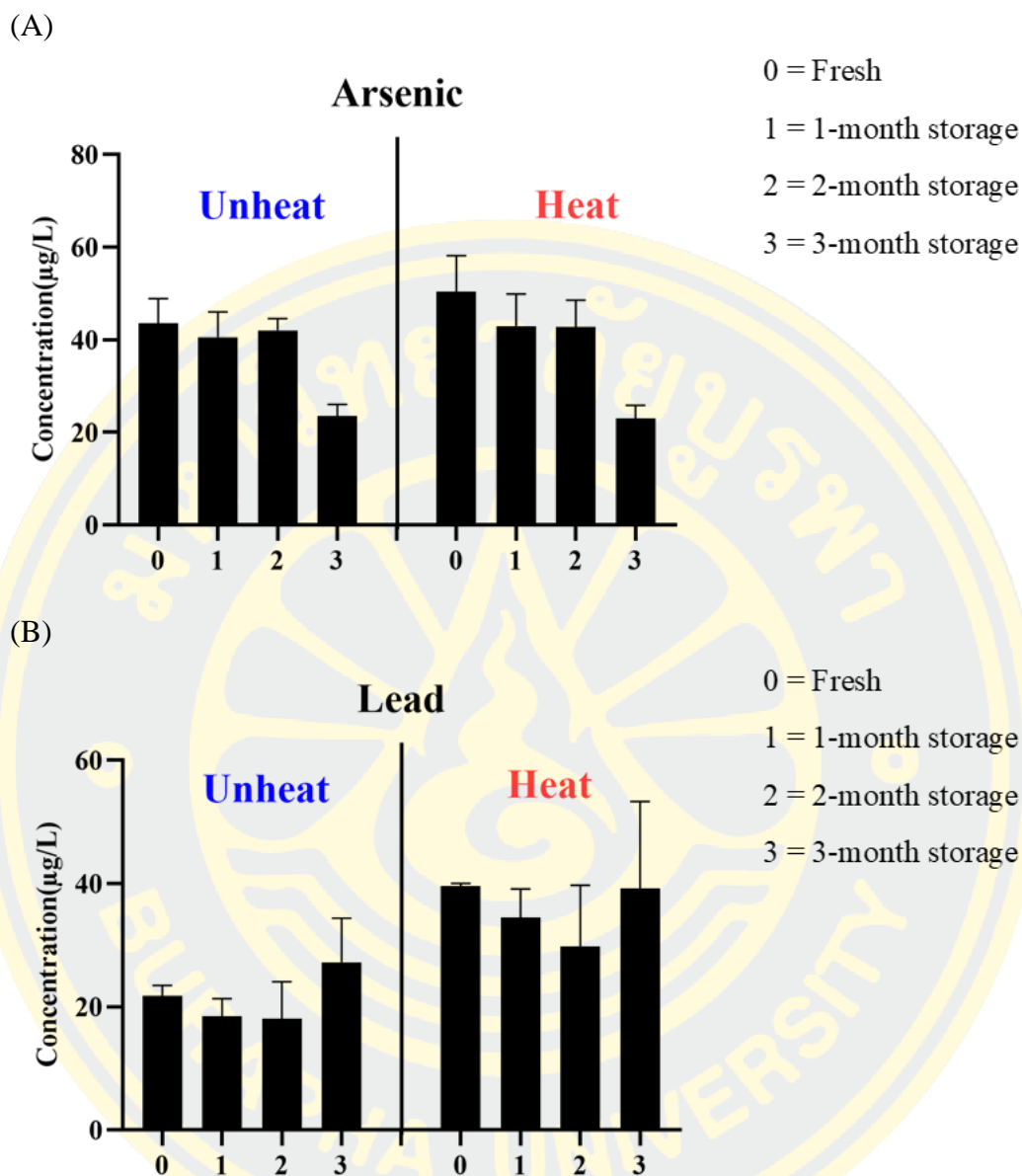
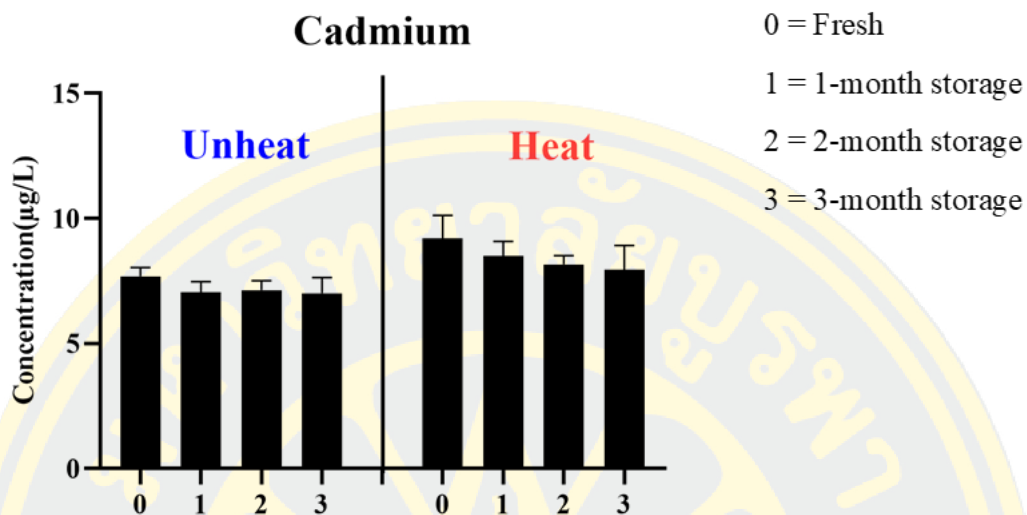


**Figure 44** Quantitation of toxic elements (As, Pb, Cd, and Cr) in each of unheated and heated BDL sample set (fresh, 1-month-, 2-month-, and 3-month-storage set). All of the toxic elements, As (A), Pb (B), Cd (C), and Cr (D), were analyzed by AAS technique. Error bars represent standard deviations (S.D.) from three replications of the data. All concentrations of toxic elements determined were summarized in Table

(C)



(D)

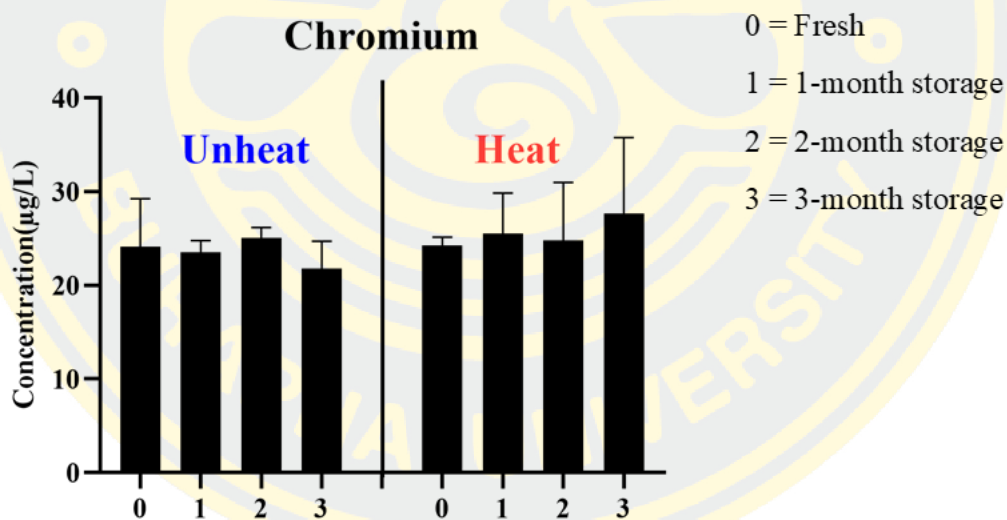


**Figure 44 (continued)** Quantitation of toxic elements (As, Pb, Cd, and Cr) in each of unheated and heated BDL sample set (fresh, 1-month-, 2-month-, and 3-month-storage set). All of the toxic elements, As (A), Pb (B), Cd (C), and Cr (D), were analyzed by AAS technique. Error bars represent standard deviations (S.D.) from three replications of the data. All concentrations of toxic elements determined were summarized in Table 7.



**Table 7** Summary of the quantitation of macronutrients, micronutrients, and toxic elements in unheated and heated BDL sample sets.

Parameters	BDL sample set											
	Fresh		1-Month storage		2-Month storage		3-Month storage					
	Unheat	Heat	Unheat	Heat	Unheat	Heat	Unheat	Heat	Unheat	Heat	Unheat	Heat
<b>Macronutrients (mg/l)</b>												
N	1321±169	923±61	1050±92	365±54	873±65	400±36	868±76	187±34				
P	122,953±	142,271±	20,919±	147,432±	360,487±	414,737±	515,416±	510,782±				
	25,085	8,389	36,553	17,025	9,376	48,379	13,727	56,087				
K	2226±153	2797±119	2345±452	2206±158	2271±254	2350±106	2111±76	2416±156				
Mg	65±11	65±10	58±3	45±14	56±7	52±15	48±8	48±6				
Ca	66±5	66±9	64±2	53±9	57±5	56±17	50±7	63±19				
<b>Micronutrients (mg/l)</b>												
Fe	3.25±0.33	3.50±0.31	3.24±0.07	3.22±0.22	2.91±0.08	3.26±0.69	2.79±0.20	3.17±0.48				
Cu	0.17±0.04	0.20±0.02	0.19±0.08	0.21±0.01	0.17±0.02	0.22±0.04	0.18±0.01	0.20±0.02				
Zn	0.84±0.12	0.93±0.05	0.94±0.06	0.89±0.08	0.83±0.07	0.93±0.18	0.86±0.04	0.87±0.07				
Mn	0.33±0.05	0.36±0.06	0.35±0.02	0.25±0.04	0.31±0.03	0.32±0.13	0.30±0.02	0.35±0.10				
Mo	0.11±0.01	0.14±0.01	0.10±0.00	0.11±0.01	0.10±0.01	0.11±0.01	0.13±0.02	0.14±0.01				
<b>Toxic elements (µg/l)</b>												
As	44±5	50±8	41±5	43±7	42±3	43±6	23±3	23±3				
Pb	22±2	40±1	19±3	34±5	18±6	30±10	27±7	40±14				
Cd	7.68±0.35	9.21±0.91	7.05±0.43	8.49±0.59	7.13±0.37	8.16±0.34	7.01±0.63	7.94±0.98				
Cr	24.16±5.10	24.26±0.89	23.53±1.28	25.52±4.33	25.04±1.15	24.78±6.22	21.77±2.96	27.66±8.12				

### 4.3 The optimal condition for HPLC-MS/MS analysis of authentic plant hormones and plant growth promoting compounds

Before analysis of plant hormones and plant-growth promoting compounds in BDL samples by HPLC-MS/MS (triple-quadrupole LC/MS), the condition for HPLC-MS/MS to monitor plant hormones and plant-growth promoting compounds were necessarily optimized. The authentic plant hormones and plant-growth promoting compounds – indole 3 acetic acid (IAA), abscisic acid (ABA), gibberellic acid (GA<sub>3</sub>), jasmonic acid (JA), salicylic acid (SA), kinetin, zeatin, 5-aminolevulinic acid (ALA), and pipercolinic acid (Pip) – at a certain concentration were used for optimizing the HPLC and MS/MS conditions.

Our results shown in Figure 45 demonstrated that the optimal HPLC-MS/MS condition for compound separation and detection was successfully carried out in a ZORBAX Eclipse Plus C<sub>18</sub> column (5 m, 4.6 x 250 mm, Agilent Technologies) with a solvent mixture of Solvents A (Milli-Q® Type I ultrapure water) and Solvent B (MeOH) (see Tables 4 and 5). It was found that these compounds were individually detected with two different modes : negative and positive modes. Most compounds were detected in a negative mode, excepting kinetin, Pip, and ALA that were detected in a positive mode (Figure 45 and Table 8). In addition, the multiple reaction mode (MRM) parameters (precursor ion, collision energy, product ion, and fragmentor voltage) were also optimized for each compound (Table 8).

In a negative mode, IAA was present at the retention time (RT) 7.9 min (Figure 45A) with the optimized MRM parameters as follows: precursor ion (Q1, 174), collision energy (Q2, 14 V), product ion (Q3, 129.6), and fragmentor voltage (135 V). The RT of GA<sub>3</sub> was present at a time about 1 min less than that of IAA (Figure 45B). It was found that there were two peaks at RT at 6.7 (minor) and 7.2 (major) min detected for GA<sub>3</sub>. The major peak at RT 7.2 min was identified as the peak of GA<sub>3</sub>. While it was primarily proposed that the minor peak with RT 6.7 min could be a decomposed isoform namely gibberellenic acid (GE), which may be occurred in aqueous solution under a certian pH or temperature (Camara et al., 2018). The optimized MRM parameters for GA<sub>3</sub> (RT 7.2 min) were as follows: precursor ion (Q1, 345), collision energy (Q2, 31 V), product ion (Q3, 143.1), and fragmentor voltage (135 V). For ABA, the RT was present at 8.4 min, about 1 min longer than

GA<sub>3</sub> (Figure 45C), with the optimized MRM parameters as follows: precursor ion (Q1, 263), collision energy (Q2, 16 V), product ion (Q3, 152.6), and fragmentor voltage (135 V). While the chromatogram of zeatin showed a peak at a shorter RT 5.4 min (Figure 45D) with the optimized MRM parameters as follows: precursor ion (Q1, 218), collision energy (Q2, 19 V), product ion (Q3, 134), and fragmentor voltage (124 V). The RT of JA was present at 9.0 min and close to ABA (Figure 45E). Its MRM parameters were optimized as follows: precursor ion (Q1, 209), collision energy (Q2, 11 V), product ion (Q3, 59.1), and fragmentor voltage (150 V). For SA (Figure 45F), its RT was present at 8.4 min the same as ABA. The MRM parameters for SA detection were optimized as follows: precursor ion (Q1, 137), collision energy (Q2, 19 V), product ion (Q3, 93), and fragmentor voltage (98 V).

In a positive mode, the chromatogram of kinetin showed a peak at RT 6.8 min (Figure 46A) with the optimized MRM parameters of precursor ion (Q1, 216), collision energy (Q2, 23 V), product ion (Q3, 81.1), and fragmentor voltage (98 V). For Pip, the RT was present at 6.0 min (Figure 46B) with the MRM parameters optimized as follows: precursor ion (Q1, 162), collision energy (Q2, 3 V), product ion (Q3, 120.9), and fragmentor voltage (46 V). Lastly, the ALA chromatogram showed its RT at 6.5 min (Figure 46C) with the optimized MRM parameters as follows: precursor ion (Q1, 132), collision energy (Q2, 59 V), product ion (Q3, 43.2), and fragmentor voltage (46 V). The optimized MRM parameters for each compound were summarized in Table 8. Our chromatographic data demonstrated that each compound can be detected by the setup and optimized HPLC-MS/MS conditions, which have been used for further studies (see later in the next sections).

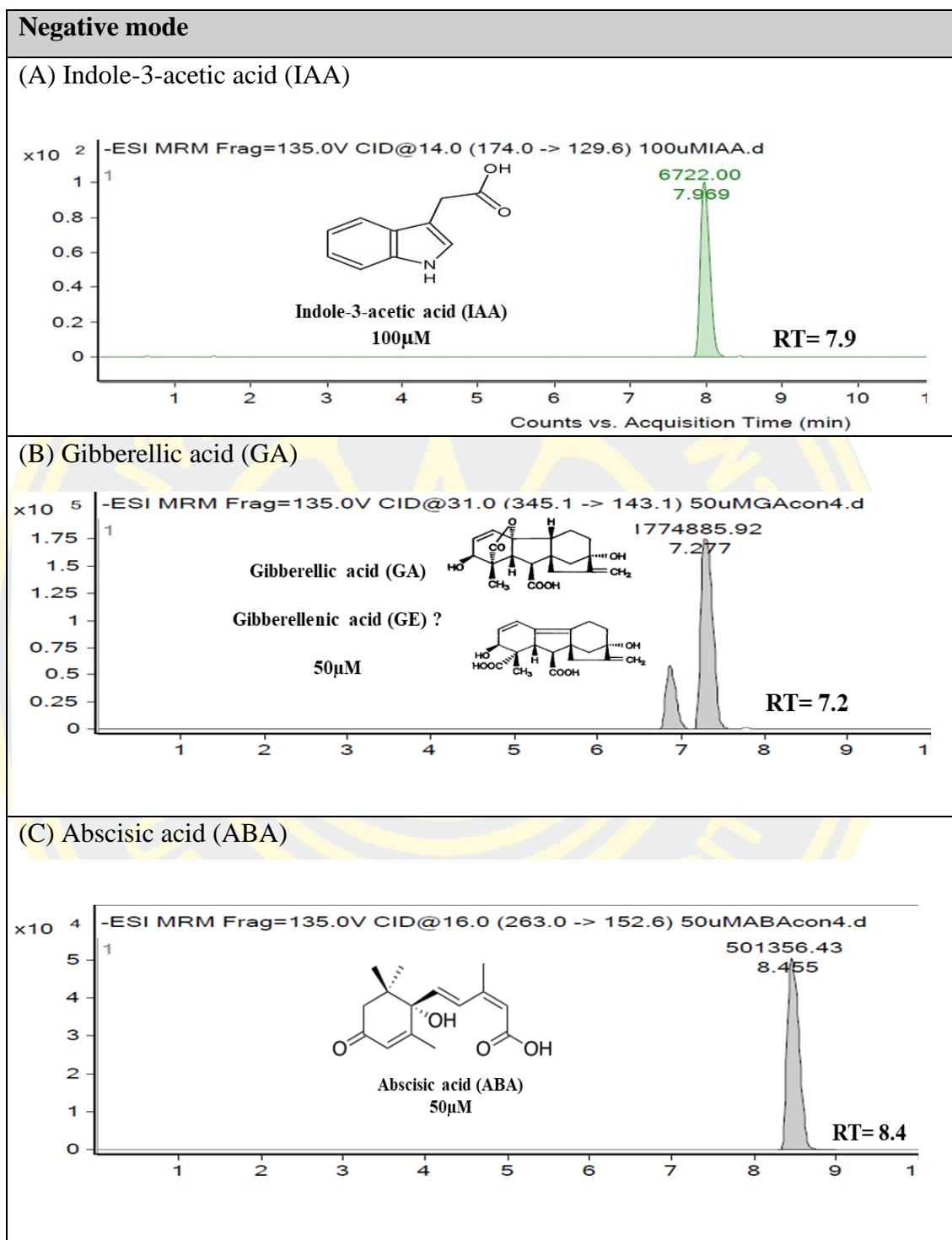


**Figure 45** The chromatograms of plant hormones and plant-growth promoting compounds together with their structures of (A) IAA, (B) GA<sub>3</sub>, (C) ABA, (D) zeatin, (E) JA, and (F) SA detected by LC-MS/MS in a negative mode.

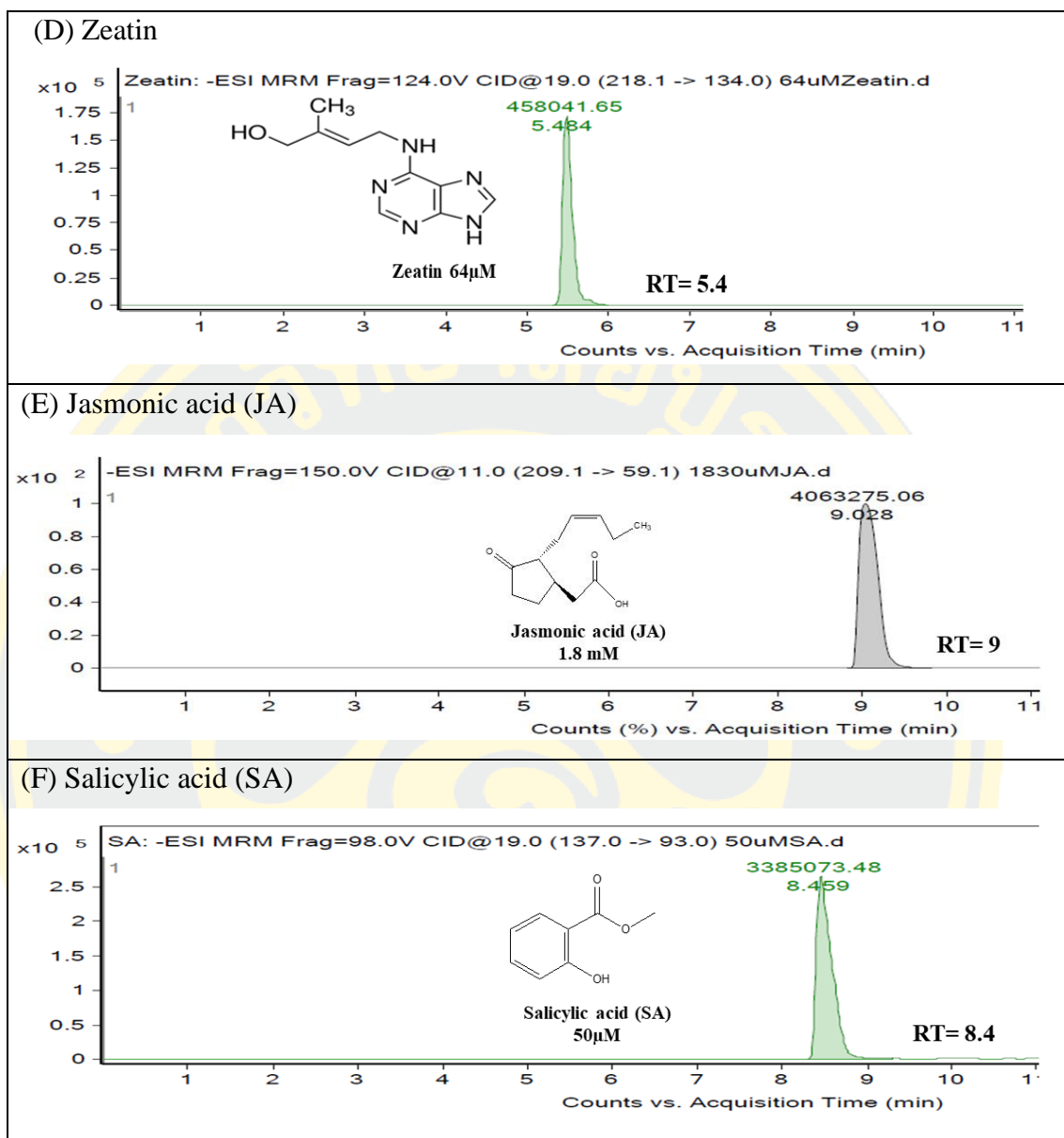


**Figure 45 (continued)** The chromatograms of plant hormones and plant-growth promoting compounds together with their structures of (A) IAA, (B) GA<sub>3</sub>, (C) ABA, (D) zeatin, (E) JA, and (F) SA detected by LC-MS/MS in a negative mode.

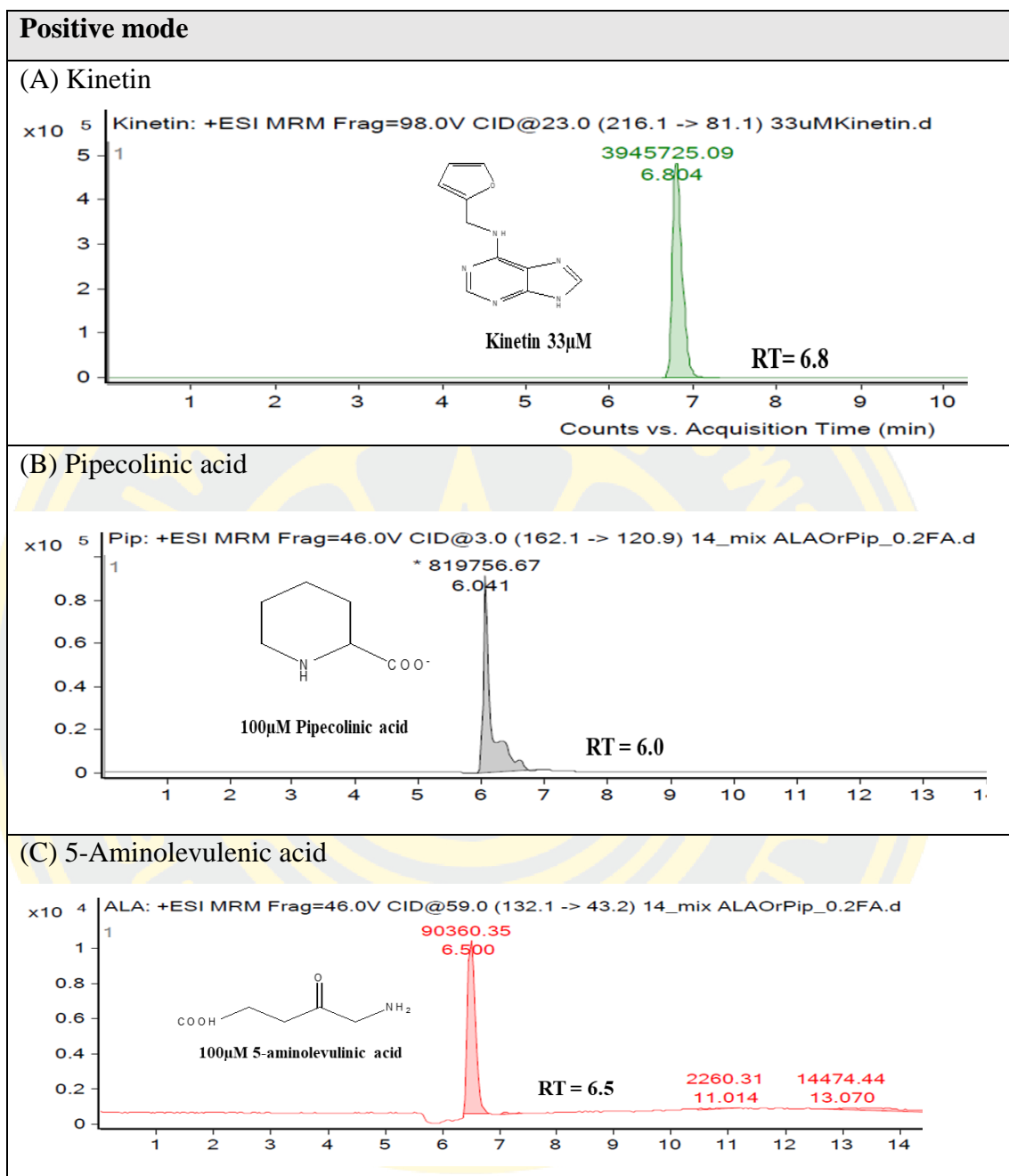


**Figure 46** The chromatograms of plant hormones and plant-growth promoting compounds together with their structures of (A) kinetin, (B) Pip, and (C) ALA detected by LC-MS/MS in a positive mode.

**Table 8** The optimized multiple reaction mode (MRM) parameters for electrospray ionization measurement of plant hormones and plant-growth promoting compounds.

Standard compound	Detection mode	Retention time (min)	Precursor ion (Q1)	Collision energy (V) (Q2)	Product ion (Q3)	Fragmentor voltage (V)
IAA	negative	7.9	174	14	129.6	135
ABA	negative	8.4	263	16	152.6	135
GA <sub>3</sub>	negative	7.2	345	31	143.1	135
SA	negative	8.4	137	19	93	98
JA	negative	9	209	11	59.1	150
Zeatin	negative	5.4	218	19	134	124
Kinetin	positive	6.8	216	23	81.1	98
Pip	positive	6.0	162	3	120.9	46
ALA	positive	6.5	132	59	43.2	46
Ampicillin (IS)	negative	6.2	348	35	74.1	100
	positive	15.0	350			
IPTG (IS)	negative	9.2	237	15	216.9	124
	positive	14.0	239	39	45.2	

#### 4.4 The optimal condition of internal standard (IS) for HPLC-MS/MS analysis

To validate the HPLC-MS/MS analysis, the internal standard (IS) was necessarily optimized. IPTG (78.12 $\mu$ M) and ampicillin (100  $\mu$ M) were chosen as candidates since they were expected to be not appeared in BDL samples. Both compounds were examined in both negative and positive modes.

The results showed that in a negative mode, the peak chromatogram of ampicillin was clear and sharp with the RT at 6.2 min (Figure 47A) with the optimized MRM parameters (Table 8) of the precursor ion (Q1, 348.1), collision energy (Q2, 35 V), product ion (Q3, 74.1), and fragmentor voltage (100 V). While the peak chromatogram of IPTG was broadened with the RT at 9.2 min (Figure 47B) with the optimized MRM parameters as follows (Table 8): precursor ion (Q1, 237.1), collision energy (Q2, 15 V), product ion (Q3, 216.9), and fragmentor voltage (124 V). For a positive mode, ampicillin was present with a clear, sharp peak at RT 15.0 min (Figure 47C) with the optimized MRM parameters similar to the negative mode (Table 8). For IPTG, it was present with a clear, sharp peak at RT 14.0 min (Figure 47D) with the optimized MRM parameters (Table 8) of the precursor ion (Q1, 239.1), collision energy (Q2, 39 V), product ion (Q3, 45.2), and fragmentor voltage (124 V). Based on the RT together with the clear peak chromatogram, ampicillin was the best compound suitable for being used as an IS for HPLC-MS/MS analysis.



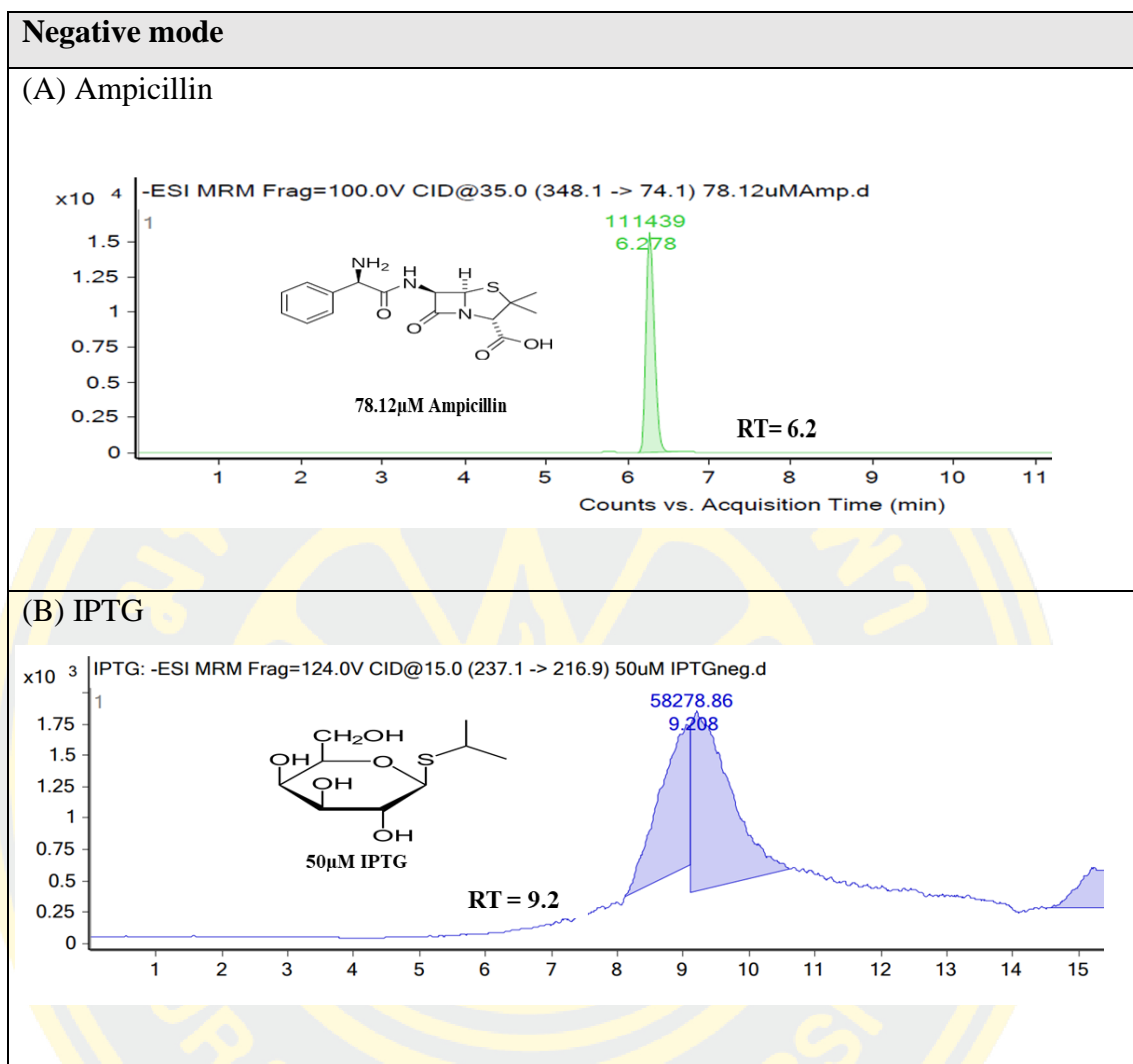


**Figure 47** The peak chromatogram of ampicillin (A and C) and IPTG (B and D) in the negative and positive modes.

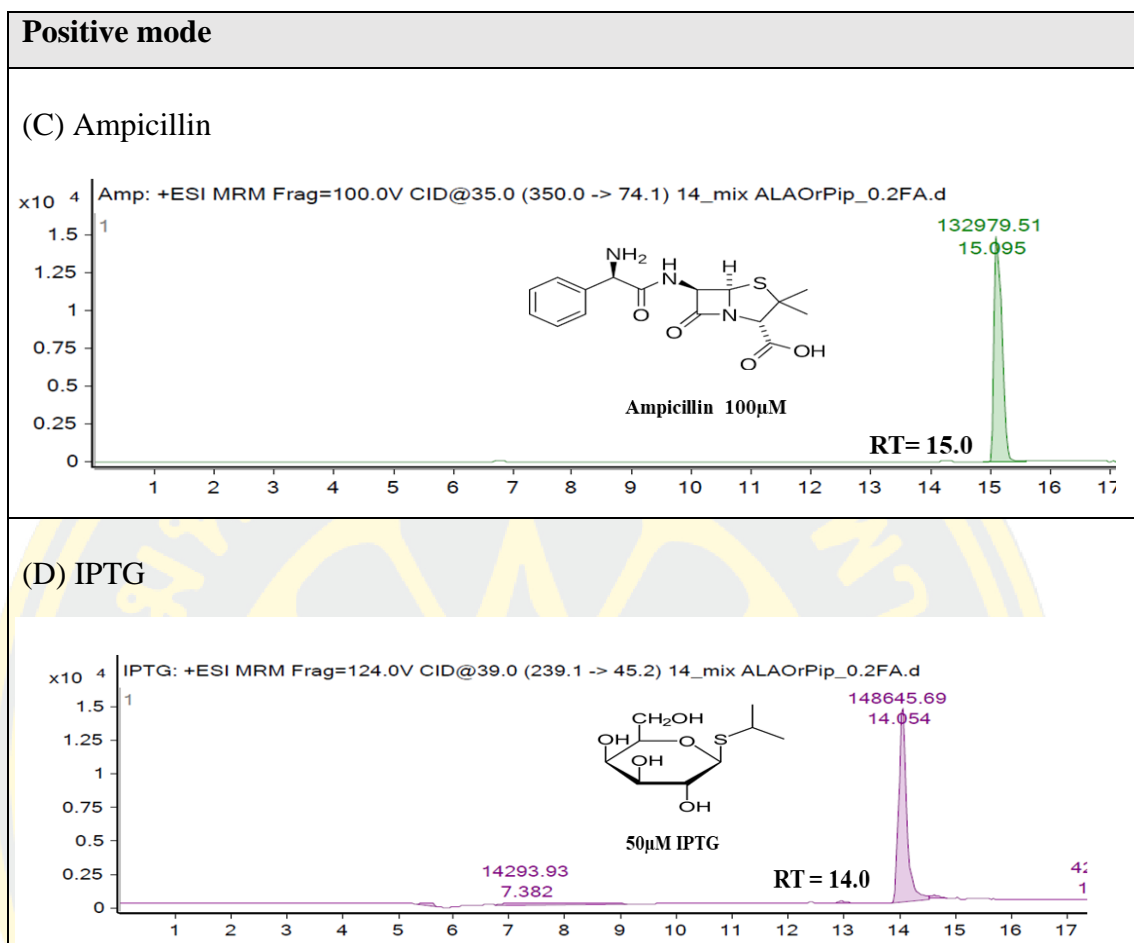


**Figure 47 (continued)** The peak chromatogram of ampicillin (A and C) and IPTG (B and D) in the negative and positive modes.

#### **4.5 Temperature effect on stability of plant hormones and plant-growth promoting compounds as well as internal standard**

Since BDL samples in this work were also subjected to heating conditions at 100 °C for 30 min, we investigated if the heating temperatures may affect the stability of plant hormones and plant-growth promoting compounds. The experiments were carried out at two different temperatures, 40 and 100 °C as described in Research Methodology section 3.11. The results are shown in Figure 48 demonstrated that the amount of plant hormones and plant-growth promoting compounds including IAA, GA<sub>3</sub>, ABA, SA, zeatin, kinetin, ALA, and Pip as well as ampicillin (an internal standard) tested remained constant under both temperatures as compared to the unheated condition. The data indicated that these compounds are not temperature-sensitive at either 40 or 100 °C. Our current data obtained were contradict to the previous report, which found that major plant hormones, such as IAA, GA<sub>3</sub>, and ABA, derived from the AD system were not tolerant to high temperatures (Li et al., 2016)

### Plant hormones stability

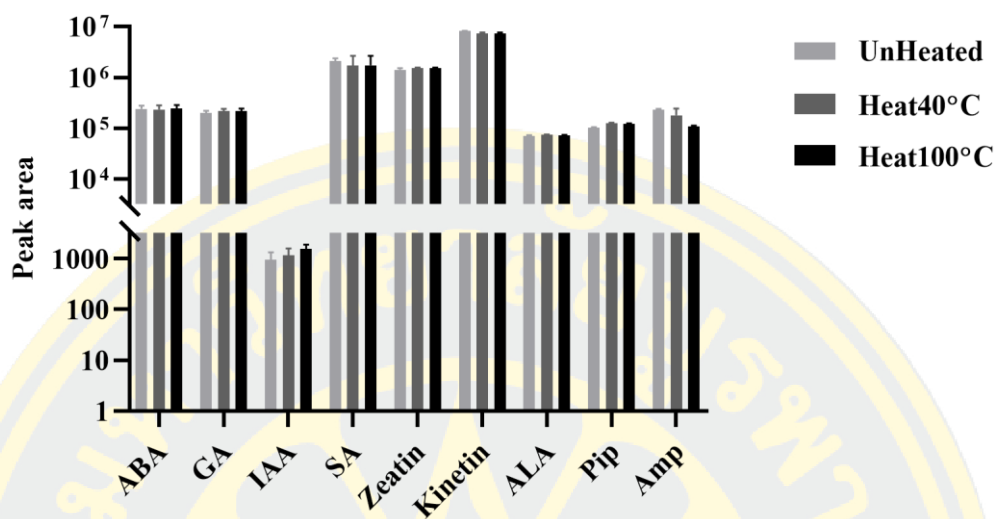


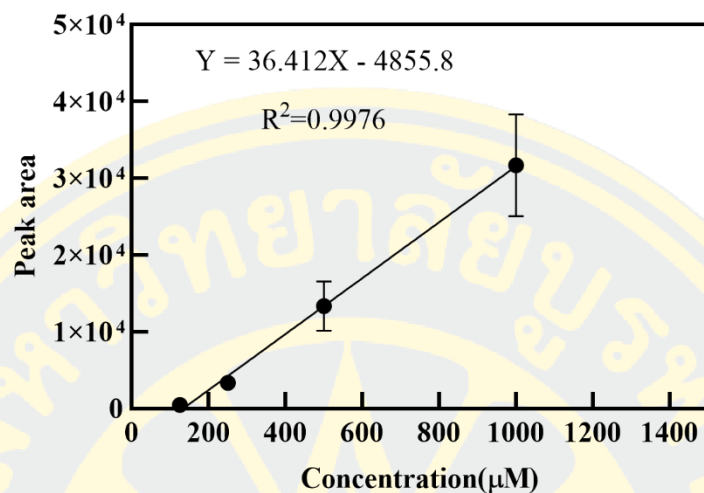
**Figure 48** Effect of temperatures at 40 and 100 °C on the stability of plant hormones and plant-growth promoting compounds including IAA, GA<sub>3</sub>, ABA, SA, zeatin, kinetin, ALA, and Pip as well as ampicillin (an internal standard). Error bars represent standard deviations (S.D.) from three replications of the data.

#### 4.6 The calibration curves of plant hormones and plant-growth promoting compounds and their limit of detection (LOD) and limit of quantitation (LOQ) values

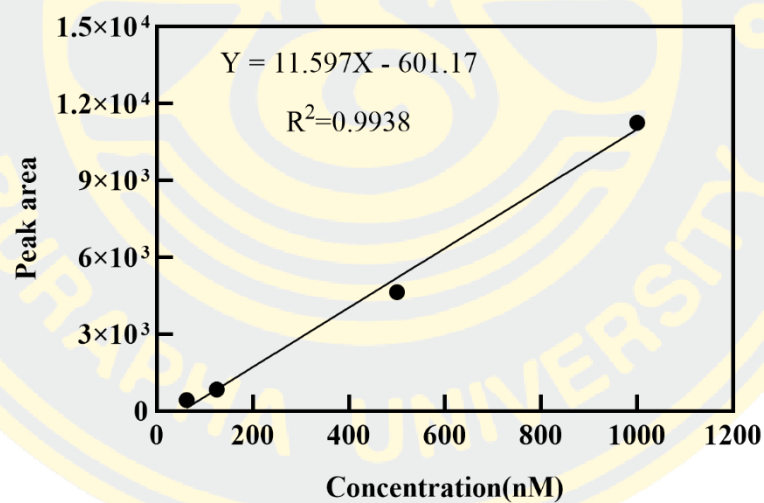
To determine LOD and LOQ values, the calibration curve plot of various concentrations of each authentic plant hormone and plant-growth promoting compound *versus* peak area were constructed. The results shown in Figure 49 demonstrated that each plant hormone and plant-growth promoting compound including IAA, GA<sub>3</sub>, ABA, SA, zeatin, kinetin, ALA, and Pip represented its calibration curve plot with different concentration ranges, coefficient of determination (R<sup>2</sup>) values for linear regression, and LOD and LOQ values (Table 9).

For IAA calibration curve (Figure 49A), the concentration ranges were 125-1,000 µM with R<sup>2</sup> value of 0.9976. The LOD and LOQ values for IAA were determined to be 32.74 and 99.21 µM, respectively (Table 9). The calibration curve of ABA was constructed in nanomolar concentration ranges of 62.5-1,000 nM and R<sup>2</sup> value of 0.9938 (Figure 49B). The LOD and LOQ values for ABA were of 51.84 and 157.23 nM, respectively (Table 9). For GA<sub>3</sub>, the concentration ranges of the calibration curve were as 39.0625-2,500 nM with R<sup>2</sup> value of 0.9983 (Figure 49C) and the calculated LOD and LOQ values were determined as 29.40 and 89.09 nM, respectively (Table 9). For SA calibration curve, the concentration ranges were of 1.56-25.00 µM with R<sup>2</sup> value of 0.9986 (Figure 49D). The LOD and LOQ values for SA were calculated to be 0.41 and 1.25 µM, respectively (Table 9). For kinetin, the concentration ranges for constructing the calibration curve were as 62.5-4,000 nM with R<sup>2</sup> value of 0.9907 (Figure 49E) and the calculated LOD and LOQ were determined to be 153.22 and 464.01 nM, respectively (Table 9). The calibration curve of zeatin was constructed by the concentration ranges of 7.80-1,000 nM with R<sup>2</sup> value of 0.9998 (Figure 49F). The LOD and LOQ values for zeatin were calculated to be 2.42 and 7.33 nM, respectively (Table 9). For Pip calibration curve (Figure 49G), the concentration ranges were 7.80-250 µM with R<sup>2</sup> value of 0.9928 and the calculated LOD and LOQ values were determined as 13.13 and 39.78 µM, respectively (Table 9). For the calibration curve of ALA, the concentration ranges were of 7.80-250 µM with R<sup>2</sup> value of 0.9986 (Figure 49H). The LOD and LOQ values for ALA were calculated to be 9.89 and 29.98 µM, respectively (Table 9).

(A)

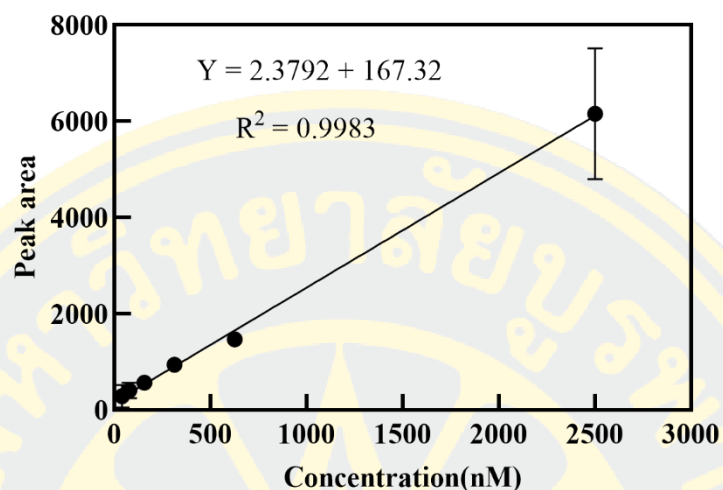
**Indole-3-acetic acid (IAA)**

(B)

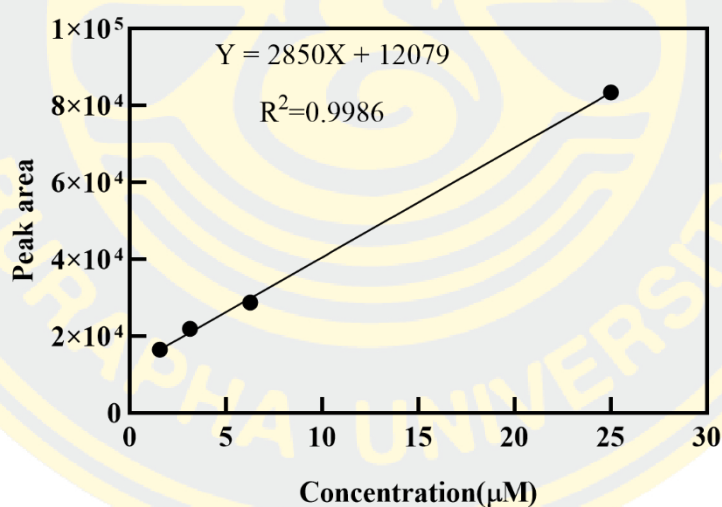
**Abscisic acid (ABA)**

**Figure 49** The calibration curve plot of various concentrations of each plant hormone and plant-growth promoting compound – (A) IAA, (B) ABA, (C)  $\text{GA}_3$ , (D) SA, (E) kinetin, (F) zeatin, (G) Pip, and (H) ALA – *versus* peak area. The coefficient of determination ( $R^2$ ) values for linear regression and the LOD and LOQ values for each calibration curve was calculated and summarized in Table 9. Error bars represent standard deviations (S.D.) from three replications of the data.

(C)

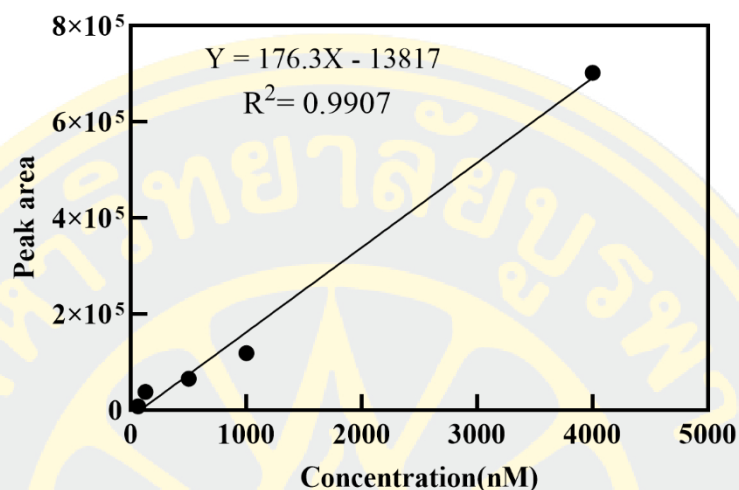
**Gibberellic acid (GA)**

(D)

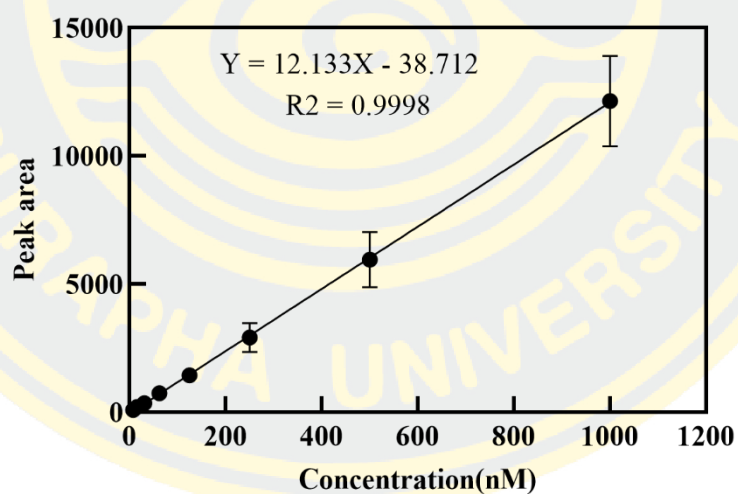
**Salicylic acid**

**Figure 49 (continued)** The calibration curve plot of various concentrations of each plant hormone and plant-growth promoting compound – (A) IAA, (B) ABA, (C) GA<sub>3</sub>, (D) SA, (E) kinetin, (F) zeatin, (G) Pip, and (H) ALA – versus peak area. The coefficient of determination ( $R^2$ ) values for linear regression and the LOD and LOQ values for each calibration curve was calculated and summarized in Table 9. Error bars represent standard deviations (S.D.) from three replications of the data.

(E)

**Kinetin**

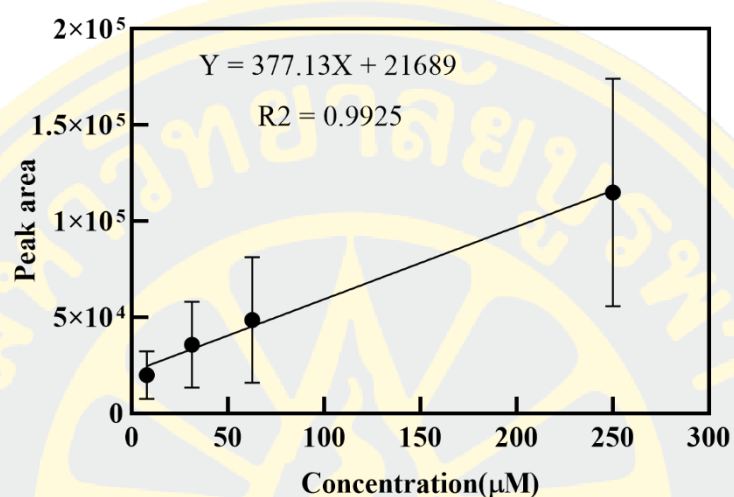
(F)

**Zeatin**

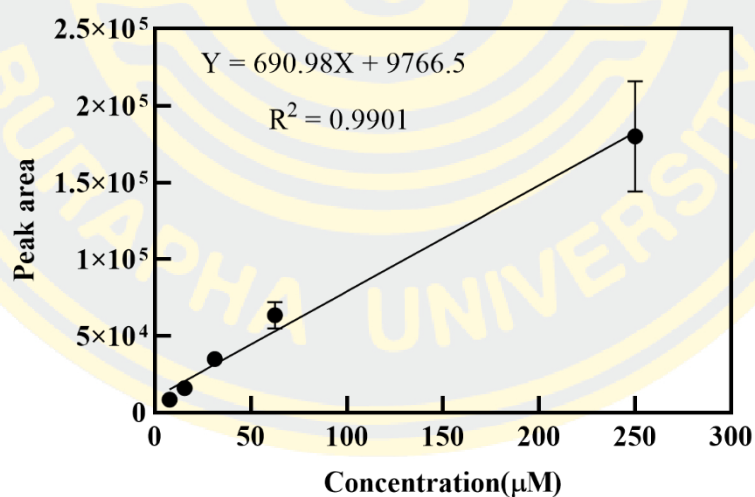
**Figure 49 (continued)** The calibration curve plot of various concentrations of each plant hormone and plant-growth promoting compound – (A) IAA, (B) ABA, (C) GA<sub>3</sub>, (D) SA, (E) kinetin, (F) zeatin, (G) Pip, and (H) ALA – versus peak area. The coefficient of determination ( $R^2$ ) values for linear regression and the LOD and LOQ values for each calibration curve was calculated and summarized in Table 9. Error bars represent standard deviations (S.D.) from three replications of the data.



(G)

**Pipecolic acid (Pip)**

(H)

**5-Aminolevulinic acid (ALA)**

**Figure 49 (continued)** The calibration curve plot of various concentrations of each plant hormone and plant-growth promoting compound – (A) IAA, (B) ABA, (C)  $\text{GA}_3$ , (D) SA, (E) kinetin, (F) zeatin, (G) Pip, and (H) ALA – versus peak area. The coefficient of determination ( $R^2$ ) values for linear regression and the LOD and LOQ values for each calibration curve was calculated and summarized in Table 9. Error bars represent standard deviations (S.D.) from three replications of the data.

**Table 9** The summary of concentration ranges, coefficient of determination ( $R^2$ ) values for linear regression, and LOD and LOQ values from the calibration curve of each plant hormone and plant-growth promoting compound.

<b>Compounds (Concentration unit)</b>	<b>Concentration range</b>	<b><math>R^2</math></b>	<b>LOD</b>	<b>LOQ</b>
IAA( $\mu$ M)	125-1,000	0.9976	32.74	99.21
ABA (nM)	62.5-1,000	0.9938	51.89	157.23
GA <sub>3</sub> (nM)	39.0625-2,500	0.9983	29.40	89.09
SA ( $\mu$ M)	1.56-25.00	0.9986	0.41	1.25
Kinetin (nM)	62.5-4,000	0.9907	153.12	464.01
Zeatin (nM)	7.80-1,000	0.9998	2.42	7.33
Pip ( $\mu$ M)	7.80-250	0.9928	13.13	39.78
ALA ( $\mu$ M)	7.80-250	0.9986	9.89	29.98

#### **4.7 The recovery yield of authentic plant hormones and plant-growth promoting compounds under solid phase extraction (SPE) method**

To ensure that the setup workflow and SPE method used were suitable for extraction of plant hormones and plant-growth promoting compounds in BDL samples, we hence measured the recovery yield of all authentic compounds including IAA, ABA, GA<sub>3</sub>, SA, kinetin, zeatin, Pip, and ALA as well as ampicillin (IS) before applying onto the real BDL samples. All authentic compounds were prepared as a mixture reagent (200  $\mu$ M each) and mixed with 1 mM ampicillin before carrying out through the workflow and SPE process.

##### **4.7.1 The recovery yield of authentic compounds under an initial workflow**

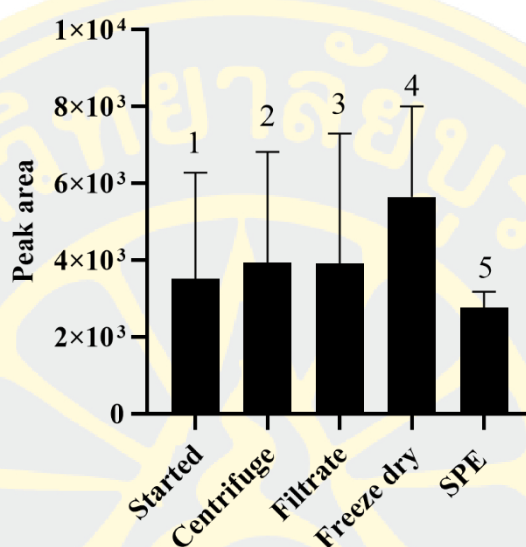
Based on the workflow and SPE process shown in Figures 39 and 40, many technical steps including centrifugation, filtration, freeze-drying, and the SPE process (washing, desalting and elution steps) were critically involved in the recovery yield of authentic compounds. Therefore, we first monitored the recovery yield of authentic compounds at each technical step using an initial workflow (Figures 39 and 40) in which an ultrapure water, 5% (v/v) MeOH and 100% ACN were used in washing, desalting, and elution steps of the SPE process, respectively. In this experiment, some key authentic compounds such as IAA, ABA, GA<sub>3</sub>, and SA, and ampicillin were examined. The peak area of each compound was determined from triple-quadrupole LC/MS chromatogram and represented for the recovery yield.

The results obtained from triple-quadrupole LC/MS analysis (Figure 50) showed that all authentic compounds examined – IAA (Figure 50A), ABA (Figure 50B), GA<sub>3</sub> (Figure 50C), and SA (Figure 50D) and ampicillin (Figure 50E) – can be recovered almost 100% after passing through centrifugation, filtration, and freeze-drying steps since their peak areas were comparable to the peak area of the starting reagent. However, the recovery yield of each compound was significantly decreased (20-75% reduction) when passed through the washing, desalting and elution steps of SPE process. The data suggest that the SPE process in the initial workflow was not well optimized. Hence, we investigated further to fine-tune the desalting and elution of authentic compounds (see next section). It should be noted that the washing step by

an ultrapure water was not optimized as it was a required preceding step prior to desalting.

(A)

### Indole-3-acetic acid (IAA)



(B)

### Abscisic acid (ABA)

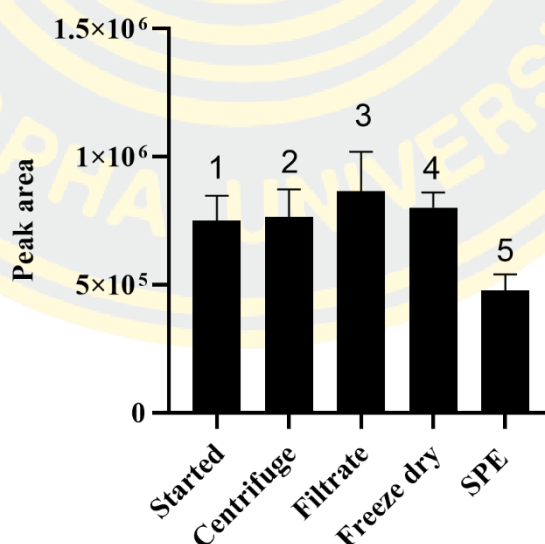
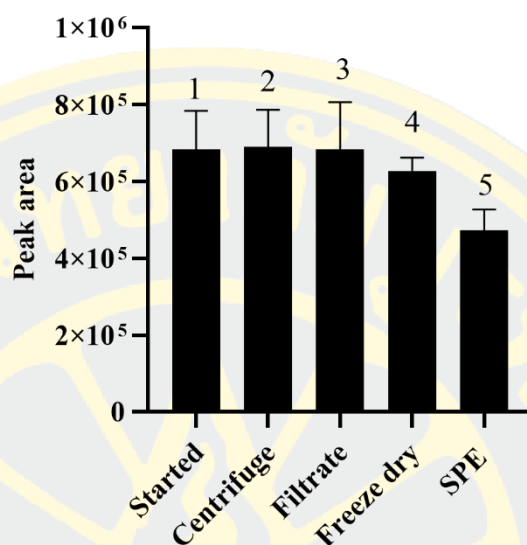


**Figure 50** The peak area determined from triple-quadrupole LC/MS chromatogram representing the recovery yield of each plant hormone and plant-growth promoting compound – (A) IAA, (B) ABA, (C) GA<sub>3</sub>, (D) SA, and (E) ampicillin – passed through the technical steps including steps (1) starting reagent, (2) centrifugation, (3)

filtration, (4) freeze-drying, and (5) SPE process (desalting and elution steps). Error bars represent standard deviations (S.D.) from three replications of the data

(C)

### Gibberellic acid (GA)



(D)

### Salicylic acid (SA)

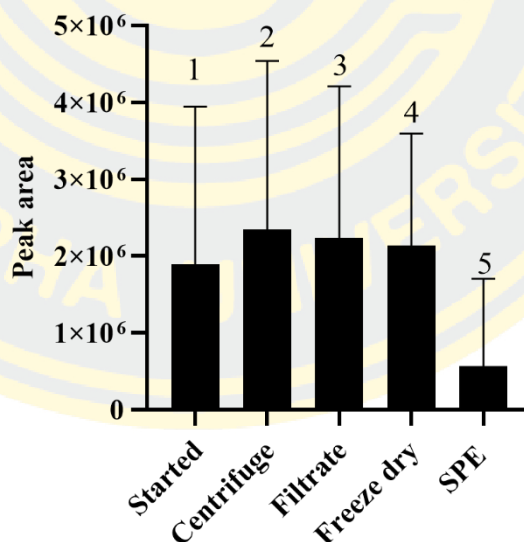


**Figure 50 (continued)** The peak area determined from triple-quadrupole LC/MS chromatogram representing the recovery yield of each plant hormone and plant-growth promoting compound – (A) IAA, (B) ABA, (C) GA<sub>3</sub>, (D) SA, and (E) ampicillin – passed through the technical steps including steps (1) starting reagent, (2) centrifugation, (3) filtration, (4) freeze-drying, and (5) SPE process (desalting and

elution steps). Error bars represent standard deviations (S.D.) from three replications of the data.

(E)

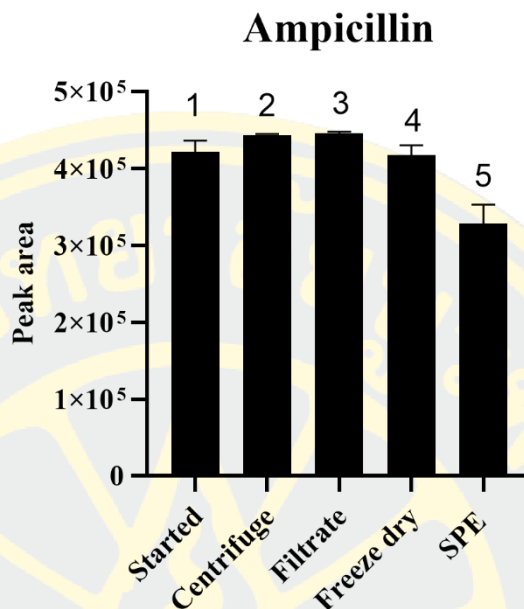


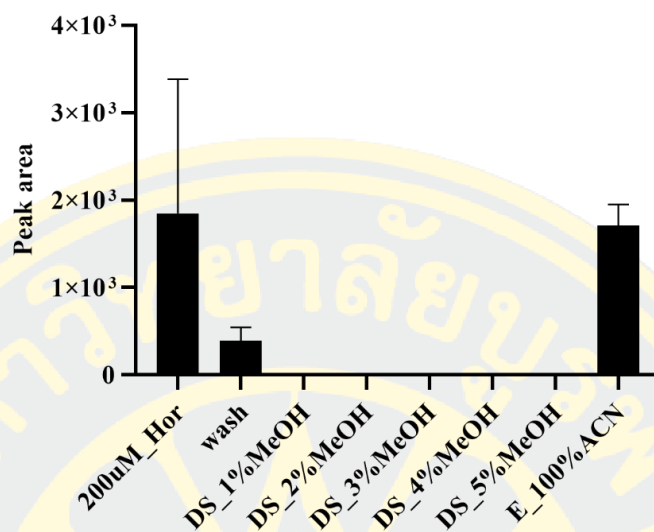
**Figure 50 (continued)** The peak area determined from triple-quadrupole LC/MS chromatogram representing the recovery yield of each plant hormone and plant-growth promoting compound – (A) IAA, (B) ABA, (C) GA<sub>3</sub>, (D) SA, and (E) ampicillin – passed through the technical steps including steps (1) starting reagent, (2) centrifugation, (3) filtration, (4) freeze-drying, and (5) SPE process (desalting and elution steps). Error bars represent standard deviations (S.D.) from three replications of the data.

#### 4.7.2 The optimal desalting step for yield recovery of authentic compounds

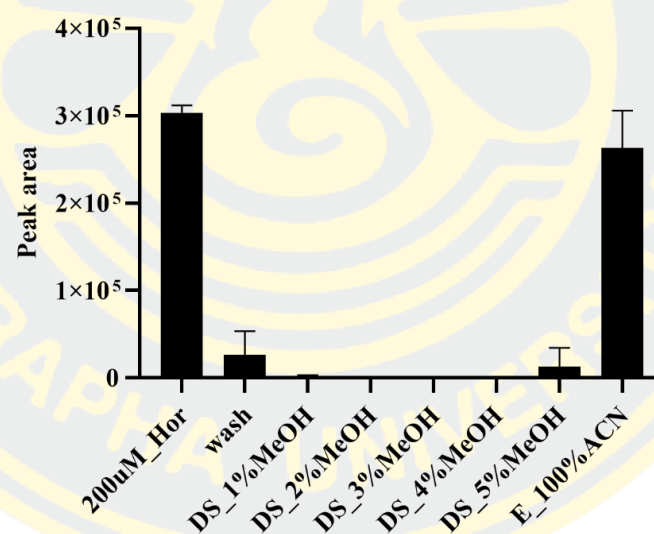
To optimize the desalting step, different % (v/v) of MeOH including 1, 2, 3, 4, and 5% (v/v) were used to remove salt from the SPE cartridge (Sep-Pak C18) after loading of a mixture reagent of authentic compounds (200  $\mu$ M each of IAA, ABA, GA<sub>3</sub>, SA, kinetin, zeatin, Pip, and ALA as well as ampicillin (IS)). 100% ACN was used for the elution step to ensure that all amounts of authentic compounds were eluted from the SPE cartridge. The peak area of each compound was determined from triple-quadrupole LC/MS chromatogram and represented for the recovery yield.

The results shown in Figure 51 demonstrated that the recovery yield of most of authentic compounds examined – IAA (Figure 51A), ABA (Figure 51B), GA<sub>3</sub> (Figure 51C), SA (Figure 51D), kinetin (Figure 51E), zeatin (Figure 51F), Pip (Figure 51G), and ALA (Figure 51H) as well as ampicillin (Figure 51I) - were lost in the desalting step with 5% (v/v) MeOH, while the desalting with 1-4 % (v/v) MeOH did not affect the binding of authentic compounds to the cartridge, excepting for Pip and ALA which was lost during all the desalting steps. It should be noted that all of the authentic compounds were lost in very low amounts, except for Pip and ALA, during the washing step with an ultrapure water (a requisite step before desalting). Pip and ALA was lost abundantly in the washing step, suggesting that these two compounds were not likely binding with the cartridge and the conditions for separation and extraction for these two compounds were not optimized yet. Based on this data, it was suggested that the optimal desalting step can be either 1, 2, 3, or 4% (v/v) MeOH. Hence, we selected 2% (v/v) MeOH as a desalting step for further studies since this MeOH concentration was not too low or too high for the desalting step.

(A)

**Indole-3-acetic acid (IAA)**

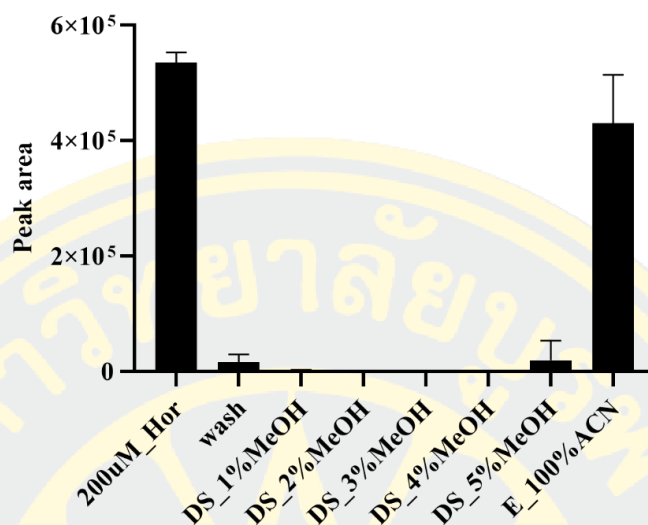
(B)

**Abscisic acid (ABA)**

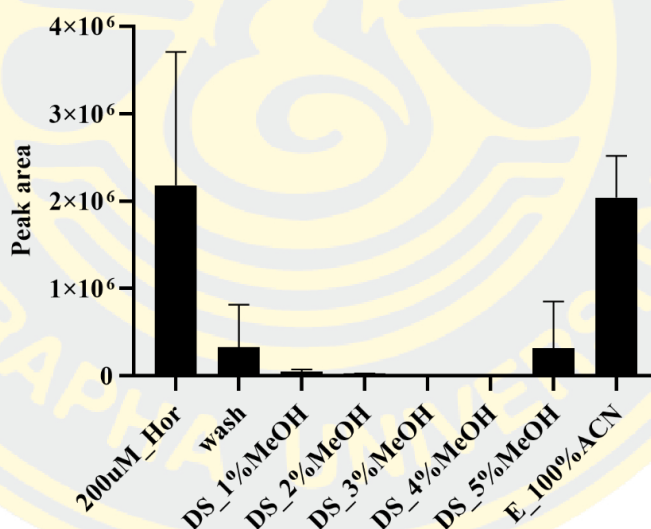
**Figure 51** The peak area determined from triple-quadrupole LC/MS chromatogram representing the recovery yield of each plant hormone and plant-growth promoting compound – (A) IAA, (B) ABA, (C) GA<sub>3</sub>, (D) SA, (E) kinetin, (F) zeatin, (G) Pip, (H) ALA, and (I) ampicillin – passed through the desalting (DS) steps with different % (v/v) MeOH (1, 2, 3, 4, and 5% v/v). The step “200  $\mu$ M\_Hor” and “E\_100ACN” denotes the starting mixture reagent (200  $\mu$ M each) and the cartridge elution with 100% ACN, respectively. Error bars represent standard deviations (S.D.) from three replications of the data



(C)

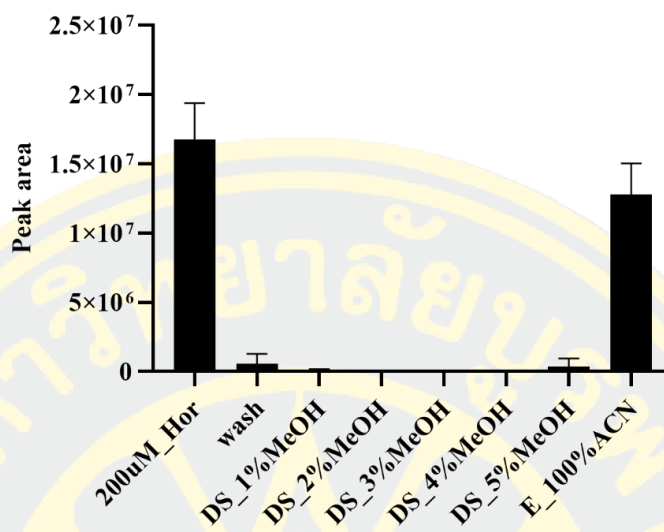
**Gibberellic acid (GA)**

(D)

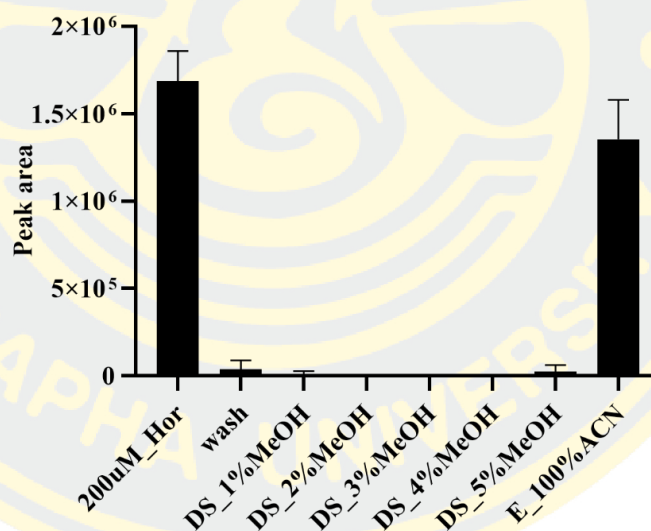
**Salicylic acid (SA)**

**Figure 51 (continued)** The peak area determined from triple-quadrupole LC/MS chromatogram representing the recovery yield of each plant hormone and plant-growth promoting compound – (A) IAA, (B) ABA, (C) GA<sub>3</sub>, (D) SA, (E) kinetin, (F) zeatin, (G) Pip, (H) ALA, and (I) ampicillin – passed through the desalting (DS) steps with different % (v/v) MeOH (1, 2, 3, 4, and 5% v/v). The step “200  $\mu$ M\_Hor” and “E\_100ACN” denotes the starting mixture reagent (200  $\mu$ M each) and the cartridge elution with 100% ACN, respectively. Error bars represent standard deviations (S.D.) from three replications of the data

(E)

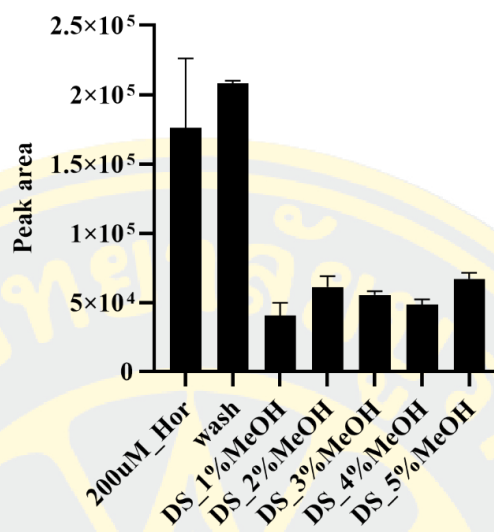
**Kinetin**

(F)

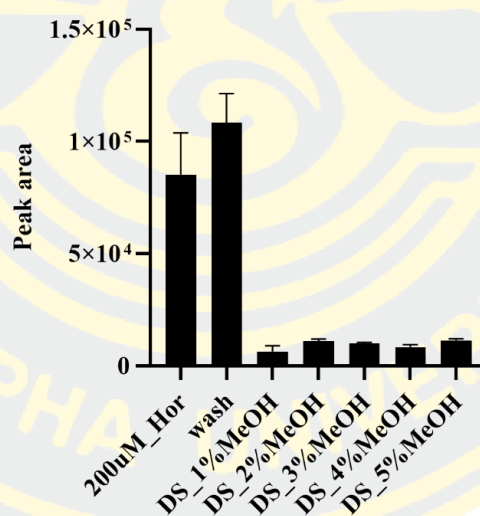
**Zeatin**

**Figure 51 (continued)** The peak area determined from triple-quadrupole LC/MS chromatogram representing the recovery yield of each plant hormone and plant-growth promoting compound – (A) IAA, (B) ABA, (C) GA<sub>3</sub>, (D) SA, (E) kinetin, (F) zeatin, (G) Pip, (H) ALA, and (I) ampicillin – passed through the desalting (DS) steps with different % (v/v) MeOH (1, 2, 3, 4, and 5% v/v). The step “200 µM\_Hor” and “E\_100ACN” denotes the starting mixture reagent (200 µM each) and the cartridge elution with 100% ACN, respectively. Error bars represent standard deviations (S.D.) from three replications of the data.

(G)

**Pipecolinic acid (Pip)**

(H)

**5-Aminolevulinic acid (ALA)**

**Figure 51 (continued)** The peak area determined from triple-quadrupole LC/MS chromatogram representing the recovery yield of each plant hormone and plant-growth promoting compound – (A) IAA, (B) ABA, (C) GA<sub>3</sub>, (D) SA, (E) kinetin, (F) zeatin, (G) Pip, (H) ALA, and (I) ampicillin – passed through the desalting (DS) steps with different % (v/v) MeOH (1, 2, 3, 4, and 5% v/v). The step “200 μM\_Hor” and “E\_100ACN” denotes the starting mixture reagent (200 μM each) and the cartridge elution with 100% ACN, respectively. Error bars represent standard deviations (S.D.) from three replications of the data.

(I)

## Ampicillin

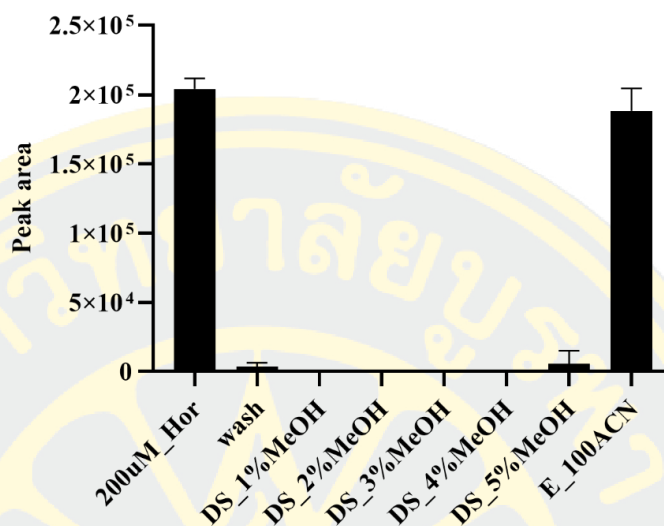


**Figure 51 (continued)** The peak area determined from triple-quadrupole LC/MS chromatogram representing the recovery yield of each plant hormone and plant-growth promoting compound – (A) IAA, (B) ABA, (C) GA<sub>3</sub>, (D) SA, (E) kinetin, (F) zeatin, (G) Pip, (H) ALA, and (I) ampicillin – passed through the desalting (DS) steps with different % (v/v) MeOH (1, 2, 3, 4, and 5% v/v). The step “200 μM\_Hor” and “E\_100ACN” denotes the starting mixture reagent (200 μM each) and the cartridge elution with 100% ACN, respectively. Error bars represent standard deviations (S.D.) from three replications of the data.

#### 4.7.3 The optimal elution step for yield recovery of authentic compounds

Not only the desalting step, but the elution step was also optimized. Although the results in the previous sections 4.7.1 and 4.7.2 showed that 100% ACN can elute the authentic compounds from the cartridge, however we still need to optimize the elution step with different % ACN including 20, 50, 80, and 100% v/v to ensure that we gain the complete recovery yield. In this experiment, some key authentic compounds such as IAA, ABA, GA<sub>3</sub>, and SA and ampicillin were examined. The peak area of each compound was determined from triple-quadrupole LC/MS chromatogram and represented for the recovery yield.

The results in Figure 52 showed that in comparison with the starting mixture reagent (200 µM each), most of the authentic compounds were eluted at early concentration of ACN at 20% v/v, except for IAA. However, not all amounts of authentic compounds were eluted at this ACN concentration, excepting ampicillin which was almost completely eluted at 20 % v/v ACN. It was reasonably found that the increasing ACN concentration can enhance the elution of authentic compounds. The recovery yield of each authentic compound was completely gained when using 80 and 100% ACN. Therefore, 100% ACN was selected as an eluent to elute all the bound authentic compounds.

### Elution step

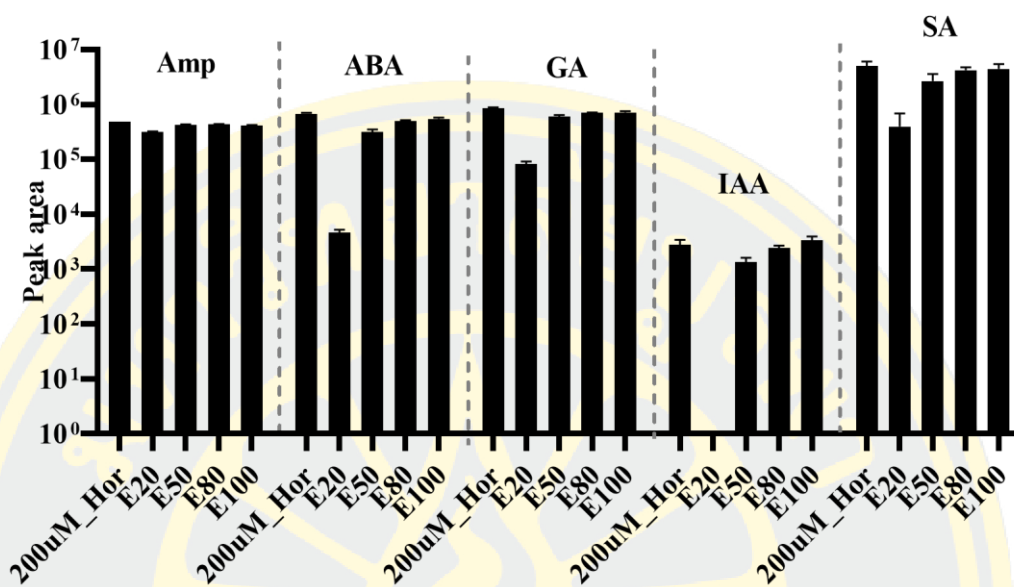


**Figure 52** The peak area determined from triple-quadrupole LC/MS chromatogram representing the recovery yield of each plant hormone and plant-growth promoting compound – IAA, ABA, GA<sub>3</sub>, SA, and ampicillin – passed through the individual elution (E) step with different % (v/v) ACN (20, 50, 80, and 100% v/v). The step “200 µM\_Hor” denotes the starting mixture reagent (200 µM each). Error bars represent standard deviations (S.D.) from three replications of the data

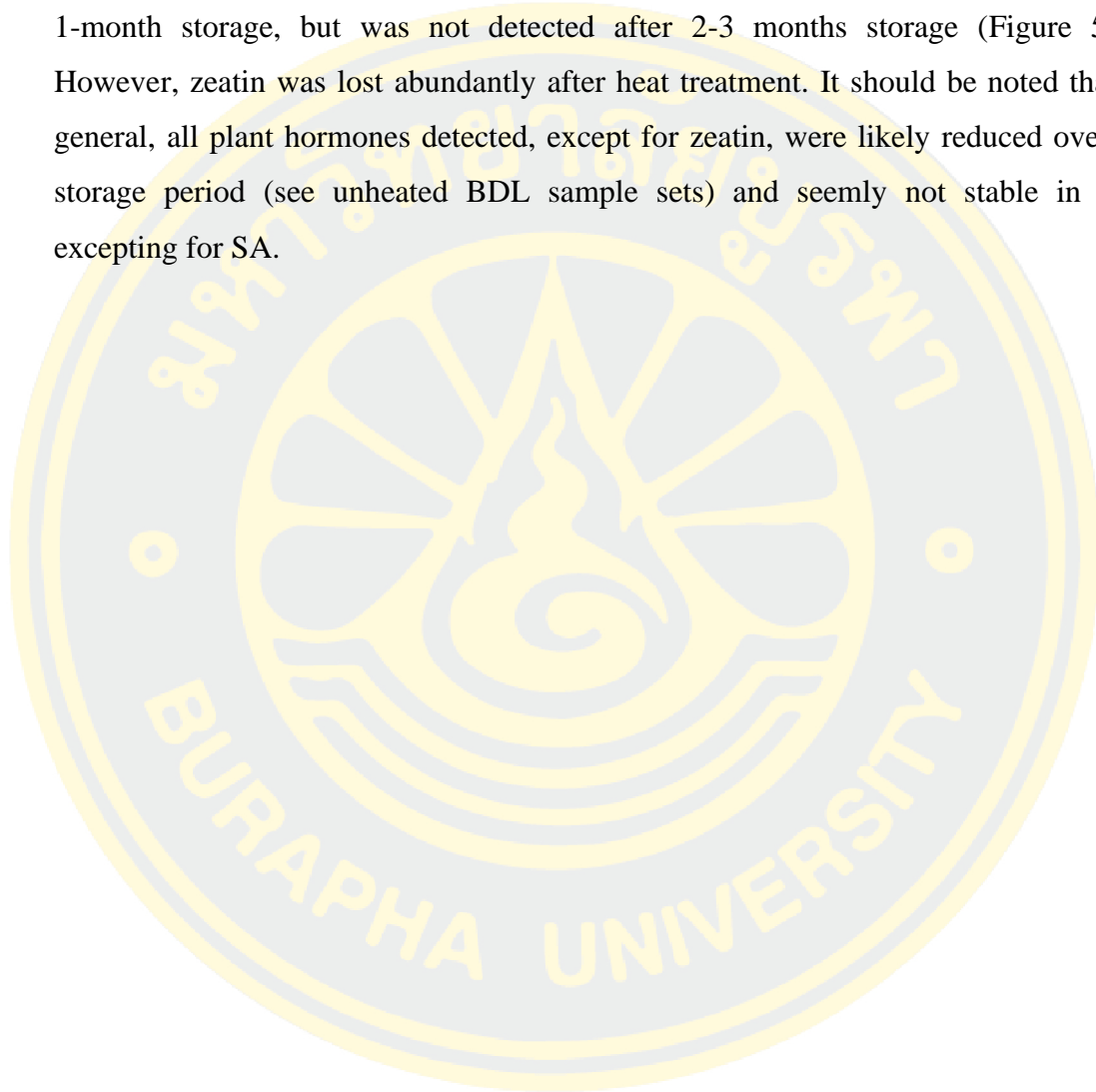
#### 4.8 Quantitation of plant hormones and plant-growth promoting compounds in unheated and heated BDL samples

Based on the established conditions obtained from the previous sections, we then quantitated plant hormones and plant-growth promoting compounds in unheated and heated BDL sample sets (fresh, 1-month-, 2-month-, and 3-month-storage set). The peak area of each compound detected was determined from triple-quadrupole LC/MS chromatogram and converted into a concentration unit by using the calibration curve as shown in the previous result section.

The results shown in Figure 53 demonstrated that only plant hormones like IAA, ABA, SA, kinetin, and zeatin were detected and quantitated, while the other plant hormones were not. For IAA (Figure 53A), it was detected in an unheated BDL sample of the fresh set with a concentration of 1.43-1.44  $\mu\text{M}$  and remained constant after heat treatment. However, it was found that IAA was trivially decreased to 1.36  $\mu\text{M}$  after storage for 1 month and cannot be detected after storages for more two months. Surprisingly, after heat treatment of the 1-month-storage BDL sample, IAA was totally lost. For ABA quantitation (Figure 53B), it can be detected in unheated BDL sample of the fresh set at 1.71 nM and was lowered to 0.77 nM after heat treatment. After 1-month storage, ABA was decreased about 3-folds (0.63 nM) as compared to unheated BDL sample of the fresh set. However, it was unexpectedly increased about 5 times after heat treatment. For storage over 1 month, ABA was not detected.

For the quantitation of SA (Figure 53C), it was found that SA was detected in unheated BDL sample of the fresh set with a concentration of about 0.17-0.18  $\mu\text{M}$  and remained constant after heat treatment. After 1-month storage, SA was decreased about a half (0.10-0.11 nM) and remained also constant after heat treatment. The data suggest that SA was thermostable. It was noted that the storage time over 1 month (2-3 months) caused the complete degradation of SA. This could be due to the aromatic ring-cleavage catabolism of SA in some aerobic microorganisms during storage periods. For kinetin (Figure 53D), in the unheated BDL sample of the fresh set, it was detected at a concentration about 1.00 nM and then trivially decreased over the storage time until 2 months. However, at the 3-month storage, kinetin was not detected. The concentration of kinetin was likely constant after heat treatment,

excepting kinetin detected in the 1-month storage BDL sample which was surprisingly increased about twice after heat treatment. Unlike the other plant hormones detected, zeatin was detected in an unheated BDL sample of the fresh set at a low concentration of about 0.2 nM and tremendously increased about 8-folds after 1-month storage, but was not detected after 2-3 months storage (Figure 53E). However, zeatin was lost abundantly after heat treatment. It should be noted that, in general, all plant hormones detected, except for zeatin, were likely reduced over the storage period (see unheated BDL sample sets) and seemly not stable in heat, excepting for SA.





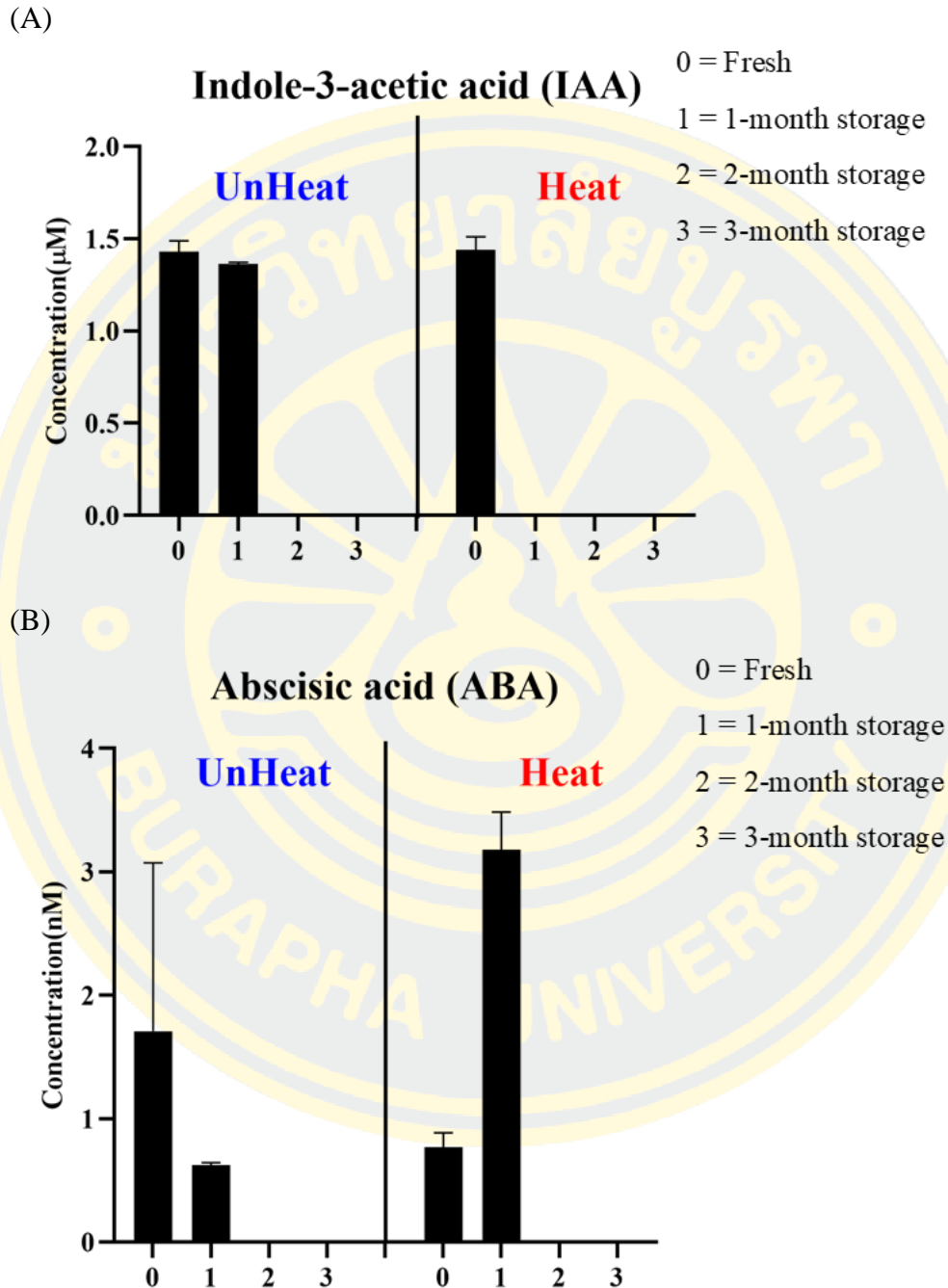
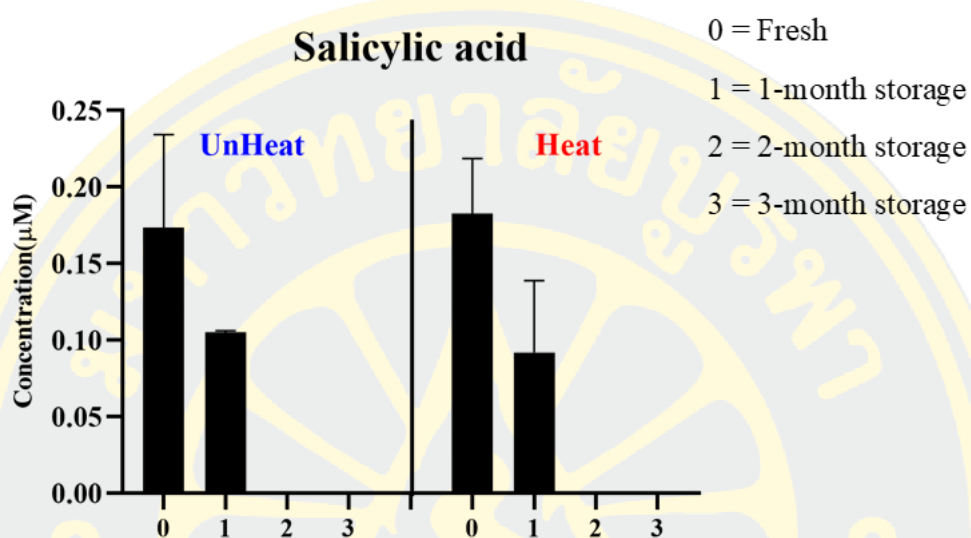


**Figure 53** Quantitation of plant hormones including (A) IAA, (B) ABA, (C) SA, (D) kinetin, and (E) zeatin in unheated and heated BDL sample sets (fresh, 1-month-, 2-month-, and 3-month-storage set) by HPLC-MS/MS analysis. Error bars represent standard deviations (S.D.) from three replications of the data.

(C)



(D)

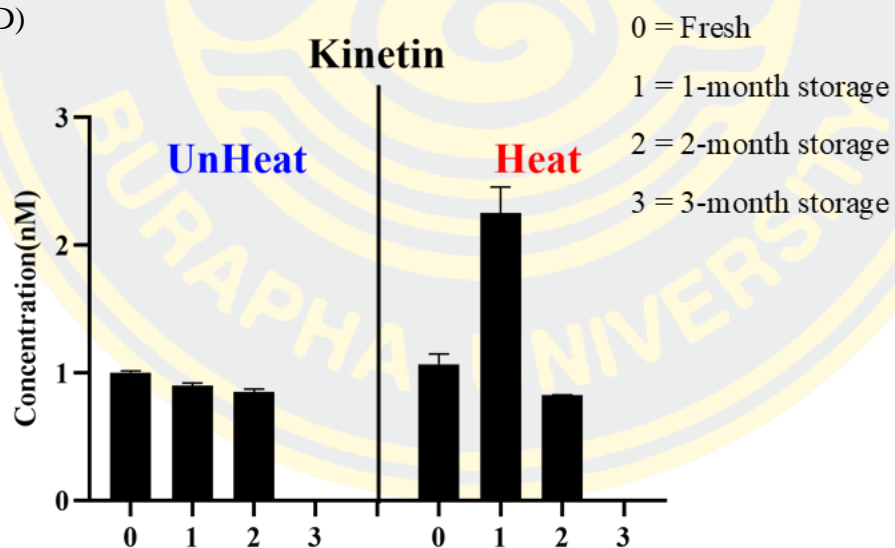


**Figure 53 (continued)** Quantitation of plant hormones including (A) IAA, (B) ABA, (C) SA, (D) kinetin, and (E) zeatin in unheated and heated BDL sample sets (fresh, 1-month-, 2-month-, and 3-month-storage set) by HPLC-MS/MS analysis. Error bars represent standard deviations (S.D.) from three replications of the data

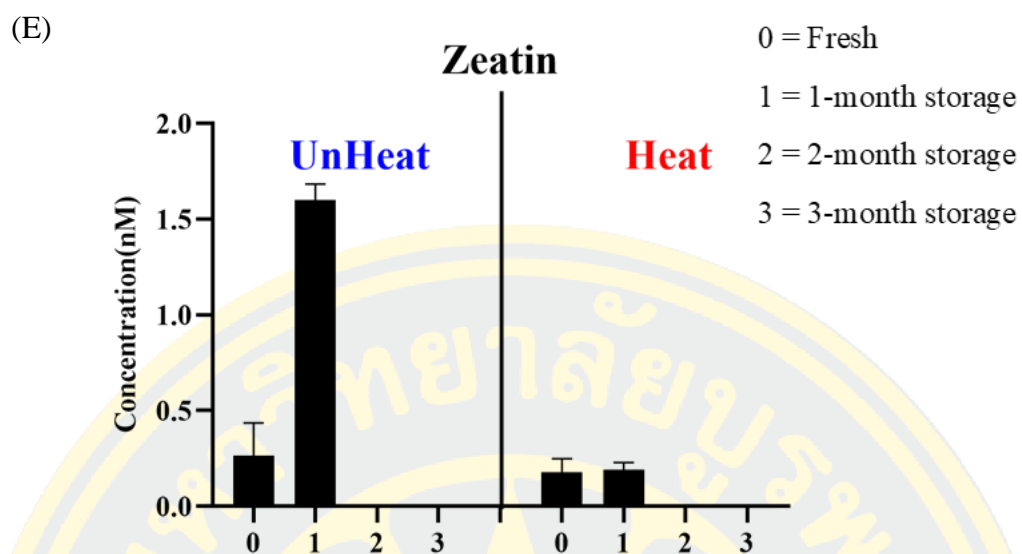


**Figure 53 (continued)** Quantitation of plant hormones including (A) IAA, (B) ABA, (C) SA, (D) kinetin, and (E) zeatin in unheated and heated BDL sample sets (fresh, 1-month-, 2-month-, and 3-month-storage set) by HPLC-MS/MS analysis. Error bars represent standard deviations (S.D.) from three replications of the data.

#### 4.9 Hydroponic bioassay

To evaluate the capability of BDL samples in promoting plant growth and development, the hydroponic assay using green oak lettuce (*Lactuca sativa L.*) as a plant model was carried out by the deep-water culture system with different treatments of only 20X-diluted BDL samples (unheated and heated samples of the fresh, 1-month-storage, 2-month-storage, and 3-month-storage sets) versus 20X-diluted BDL samples (unheated and heated samples of the fresh, 1-month-storage-, 2-month-storage, and 3-month-storage sets) mixed with 170X-diluted hydroponic fertilizer, comparing to negative control (tap water) and a positive control (170X-diluted hydroponic fertilizer). There were 3 parameters measured for monitoring plant growth including wet weight, dried weight, and canopy diameter.

The results demonstrated that the use of only 20X-diluted BDL samples (unheated and heated samples of the fresh, 1-month-storage-, 2-month-storage, and 3-month-storage sets) in the deep-water culture system did not promote the growth of green oak lettuce, like the system that used only tap water (see later in Figures 55A and 55B). In contrast, the mix of 170X-diluted hydroponic fertilizer and BDL samples (unheated and heated samples of the fresh, 1-month-storage-, 2-month-storage, and 3-month-storage sets) can promote the growth of green oak lettuce (Figure 54). However, only the condition of the heated BDL sample of the 1-month-storage set mixed with 170X-diluted hydroponic fertilizer (1HO+) can enhance the growth of green oak lettuce since three parameters – wet weight (Figure 54A), dried weight (Figure 54B), and canopy diameter (Figures 54C and 55D) – of green oak lettuce were increased significantly, compared to the positive control (Figures 54C and 55C). While other conditions (FUO+, unheated BDL sample of the fresh set mixed with 170X-diluted hydroponic fertilizer; FHO+, heated BDL sample of the fresh set mixed with 170X-diluted hydroponic fertilizer; 1UO+, unheated BDL sample of the 1-month-storage set mixed with 170X-diluted hydroponic fertilizer; 1HO+, heated BDL sample of the 1-month-storage set mixed with 170X-diluted hydroponic fertilizer; 2UO+, unheated BDL sample of the 2-month-storage set mixed with 170X-diluted hydroponic fertilizer; 2HO+, heated BDL sample of the 2-month-storage set mixed with 170X-diluted hydroponic fertilizer; 3UO+, unheated BDL sample of the 3-month-storage set mixed with 170X-diluted hydroponic fertilizer; and 3HO+,

heated BDL sample of the 3-month-storage set mixed with 170X-diluted hydroponic fertilizer) did not enhance plant growth. Our results indicated that BDL samples can act only as the plant-growth supplement.



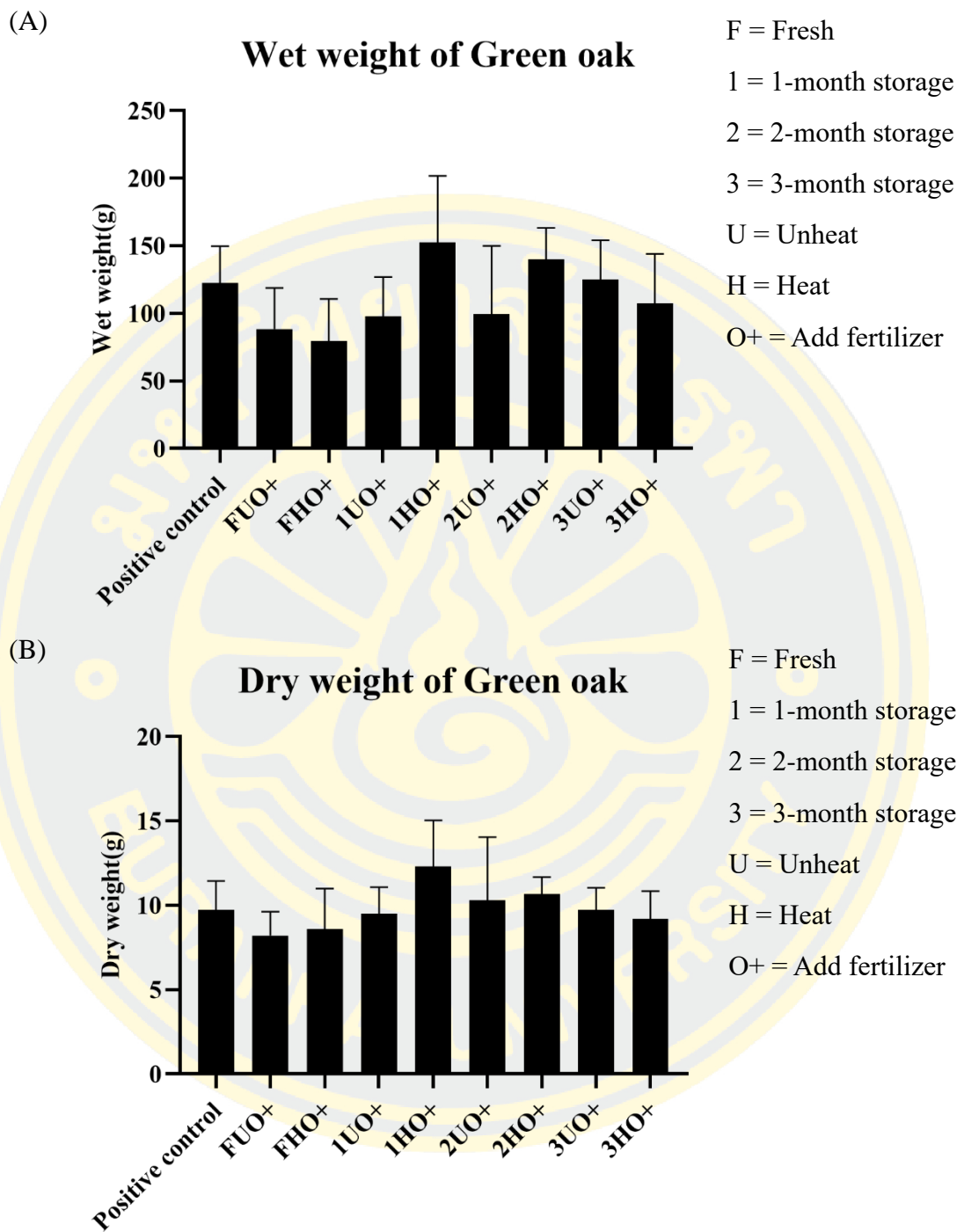


**Figure 54** Green oak lettuce (*Lactuca sativa L.*) wet weight (A), dry weight (B) and canopy diameter (C) were used to test the quality of BDL samples to promote plant growth and development

(C)

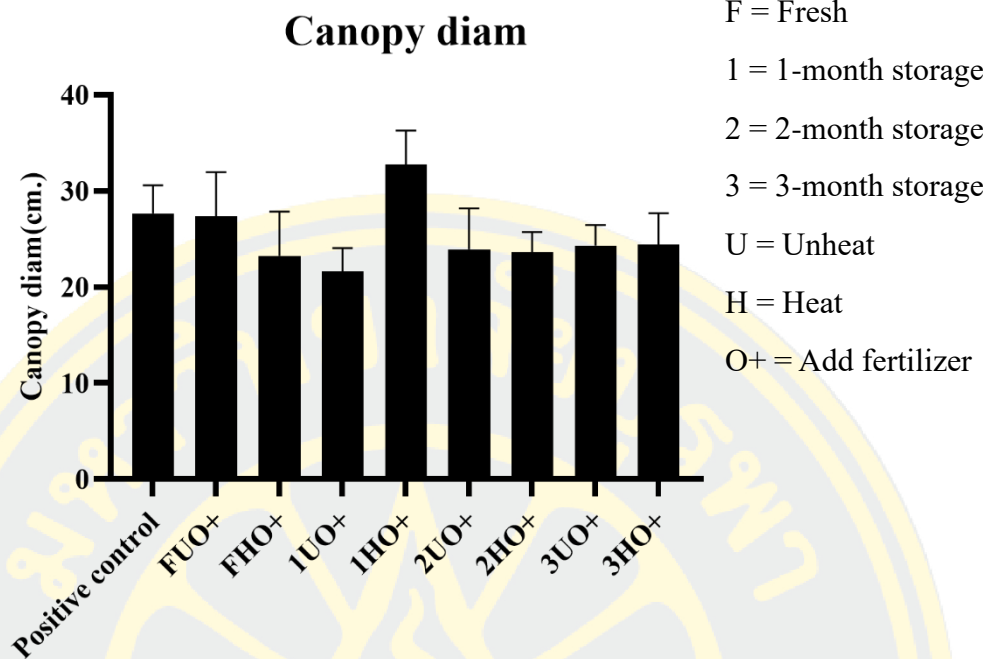


**Figure 54 (continued)** Green oak lettuce (*Lactuca sativa L.*) wet weight (A), dry weight (B) and canopy diameter (C) were used to test the quality of BDL samples to promote plant growth and development.

(A) Negative control



(B) Only BDL sample



**Figure 55** Photographs of green oak lettuce (*Lactuca sativa L.*) treated with different conditions, (A) negative control, (B) only BDL sample, (C) positive control, and (D) the mix of BDL sample and hydroponic fertilizer.



(C) Positive control



**Figure 55 (continued)** Photographs of green oak lettuce (*Lactuca sativa L.*) treated with different conditions, (A) negative control, (B) only BDL sample, (C) positive control, and (D) the mix of BDL sample and hydroponic fertilizer.

(D) Mixture of BDL sample and hydroponic fertilizer



**Figure 55 (continued)** Photographs of green oak lettuce (*Lactuca sativa* L.) treated with different conditions, (A) negative control, (B) only BDL sample, (C) positive control, and (D) the mix of BDL sample and hydroponic fertilizer.

## CHAPTER 5

### DISCUSSION AND CONCLUSION

This thesis work has shown that biogas digestate liquid (BDL) samples obtained from the anaerobic co-digestion of animal manure inoculum and food waste contain essential plant nutrients (macronutrients and micronutrients) and some plant hormones/plant-growth promoting compounds, which are supplemental for plant growth. In addition, the quantitative analyses of plant nutrients and plant hormones/plant-growth promoting compounds have been established and used as a measure of quality control of BDL production.

The measurement of basic physicochemical parameters, pH and EC values, of BDL samples showed that pH values measured for unheated and heated BDL samples were in a pH range of 8-9, which was slightly higher than the pH 5.5-8.5 specified for the compost (Thai Agricultural Standard, TAS 9503 – 2005). While the EC values of 10-13 mS/cm in BDL samples, which was equivalent to the EC of industrial wastewater (~10 mS/cm) and much higher than that of the tap water (0.05-0.8 mS/cm) (Fondriest Environmental, Inc. “Conductivity, Salinity and Total Dissolved Solids.” Fundamentals of Environmental Measurements. 3 Mar 2014.), were about 3-4 folds higher than that the EC values of  $\leq 3.5$  mS/cm specified for the compost (Thai Agricultural Standard, TAS 9503 – 2005). Based on this data, it was suggested that BDL samples could be applied in field application as their pH values were in a range of the specified values, however high salt contents were optimally diluted before use.

The analysis of macronutrients especially for major nutrients N, P, and K demonstrated that in an unheated condition, the total N content was gradually reduced over the storage time (Figure 42A). At least 50% of digestate N is found in the AD process occurs as a volatile  $\text{NH}_4^+\text{-N}$  (S. Wu & Dong, 2020), it was hypothesized that the decrease of the N contents during storage (1-3 months) could be because of the vaporization and the consumption by ammonia oxidizing bacteria (AOB) and nitrite oxidizing bacteria (NOB) that can convert  $\text{NH}_4^+$  to  $\text{NO}_3^-$  and  $\text{NO}_3^-$  is then reduced to dinitrogen gas ( $\text{N}_2$ ) under anoxic conditions by heterotrophic denitrifying bacteria

(DNB) (Iannacone, Di Capua, Granata, Gargano, & Esposito, 2020). With heating condition, it was likely that the volatile  $\text{NH}_4^+\text{-N}$  was vaporized and thus the N contents were tremendously lost. Unlike N, the P contents was increased over the storage time in unheated condition and stable under heated condition (Figure 42B). It was hypothesized that the increase in the P contents in unheated conditions could be resulted from some biological processes that occurred during storage could enhance synthesis of the P-containing compounds. In contrast to N and P, the K contents were kept constant over the storage period in an unheated condition and stable under heat treatment (Figure 42C). It should be noted that the amounts of N (~1,000-1,300 mg/l equivalent to ~0.1-0.13% w/w), P (~20,000-500,000 mg/l equivalent to ~2-50% w/w), and K (~2,000 mg/l equivalent to ~0.2% w/w) found in BDL samples (Table 7) were higher than the values recommended for the compost in the USA (N, 100-300 mg/l; P, 800-2,500 mg/l; and K, 500-2,000 mg/l) (Brinton, 2000). Based on Thai Agricultural Standard (TAS 9503 – 2005), it was found that the N and K contents found in BDL samples were about 10- and 2.5-folds, respectively, lower than the specified values for the compost (N,  $\geq 1\%$  w/w; K,  $\geq 0.5\%$  w/w), while the P contents were higher than the standard value (P,  $\geq 0.5\%$  w/w). Nevertheless, it should be noted that the physical appearance of the compost and BDL samples were different, therefore the values determined in BDL samples may not be comparable with the specified values for the compost.

Not only macronutrients, the micronutrients including Fe, Cu, Zn, Mn and Mo were also detected in a broad range of 0.1-3 mg/l for both unheated and heated BDL samples (Table 7). Interestingly, the amounts of toxic elements (As, Pb, Cd, and Cr) found in BDL samples were about 500-10,000-folds lower than the specified values for the compost (As,  $\leq 10\text{-}50$  mg/Kg; Pb,  $\leq 500\text{-}1,000$  mg/Kg; Cd,  $\leq 5\text{-}10$  mg/Kg; and Cr,  $\leq 200\text{-}300$  mg/Kg) (Brinton, 2000). As the previous report showed that toxic elements such as Pb and Cd can affect the bioaccumulation of macro- and micronutrients (Khan et al., 2016), therefore low abundances of toxic elements in BDL samples used in this present work support the use of BDL samples as an environmentally friendly organic fertilizer.

To quantitate plant hormones/plant-growth promoting compounds (IAA, ABA, GA<sub>3</sub>, JA, SA, kinetin, zeatin, ALA, and Pip) in BDL samples, the LC-MS/MS conditions for the authentic compounds were successfully optimized (Figures 45 and 46, Table 8). Most authentic compounds were suitably detected in a negative mode, while the rests (kinetin, ALA, and Pip) were detected in a positive mode. Unlike the work presented herein, IAA and zeatin were detected in a positive mode in the previous report (H.-x. WANG et al., 2020). All of the authentic compounds were detected in a single peak at a particular retention time (Figures 45 and 46, Table 8), excepting for GA<sub>3</sub> which has been found at two separate retention times, 6.7 min (minor peak) and 7.2 min (major peak) (Figure 45B), with the same  $m/z$  345 and 143.1 of the precursor and product ion, respectively. It can be hypothesized that the appearance of the minor peak could be a result of the decomposition of GA<sub>3</sub> to form a decomposed isoform, namely gibberellenic acid (GE), which may occur in aqueous solution under certain pH or temperature conditions (see the chemical structure of GE compared to GA<sub>3</sub> in Figure 45B). This is because the molecular masses of GA<sub>3</sub> and GE were the same (C<sub>19</sub>H<sub>22</sub>O<sub>6</sub>, 346.37 g/mol), but their chemical structures were different. The chemical structure of GA<sub>3</sub> belongs to a tetracyclic dihydroxy-lactone acid which contains a C<sub>1</sub>-C<sub>2</sub> double bond, a C<sub>10</sub>-lactone ring, and an OH group in C<sub>13</sub>. The GE has the same core structure but differs with the occurrence of a double bond in a 5-membered ring, thus possibly causing a different retention time (Camara et al., 2018; Tang, Huang, Zhang, Jiang, & Zhong, 2015). In addition to authentic plant hormones/plant-growth promoting compounds, we also optimized the LC-MS/MS condition for the internal standard (IS). Ampicillin was selected as a suitable IS for LC-MS/MS method validation since it can give a better signal with a shorter retention time than IPTG in either negative or positive mode (Figure 47 and Table 8).

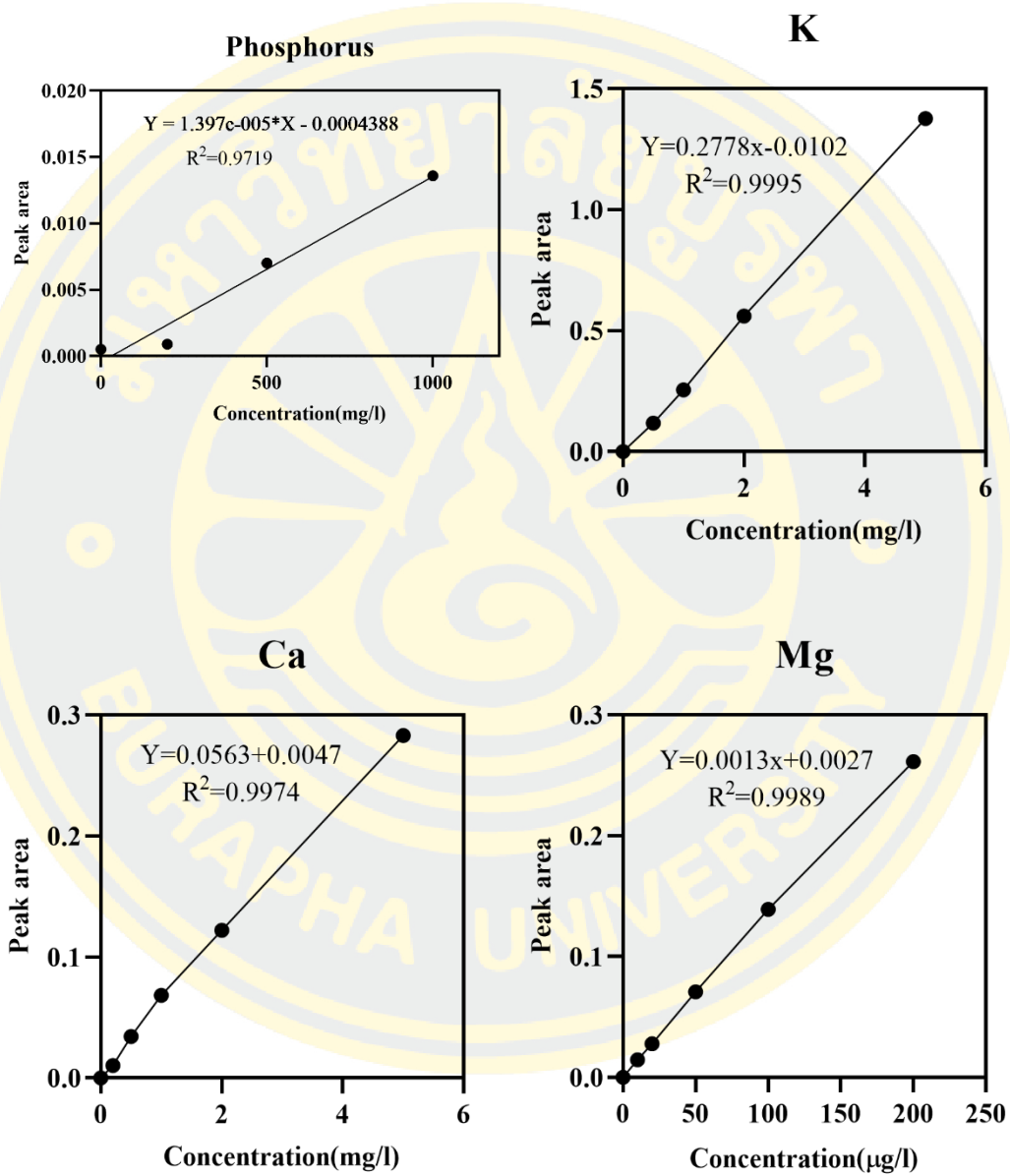
The workflow and SPE preparation method for determining plant hormones/plant-growth promoting compounds in BDL samples have been successfully established (Figures 39 and 40). Most of the plant hormones/plant-growth promoting compounds can be quantitated by this setup method, except for ALA and Pip. Since both ALA and Pip contain polar functional groups such as amino and carboxylic groups which may not be able to bind the SPE C<sub>18</sub> cartridge, but instead be compatible with the SPE polar cartridge like a cation-exchange AG

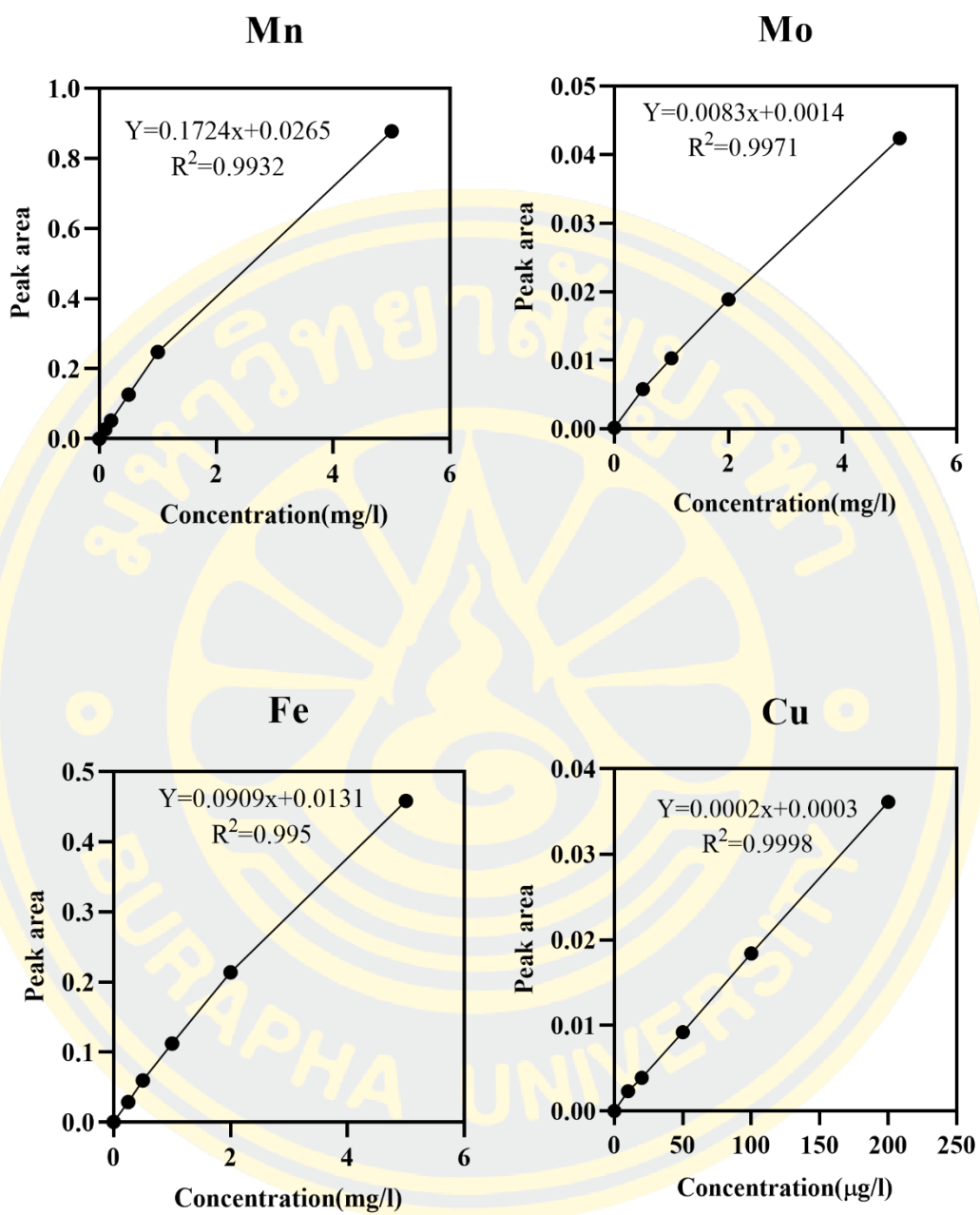
50WX8-(H+) resin and Oasis MCX (Servillo et al., 2012). Based on our analyses, only five plant hormones including IAA, ABA, SA, kinetin and zeatin were found in BDL samples (Figure 53). In unheated condition, all of these plant hormones were decreased after storage for 1 month, excepting zeatin which was unexpectedly increased. However, they were not detected after storage for further 2-3 months. According to our results, the amount of IAA detected in the unheated BDL sample (~1.5  $\mu\text{M}$ ) was likely sufficient for stimulating plant growth as previously reported (Srivastava, 2002). As the previous report showed that SA at a concentration of 5.6 mM can induce flowering (Sahu, 2013), the amount of SA detected in this work (~0.1-0.2  $\mu\text{M}$ ) was therefore likely insufficient for accelerating the flowering. It was interesting to note that all of plant hormones detected, except zeatin, were likely stable over heat treatment, which was agreed well with the finding that these plant hormones were stable at 40 and 100 °C (Figure 48).

On the basis of plant nutrients and hormones detected in BDL samples, we hence tested the capability of BDL samples with different treatments (see details in section 4.9) in promoting plant growth by using green oak lettuce (*Lactuca sativa L.*) as a plant model grown by the hydroponic method. It was found that only the 1HO+ formula (heated BDL sample of 1-month-storage set mixed with 170X-diluted hydroponic fertilizer) can promote the growth of green oak (Figures 54 and 55). It could be possible that the amounts of ABA, SA, kinetin, and zeatin remained after heat treatment may be proper for plant growth in the presence of hydroponic fertilizer. This indicates that the heated BDL sample of the 1-month-storage set was suitably used as a supplement to enhance plant growth, while other conditions, particularly those with only BDL samples, cannot.

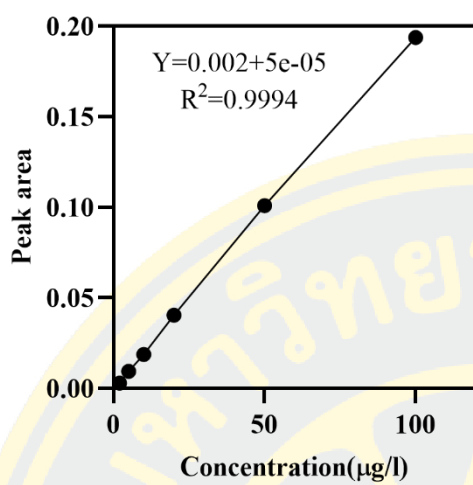
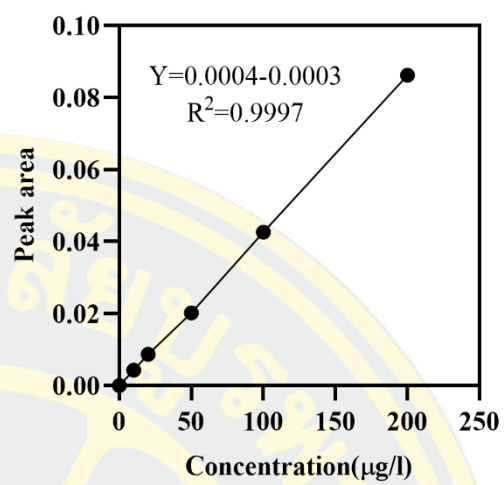
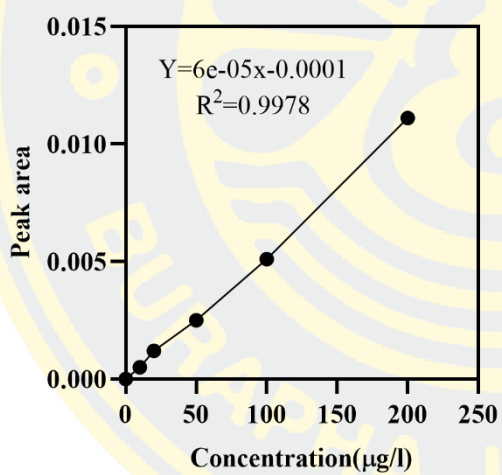
In conclusion, the present study demonstrated that BDL sample obtained from the anaerobic co-digestion of animal manure inoculum and food waste contain plant nutrients and certain amounts of plant hormones which are useful for plant growth. Furthermore, the detection of toxic elements at substantially low ppb ranges suggests that BDL sample can serve as an environmentally friendly organic supplement to promote plant growth. Besides that, the quantitative analyses of plant nutrients and plant hormones have been successfully established and used as a measure of quality control of BDL production.

## APPENDIX







**Arsenic****Cd****Cr**

## REFERENCES

- Adio, A. M., Casteel, C. L., De Vos, M., Kim, J. H., Joshi, V., Li, B., . . . Jander, G. (2011). Biosynthesis and defensive function of N $\delta$ -acetylornithine, a jasmonate-induced *Arabidopsis* metabolite. *The Plant Cell*, 23(9), 3303-3318.
- Andrabi, S. B. A., Tahara, M., Matsubara, R., Toyama, T., Aonuma, H., Sakakibara, H., . . . Nagamune, K. (2018). Plant hormone cytokinins control cell cycle progression and plastid replication in apicomplexan parasites. *Parasitology International*, 67(1), 47-58. doi:<https://doi.org/10.1016/j.parint.2017.03.003>
- Brinton, W. F. (2000). Compost quality standards and guidelines. *Final Report by Woods End Research Laboratories for the New York State Association of Recyclers*.
- Burló, F., Guijarro, I., Carbonell-Barrachina, A. A., Valero, D., & Martínez-Sánchez, F. (1999). Arsenic Species: Effects on and Accumulation by Tomato Plants. *Journal of Agricultural and Food Chemistry*, 47(3), 1247-1253. doi:10.1021/jf9806560
- Camara, M. C., Vandenberghe, L. P., Rodrigues, C., de Oliveira, J., Faulds, C., Bertrand, E., & Soccol, C. R. (2018). Current advances in gibberellic acid (GA 3) production, patented technologies and potential applications. *Planta*, 248(5), 1049-1062.
- Carmona-Cabello, M., García, I. L., Sáez-Bastante, J., Pinzi, S., Koutinas, A. A., & Dorado, M. P. (2020). Food waste from restaurant sector – Characterization for biorefinery approach. *Bioresource Technology*, 301, 122779. doi:<https://doi.org/10.1016/j.biortech.2020.122779>
- Chapman, E. J., & Estelle, M. (2009). Mechanism of auxin-regulated gene expression in plants. *Annual review of genetics*, 43, 265-285.
- Chen, Z., Zheng, Z., Huang, J., Lai, Z., & Fan, B. (2009). Biosynthesis of salicylic acid in plants. *Plant signaling & behavior*, 4(6), 493-496.
- Cheong, J. C., Lee, J. T. E., Lim, J. W., Song, S., Tan, J. K. N., Chiam, Z. Y., . . . Tong, Y. W. (2020). Closing the food waste loop: Food waste anaerobic digestate as fertilizer for the cultivation of the leafy vegetable, xiao bai cai (*Brassica rapa*). *Science of The Total Environment*, 715, 136789. doi:<https://doi.org/10.1016/j.scitotenv.2020.136789>
- Chojnacka, K., Moustakas, K., & Witek-Krowiak, A. (2020). Bio-based fertilizers: A practical approach towards circular economy. *Bioresource Technology*, 295, 122223.
- Cox, C. E., Brandl, M. T., de Moraes, M. H., Gunasekera, S., & Teplitski, M. (2018). Production of the plant hormone auxin by *Salmonella* and its role in the interactions with plants and animals. *Frontiers in microbiology*, 8, 2668.
- Dahiya, S., Kumar, A. N., Shanthi Sraavan, J., Chatterjee, S., Sarkar, O., & Mohan, S. V. (2018). Food waste biorefinery: Sustainable strategy for circular bioeconomy. *Bioresource Technology*, 248, 2-12. doi:<https://doi.org/10.1016/j.biortech.2017.07.176>
- Dilworth, L., Riley, C., & Stennett, D. (2017). Plant Constituents: Carbohydrates, oils, resins, balsams, and plant hormones. In *Pharmacognosy* (pp. 61-80): Elsevier.
- Duca, D., Lorv, J., Patten, C. L., Rose, D., & Glick, B. R. (2014). Indole-3-acetic acid in plant-microbe interactions. *Antonie Van Leeuwenhoek*, 106(1), 85-125.

- Esposito, G., Frunzo, L., Giordano, A., Liotta, F., Panico, A., & Pirozzi, F. (2012). Anaerobic co-digestion of organic wastes. *Reviews in Environmental Science and Bio/Technology*, 11(4), 325-341.
- Fatima, Z., Saleemi, M., Zia, M., Sultan, T., Aslam, M., Rehman, R., & Chaudhary, M. F. (2009). Antifungal activity of plant growth-promoting rhizobacteria isolates against *Rhizoctonia solani* in wheat. *African Journal of Biotechnology*, 8(2).
- Fisgativa, H., Tremier, A., & Dabert, P. (2016). Characterizing the variability of food waste quality: A need for efficient valorisation through anaerobic digestion. *Waste management*, 50, 264-274.
- Geilfus, C.-M. (2019). Hormones. In *Controlled Environment Horticulture* (pp. 163-173): Springer.
- Gouffi, K., Bernard, T., & Blanco, C. (2000). Osmoprotection by Pipecolic Acid in *Sinorhizobium meliloti*: Specific Effects of d and l Isomers. *Applied and environmental microbiology*, 66(6), 2358-2364.
- Gujjar, R. S., & Supaibulwatana, K. (2019). The mode of cytokinin functions assisting plant adaptations to osmotic stresses. *Plants*, 8(12), 542.
- Han, H., Zhang, S., & Sun, X. (2009). A review on the molecular mechanism of plants rooting modulated by auxin. *African Journal of Biotechnology*, 8(3).
- Han, X., Zeng, H., Bartocci, P., Fantozzi, F., & Yan, Y. (2018). Phytohormones and effects on growth and metabolites of microalgae: a review. *Fermentation*, 4(2), 25.
- Hao, Y., Wang, H., Qiao, S., Leng, L., & Wang, X. (2016). Histone deacetylase HDA6 enhances brassinosteroid signaling by inhibiting the BIN2 kinase. *Proceedings of the National Academy of Sciences*, 113(37), 10418-10423.
- Hartmann, M., Kim, D., Bernsdorff, F., Ajami-Rashidi, Z., Scholten, N., Schreiber, S., . . . Zeier, J. (2017). Biochemical principles and functional aspects of pipecolic acid biosynthesis in plant immunity. *Plant physiology*, 174(1), 124-153.
- Hernández, J. A., Diaz-Vivancos, P., Barba-Espín, G., & Clemente-Moreno, M. J. (2017). On the role of salicylic acid in plant responses to environmental stresses. In *Salicylic Acid: A Multifaceted Hormone* (pp. 17-34): Springer.
- Hussein, H.-A. A., Mekki, B. B., El-Sadek, M. E. A., & El Lateef, E. E. (2019). Effect of L-Ornithine application on improving drought tolerance in sugar beet plants. *Heliyon*, 5(10), e02631. doi:<https://doi.org/10.1016/j.heliyon.2019.e02631>
- Iannacone, F., Di Capua, F., Granata, F., Gargano, R., & Esposito, G. (2020). Simultaneous nitrification, denitrification and phosphorus removal in a continuous-flow moving bed biofilm reactor alternating microaerobic and aerobic conditions. *Bioresource Technology*, 310, 123453.
- Iocoli, G. A., Zabaloy, M. C., Pasdevicelli, G., & Gómez, M. A. (2019). Use of biogas digestates obtained by anaerobic digestion and co-digestion as fertilizers: Characterization, soil biological activity and growth dynamic of *Lactuca sativa* L. *Science of The Total Environment*, 647, 11-19. doi:<https://doi.org/10.1016/j.scitotenv.2018.07.444>
- Javidnia, K., Faghih-Mirzaei, E., Miri, R., Attaroshan, M., & Zomorodian, K. (2016). Biotransformation of acetoin to 2, 3-butanediol: Assessment of plant and microbial biocatalysts. *Research in pharmaceutical sciences*, 11(4), 349.
- Kanto, U., Jutamanee, K., Osotsapar, Y., Chai-arree, W., Jintanawich, W., Promdang, S., & Junjerm, J. (2013). Quantification of 5-aminolevulinic acid in swine

- manure extract by HPLC-fluorescence. *Journal of Liquid Chromatography & Related Technologies*, 36(19), 2731-2748.
- Khalaf, E., & Raizada, M. (2020). Draft genome sequences of seven strains of *Paenibacillus* spp.(phylum Firmicutes) inhabiting the seeds of *Cucumis melo* L.(cantaloupe) and exhibiting plant probiotic traits. *Microbiol Resour Announc* 9: e00715-20. In.
- Khan, A., Khan, S., Alam, M., Khan, M. A., Aamir, M., Qamar, Z., . . . Perveen, S. (2016). Toxic metal interactions affect the bioaccumulation and dietary intake of macro-and micro-nutrients. *Chemosphere*, 146, 121-128.
- Kim, J. K., Oh, B. R., Chun, Y. N., & Kim, S. W. (2006). Effects of temperature and hydraulic retention time on anaerobic digestion of food waste. *Journal of Bioscience and bioengineering*, 102(4), 328-332.
- Kim, M.-S., Kim, D.-H., & Yun, Y.-M. (2017). Effect of operation temperature on anaerobic digestion of food waste: Performance and microbial analysis. *Fuel*, 209, 598-605.
- Kumar, D. (2014). Salicylic acid signaling in disease resistance. *Plant Science*, 228, 127-134.
- Labatut, R. A., & Pronto, J. L. (2018). Sustainable Waste-to-Energy Technologies: Anaerobic Digestion. In *Sustainable Food Waste-To-energy Systems* (pp. 47-67): Elsevier.
- Lefevre, H., Bauters, L., & Gheysen, G. (2020). Salicylic acid biosynthesis in plants. *Frontiers in plant science*, 11, 338.
- Li, X., Guo, J., Pang, C., & Dong, R. (2016). Anaerobic digestion and storage influence availability of plant hormones in livestock slurry. *ACS Sustainable Chemistry & Engineering*, 4(3), 719-727.
- Liang, X., Yuan, J., Yang, E., & Meng, J. (2017). Responses of soil organic carbon decomposition and microbial community to the addition of plant residues with different C:N ratio. *European Journal of Soil Biology*, 82, 50-55. doi:<https://doi.org/10.1016/j.ejsobi.2017.08.005>
- LoGiudice, N., Le, L., Abuan, I., Leizorek, Y., & Roberts, S. C. (2018). Alpha-difluoromethylornithine, an irreversible inhibitor of polyamine biosynthesis, as a therapeutic strategy against hyperproliferative and infectious diseases. *Medical Sciences*, 6(1), 12.
- Lu, J., Muhmood, A., Czekala, W., Mazurkiewicz, J., Dach, J., & Dong, R. (2019). Untargeted metabolite profiling for screening bioactive compounds in digestate of manure under anaerobic digestion. *Water*, 11(11), 2420.
- Lu, J., Muhmood, A., Liu, H., Dong, R., Pang, S., & Wu, S. (2020). Exploring Bioactive Compounds in Anaerobically Digested Slurry: Extraction, Characterization, and Assessment of Antifungal Activity. *Waste and Biomass Valorization*, 11(5), 1863-1872.
- Ma, Y., Cao, J., He, J., Chen, Q., Li, X., & Yang, Y. (2018). Molecular mechanism for the regulation of ABA homeostasis during plant development and stress responses. *International journal of molecular sciences*, 19(11), 3643.
- Maathuis, F. J., & Diatloff, E. (2013). Roles and functions of plant mineral nutrients. In *Plant Mineral Nutrients* (pp. 1-21): Springer.
- Mahjoub, B., & Domscheit, E. (2020). Chances and challenges of an organic waste-based bioeconomy. *Current Opinion in Green and Sustainable Chemistry*, 25,

100388. doi:<https://doi.org/10.1016/j.cogsc.2020.100388>
- Melikoglu, M., Lin, C. S. K., & Webb, C. (2013). Analysing global food waste problem: pinpointing the facts and estimating the energy content. *Central European Journal of Engineering*, 3(2), 157-164.
- Miransari, M., & Smith, D. L. (2014). Plant hormones and seed germination. *Environmental and Experimental Botany*, 99, 110-121. doi:<https://doi.org/10.1016/j.envexpbot.2013.11.005>
- Möller, K., & Müller, T. (2012). Effects of anaerobic digestion on digestate nutrient availability and crop growth: A review. *Engineering in Life Sciences*, 12(3), 242-257.
- Moreau, M., Tian, M., & Klessig, D. F. (2012). Salicylic acid binds NPR3 and NPR4 to regulate NPR1-dependent defense responses. *Cell research*, 22(12), 1631-1633.
- Ng, L. M., Melcher, K., Teh, B. T., & Xu, H. E. (2014). Abscisic acid perception and signaling: structural mechanisms and applications. *Acta Pharmacologica Sinica*, 35(5), 567-584.
- Osman, K. T. (2013). Plant nutrients and soil fertility management. In *Soils* (pp. 129-159): Springer.
- Pandey, A., Sharma, M., & Pandey, G. K. (2016). Emerging roles of strigolactones in plant responses to stress and development. *Frontiers in plant science*, 7, 434.
- Paritosh, K., Kushwaha, S. K., Yadav, M., Pareek, N., Chawade, A., & Vivekanand, V. (2017). Food waste to energy: an overview of sustainable approaches for food waste management and nutrient recycling. *BioMed Research International*, 2017.
- Park, K. Y., Seo, S. Y., Oh, B.-R., Seo, J.-W., & Kim, Y. J. (2018). 2, 3-butanediol induces systemic acquired resistance in the plant immune response. *Journal of Plant Biology*, 61(6), 424-434.
- Paul, V., Pandey, R., Ramesh, K., & Meena, R. (2017). Atomic Absorption Spectroscopy (AAS) for Elemental Analysis of Plant Samples. *Manual of ICAR Sponsored Training Programme for Technical Staff of ICAR Institutes on "Physiological Techniques to Analyze the Impact of Climate Change on Crop Plants"*, 84.
- Pelayo Lind, O., Hultberg, M., Bergstrand, K.-J., Larsson-Jönsson, H., Caspersen, S., & Asp, H. (2021). Biogas digestate in vegetable hydroponic production: pH dynamics and pH management by controlled nitrification. *Waste and Biomass Valorization*, 12(1), 123-133.
- Phibunwatthanawong, T., & Riddech, N. (2019). Liquid organic fertilizer production for growing vegetables under hydroponic condition. *International Journal of Recycling of Organic Waste in Agriculture*, 8(4), 369-380.
- Pieterse, C. M., & Van Loon, L. C. (1999). Salicylic acid-independent plant defence pathways. *Trends in plant science*, 4(2), 52-58.
- Pramanik, S. K., Suja, F. B., Zain, S. M., & Pramanik, B. K. (2019). The anaerobic digestion process of biogas production from food waste: Prospects and constraints. *Bioresource Technology Reports*, 8, 100310. doi:<https://doi.org/10.1016/j.biteb.2019.100310>
- Raksasat, R., Lim, J. W., Kiatkittipong, W., Kiatkittipong, K., Ho, Y. C., Lam, M. K., . . . Cheng, C. K. (2020). A review of organic waste enrichment for inducing palatability of black soldier fly larvae: Wastes to valuable resources.

- Environmental Pollution*, 267, 115488.  
doi:<https://doi.org/10.1016/j.envpol.2020.115488>
- Sahu, G. K. (2013). Salicylic acid: Role in plant physiology and stress tolerance. In *Molecular stress physiology of plants* (pp. 217-239): Springer.
- Sakakibara, H. (2005). Cytokinin biosynthesis and regulation. *Vitamins & Hormones*, 72, 271-287.
- Sanchez, E., Borja, R., Weiland, P., Travieso, L., & Martin, A. (2001). Effect of substrate concentration and temperature on the anaerobic digestion of piggery waste in a tropical climate. *Process Biochemistry*, 37(5), 483-489.
- Santner, A., Calderon-Villalobos, L. I. A., & Estelle, M. (2009). Plant hormones are versatile chemical regulators of plant growth. *Nature chemical biology*, 5(5), 301-307.
- Santner, A., & Estelle, M. (2009). Recent advances and emerging trends in plant hormone signalling. *Nature*, 459(7250), 1071-1078.
- Sasaki, K., Tanaka, T., Nishizawa, Y., & Hayashi, M. (1990). Production of a herbicide, 5-aminolevulinic acid, by *Rhodobacter sphaeroides* using the effluent of swine waste from an anaerobic digester. *Applied microbiology and biotechnology*, 32(6), 727-731.
- Sawyer, N., Trois, C., Workneh, T., & Okudoh, V. I. (2019). An overview of biogas production: fundamentals, applications and future research. *International Journal of Energy Economics and Policy*.
- Scaglia, B., Pognani, M., & Adani, F. (2015). Evaluation of hormone-like activity of the dissolved organic matter fraction (DOM) of compost and digestate. *Science of The Total Environment*, 514, 314-321.
- Scaglia, B., Pognani, M., & Adani, F. (2017). The anaerobic digestion process capability to produce biostimulant: the case study of the dissolved organic matter (DOM) vs. auxin-like property. *Science of The Total Environment*, 589, 36-45.  
doi:<https://doi.org/10.1016/j.scitotenv.2017.02.223>
- Servillo, L., Giovane, A., Balestrieri, M. L., Ferrari, G., Cautela, D., & Castaldo, D. (2012). Occurrence of pipercolic acid and pipercolic acid betaine (homostachydrine) in Citrus genus plants. *Journal of Agricultural and Food Chemistry*, 60(1), 315-321.
- Shan, L., & He, P. (2018). Pipped at the post: pipercolic acid derivative identified as SAR regulator. *Cell*, 173(2), 286-287.
- Shargool, D., Jain, J., & McKay, G. (1988). Ornithine biosynthesis, and arginine biosynthesis and degradation in plant cells. *Phytochemistry*, 27(6), 1571-1574.
- Sharma, N., Acharya, S., Kumar, K., Singh, N., & Chaurasia, O. (2018). Hydroponics as an advanced technique for vegetable production: An overview. *Journal of Soil and Water Conservation*, 17(4), 364-371.
- Shrivastava, A., & Gupta, V. B. (2011). Methods for the determination of limit of detection and limit of quantitation of the analytical methods. *Chronicles of young scientists*, 2(1), 21-25.
- Sindhu, R., Gnansounou, E., Rebello, S., Binod, P., Varjani, S., Thakur, I. S., . . . Pandey, A. (2019). Conversion of food and kitchen waste to value-added products. *Journal of Environmental Management*, 241, 619-630.
- Spaepen, S., & Vanderleyden, J. R. Firemans. (2007). *Indole-3-acetic acid in microbial and microorganism-plant signaling*. *Federation of European Microbiological*

- Societies Microbiology Reviews*, 31, 425-448.
- Srisowmeya, G., Chakravarthy, M., & Nandhini Devi, G. (2020). Critical considerations in two-stage anaerobic digestion of food waste – A review. *Renewable and Sustainable Energy Reviews*, 119, 109587.  
doi:<https://doi.org/10.1016/j.rser.2019.109587>
- Srivastava, L. (2002). General features of plant hormones, their analysis, and quantitation. *Plant Growth and Development. Hormones and Environment*, 141-153.
- Talan, A., Tiwari, B., Yadav, B., Tyagi, R., Wong, J., & Drogui, P. (2020). Food Waste Valorization: Energy Production Using Novel Integrated Systems. *Bioresource Technology*, 124538.
- Tang, X., Huang, L., Zhang, W., Jiang, R., & Zhong, H. (2015). Photo-catalytic activities of plant hormones on semiconductor nanoparticles by laser-activated electron tunneling and emitting. *Scientific reports*, 5(1), 1-9.
- Tian, H., Xu, Y., Liu, S., Jin, D., Zhang, J., Duan, L., & Tan, W. (2017). Synthesis of gibberellic acid derivatives and their effects on plant growth. *Molecules*, 22(5), 694.
- Tinikul, R., Chenprakhon, P., Maenpuen, S., & Chaiyen, P. (2018). Biotransformation of plant-derived phenolic acids. *Biotechnology Journal*, 13(6), 1700632.
- Uchida, R. (2000). Essential nutrients for plant growth: nutrient functions and deficiency symptoms. *Plant nutrient management in Hawaii's soils*, 31-55.
- Wang, C., Liu, R., Lim, G.-H., de Lorenzo, L., Yu, K., Zhang, K., . . . Kachroo, P. (2018). Pipecolic acid confers systemic immunity by regulating free radicals. *Science advances*, 4(5), eaar4509.
- WANG, H.-x., WANG, M.-l., WANG, X.-z., & DING, Y.-l. (2020). Detection of seven phytohormones in peanut tissues by ultra-high-performance liquid chromatography-triple quadrupole tandem mass spectrometry. *Journal of Integrative Agriculture*, 19(3), 700-708.
- Werner, T., & Schmülling, T. (2009). Cytokinin action in plant development. *Current opinion in plant biology*, 12(5), 527-538.
- Westerman, P. W., & Bicudo, J. R. (2005). Management considerations for organic waste use in agriculture. *Bioresource Technology*, 96(2), 215-221.  
doi:<https://doi.org/10.1016/j.biortech.2004.05.011>
- Wu, S., & Dong, R. (2020). Nutrients and Plant Hormones in Anaerobic Digestates: Characterization and Land Application. *Biorefinery of Inorganics: Recovering Mineral Nutrients from Biomass and Organic Waste*, 231-246.
- Wu, Y., Jin, X., Liao, W., Hu, L., Dawuda, M. M., Zhao, X., . . . Yu, J. (2018). 5-Aminolevulinic acid (ALA) alleviated salinity stress in cucumber seedlings by enhancing chlorophyll synthesis pathway. *Frontiers in plant science*, 9, 635.
- Wu, Y., Liao, W., Dawuda, M. M., Hu, L., & Yu, J. (2019). 5-Aminolevulinic acid (ALA) biosynthetic and metabolic pathways and its role in higher plants: a review. *Plant Growth Regulation*, 87(2), 357-374.
- Xu, F., Li, Y., Ge, X., Yang, L., & Li, Y. (2018). Anaerobic digestion of food waste—Challenges and opportunities. *Bioresource Technology*, 247, 1047-1058.
- Yamaguchi, I., Cohen, J. D., Culler, A. H., Quint, M., Slovin, J. P., Nakajima, M., . . . Sakagami, Y. (2010). 4.02 - Plant Hormones. In H.-W. Liu & L. Mander (Eds.), *Comprehensive Natural Products II* (pp. 9-125). Oxford: Elsevier.

- Yang, J., Duan, G., Li, C., Liu, L., Han, G., Zhang, Y., & Wang, C. (2019). The crosstalks between jasmonic acid and other plant hormone signaling highlight the involvement of jasmonic acid as a core component in plant response to biotic and abiotic stresses. *Frontiers in plant science*, 10.
- Yi, H.-S., Ahn, Y.-R., Song, G. C., Ghim, S.-Y., Lee, S., Lee, G., & Ryu, C.-M. (2016). Impact of a bacterial volatile 2, 3-butanediol on *Bacillus subtilis* rhizosphere robustness. *Frontiers in microbiology*, 7, 993.
- Yoneyama, K., Xie, X., Yoneyama, K., & Takeuchi, Y. (2009). Strigolactones: structures and biological activities. *Pest Management Science: formerly Pesticide Science*, 65(5), 467-470.
- Zhang, C., Su, H., Baeyens, J., & Tan, T. (2014). Reviewing the anaerobic digestion of food waste for biogas production. *Renewable and Sustainable Energy Reviews*, 38, 383-392. doi:<https://doi.org/10.1016/j.rser.2014.05.038>
- Zhang, W., Wei, Q., Wu, S., Qi, D., Li, W., Zuo, Z., & Dong, R. (2014). Batch anaerobic co-digestion of pig manure with dewatered sewage sludge under mesophilic conditions. *Applied energy*, 128, 175-183.





**BIOGRAPHY**

**NAME** Miss Thipwan Jiemanukunkij

**DATE OF BIRTH** August 6,1995

**PLACE OF BIRTH** Chanthaburi

**PRESENT ADDRESS** 156 Moo1, Khlong Pun, Klaeng, Rayong , Thailand

**POSITION HELD** 2018-2019 Research assistant at Vidyasirimedhi Institute of Science and Technology (VISTEC),Rayong

**EDUCATION** 2014-2018 Bachelor of biomedical sciences (B.Sc.), Faculty of Allied Health Sciences

